UNIVERSITY OF SOUTHAMPTON

FACULTY OF ENGINEERING, SCIENCE AND MATHEMATICS

School of Electronics and Computer Science

Finite Element Analysis of Electrical Devices Coupled to Electric Circuits

by

Tony Jay

Thesis for the degree of Master of Philosophy

October 2003

Acknowledgements

I would like to express my gratitude to Vector Fields for supporting my studies. In particular, John Simkin was always available to answer questions and Chris Biddlecombe and Simon Taylor provided valuable discussions and encouragement.

Thanks to my supervisor, Jan Sykulski, without whose enthusiasm this thesis would not have been completed.

Thanks to Mum and Dad who fostered my interest in science and engineering and to my wife, Victoria, for giving me time and support.

UNIVERSITY OF SOUTHAMPTON

ABSTRACT

FACULTY OF ENGINEERING, SCIENCE AND MATHEMATICS
SCHOOL OF ELECTRONICS AND COMPUTER SCIENCE

Master of Philosophy

FINITE ELEMENT ANALYSIS OF ELECTRICAL DEVICES COUPLED TO ELECTRIC CIRCUITS

by Tony Jay

This report presents the coupling of circuit equations with two dimensional finite element electromagnetic analysis. Time transient and time harmonic analysis are both considered.

Conventional finite element analysis uses prescribed currents within domains to represent electrical conductors. Real devices are normally supplied by power supplies and external circuits can be used to represent their voltage sources and impedances. A two dimensional (2d) cross section may be adequate for magnetic analysis, but the electrical connection between components is lost. External circuits can be used to supply this lost information.

Coupling has been implemented in this report by combining both the circuit and finite element equations into one system. The 'directly' coupled system is then processed so that it can be analysed using conventional linear algebra methods

Two different techniques are presented for entering a circuit into the finite element model. The first requires the user to identify network loops within the circuit. The second uses an extended form of a SPICE circuit definition file. An automatic loop generation algorithm is presented to convert a SPICE format file into network loops.

Results are presented for both the time harmonic and time transient cases. Analytical results are discussed which demonstrate the accuracy of the coupling technique and a model of a motor is presented which shows that complex models can be successfully simulated and also demonstrates the commercial importance of this work.

Table of Contents

Table of Figures

1. Introduction

1.1 Background

In industry and academia it is of great interest to model the behaviour of electromagnetic fields in real devices. Most electromagnetic devices use the field produced by currents in conductors or permanent magnets to produce the action of a force at a distance, or use the induced fields caused by motion to measure displacement. Devices may range from coils costing a few pence to generators, motors and Magnetic Resonance Imagers (MRIs) costing millions of pounds.

The theory required to describe the electromagnetic fields in real devices is contained in Maxwell's Equations published at the end of the 19^{th} Century [1]. Electromagnetic analysis is the problem of solving Maxwell's equations subject to given boundary conditions. The analytical solutions of Maxwell's equations are limited in that they can be only found for simple geometries such as semi-infinite planes, cylinders, spheres or to a small section of a device [2,3,4]. Analytical solutions are also available for static, time harmonic and time transient fields, but tend to be restricted to homogenous magnetic materials with constant permeability.

In order to calculate the transient solution of Maxwell's equations for models in three dimensions which contain materials with non-linear permeability, numerical solutions are required. Electrical machines are an important application which demand this complexity [5,6]. Numerical solutions require the spatial discretisation of a model, and large models can only be analysed with the use of efficient computer programs.

There are various techniques for creating a discrete model of a real device. The finite element method [7,8] is the most popular for electromagnetic analysis although the boundary element method [9] and hybrid methods [10] are also successful. For all techniques it is important to use computer processing speed and memory efficiently as well as using efficient algorithms. Greater accuracy can be achieved in numerical methods by decreasing the size of elements, i.e. increasing the spatial discretisation of a model. Discretisation produces a system of equations that describe the fields. The penalty for increased accuracy is therefore an increased number of equations. To solve more equations requires more floating point calculations and computer memory which results in longer solution times. The compromise of computer resources versus accuracy is one of the dichotomies of computation techniques. It is common to reduce the

degrees of freedom of a model by exploiting any periodic symmetry. This allows the size of the model to be reduced. It is not just the symmetry of the model itself which is important but the symmetry of the magnetic fields within the model.

This thesis will exploit the finite element method due to its flexibility and efficiency. Finite element analysis (FEA) has been used successfully for calculating the electromagnetic fields in real devices for over thirty years, and as early as 1970 the method was applied to a rotational electrical machine [8]. Thirty years of advancement and the increase in computing power have allowed more effects to be included in the computer models such as the non-linearity of magnetic permeability and motion.

In two dimensions external circuits are needed to correctly describe the connectivity of the conductors outside of the finite element problem [11], whereas in 3d it may be possible to model them as part of a finite element mesh. External circuits are also needed when the drive of a conductor or a circuit must be expressed as a voltage rather than a current density.

The goal of an electrical machine designer is to predict the performance of a machine and its behaviour over a range of operating conditions. This can be achieved using computer aided engineering software. A discrete model of the device can be created, the non-linear behaviour of the magnetic materials can be modelled and the device can be coupled to external circuits and motion. For most applications this is currently impractical using 3d discrete models as solution times are unacceptably long for commercial use. If a model can be approximated to be infinite in the one direction (XY symmetry), or exhibits axi-symmetry around the axis, then the model can be reduced to two dimensions and the number of equations is therefore reduced compared to a 3d model of the same discretisation. A reduction in the number of equations is translated to reduction of solution time or can allow for an increased discretisation within a model. Coupling to external circuits in this thesis is restricted to two classes of 2d applications, but also involves coupling to other effects such as motion and non-linearity.

There are at least three approaches to modelling external circuits and each has its own merits.

1.2 Approaches to circuit coupling.

The three main approaches to coupling finite elements with external circuits, are

1. Circuit and parameter extraction
2. Indirect coupling
3. Direct coupling

Each technique has its own advantages and disadvantages in terms of memory requirement, accuracy, calculation time and ease of use.

1.2.1 Circuit and parameter extraction

It is very convenient for designers of the supply circuit for an electrical device, such as an induction motor, to be able to use their normal circuit simulation tools to analyse the system performance. If equivalent 'circuit' parameters are extracted from a FEA solution they can be incorporated directly into a circuit simulator. Two closely related approaches are

- Equivalent circuits
- Tables of parameters

The first technique uses an "equivalent circuit", which is a theoretical electrical circuit containing resistances and impedances representing the real device to be analysed [12]. Figure 1.1 shows two different simple equivalent circuits for an air-cored two-winding transformer [13] consisting of a primary and secondary windings.

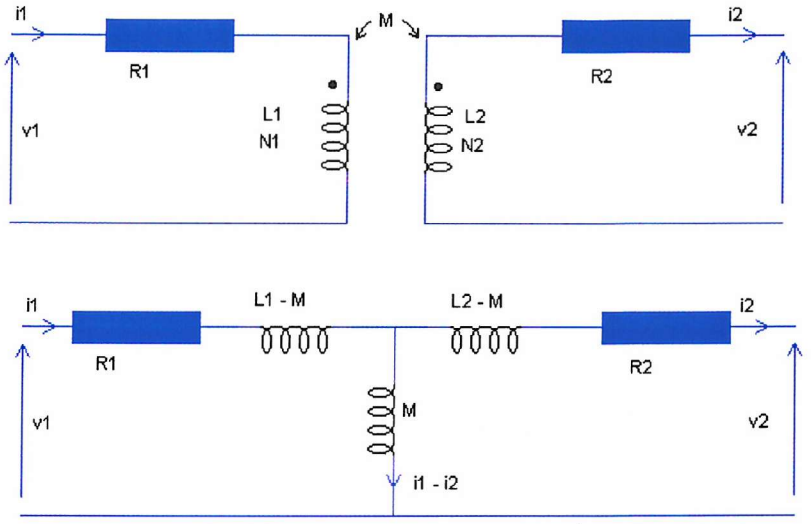

Figure 1.1 Equivalent circuit of an air core transformer

Here v1 and v2 are the potential differences across the primary and secondary windings, i1 and i2 the currents in the windings, L1 and L2 the inductances of the windings, N1 and N2 the number of turns of the windings, R1 and R2 the DC resistances of the windings and M the mutual inductance.

An equivalent circuit is proposed for a device by a designer and then a finite element package can be used to extract the equivalent circuit component values. Circuit analysis can then be performed on the equivalent circuit using the designer's favourite off the shelf circuit simulator.

It is even possible to build an expert system for a particular type of model which performs the FEA with the user knowing very little about finite elements, and then extract the parameters automatically [15]. This technique relies on the expert system being flexible enough to produce accurate models for all of the designer's needs.

The equivalent circuit is an approximation, and the approximation typically becomes less valid when the device exhibits strong non-linear characteristics. Models containing non-linear materials, motion or effects with a wide range of time constants cannot be represented accurately by a single equivalent circuit model. However, there has been work [14], where very elaborate equivalent circuits have been used for the transient analysis of electrical machines

where motion is present. The motion of the device is simulated by the reconnection of resistors which represent the air gap between the stationary and moving parts. This technique can even calculate electromagnetic torque. The equivalent circuit method is also an efficient way to couple high frequency problems to circuits where scattering parameters are calculated at different frequencies [16].

The second circuit parameter technique involves solving the finite element model of the device using many different excitation conditions. A variety of drive currents are applied to the model and a look up table is created of force and flux linkage versus current and position in a device [17]. The look up table can be integrated into the circuit simulator as a component which returns flux and force for a given position and current [18]. The circuit simulator can also be used to model the mechanical systems by using their electric analogs. For example, a rotating mass is represented by a capacitor and viscous damping is modelled by a resistor.

There are many commercial circuit simulators which can include the calculated circuit parameters such as Saber [19] or those based on the 1970's Berkely University package SPICE [20]. These and other packages contain extensive libraries characterising real components such as diodes and thyristers from many different manufacturers. The equivalent circuit approach is favoured by circuit designers as it gives a compact characterisation of a device that can give insight into system performance. The simulator package will be easy to use as it will also have schematic capture of the external circuit along with extensive visualisation tools for the results. The parameter table technique has limitations as the complexity of the driving circuits are increased many more FEA simulations are required to produce the tables. When many FEA solutions are required it may be easier to more closely couple the circuit and finite element systems.

1.2.2 Indirect coupling

An attractive proposition in circuit modelling is to use an engineer's favourite circuit simulator to solve the circuit equations in parallel with a finite element program solving the electromagnetic equations. Either of the two programs could be considered as the controlling program. For example, a circuit modelling program could request from a FEA program the current in a particular element when providing a certain voltage. Communication between the two programs could be by shared memory or sockets either on the same or different computers over

a network. The close coupling could involve the circuit simulation requesting the flux and forces at each time step in a transient solution, having supplied the currents. This approach exploits both the accuracy and flexibility of both programs. To be able to establish effective communication between two programs, the requirements of both types of simulation must be considered.

A second type of indirect coupling integrates the finite element equations and the circuit equations in the same program. The two different sets of equations are formed when analysing a model, one matrix describing the FEA problem and one describing the circuits [22]. The two matrices are not combined together; this has advantages because the matrices have different properties and structures. The FEA matrix is very large, sparse and symmetric, requiring special solvers performing iterative solutions [23]. The circuit matrix is often a small dense matrix which can be solved by an exact method such as Gauss-Jordon elimination [23]. The excitation terms for the circuit equations are calculated from the coupling coefficients between the circuit and FEA equations. These right hand side terms can be calculated by changing the drive on each conductor in turn. This procedure requires an efficient matrix solver which can solve the same matrix equations with multiple right hand sides [22].

1.2.3 Direct coupling

If the circuit equations and the symmetric finite element equation matrices are merged into one large system of equations, the final system of equations can be solved simultaneously. This approach requires the extension of a finite element code and has the limitation that the circuit simulation will not have the flexibility of a fully functioning circuit simulation package, but all the features of the FEA program will be available [21].

The combined system of equations is not symmetric and contains two blocks of coefficients from different types of equations. The terms therefore may be poorly conditioned and an iterative matrix solver will require more iterations than in the case of a well-conditioned symmetric matrix. The symmetry of the matrix can be retained, by the correct use of scaling, in order to minimise the size of the matrix that must be calculated and stored. The scaling process adds extra complications within a program, especially when matrices are recalculated at each time step in a time marching scheme.

A second method of direct coupling in frequency domain analysis replaces the inductors and capacitances by equivalent circuits of resistances using Dommel's analysis [24]. The electrical components are represented by one dimensional finite elements within the finite element matrix. This method produces a single matrix which can be solved in a conventional way. The proponents of this method do not claim that it has any advantage over including inductances and capacitances explicitly and the resulting final matrix equations are identical.

Direct coupling can achieve very efficient and simulations, that can include effects such as linear or rotational motion. The complexity of the circuit which can be modelled is only limited by the implementation of the circuit equations within the FEA code. Some components are easily included such as resistors and inductors, whereas other components such as diodes and capacitors require recalculation of their properties at each step in a transient solution. As the expectations and demands of machine designers increase it is possible to increase the functionality of the circuit modelling code within the FEA program. The direct method will never provide as good a circuit simulator as a stand alone tool, but a stand alone tool can only use an equivalent circuit representation of a machine which is by definition an approximation.

If direct coupling is implemented, a very large range of voltage driven finite element problems can by solved, where the characteristics of a device are not known *a priori.*

1.3 The development of direct circuit coupling.

1.3.1 Nodal analysis of circuits

The first attempt to model the external circuit was in 1976 [25], but it was only later understood that to include circuits in a typical vector potential formulation a scalar potential term must be included. Every conductor which is in a circuit must have a scalar potential associated with it and each conductor is represented as an element between two circuit nodes. The simplest external circuit which can be considered is a short circuit in a 2d model, where a group of conductors can be joined together by short circuit connections, as described in [26] for the frequency domain case and [27] for the time transient case. Consider the simple physical system described in figure 1.2 of two conducting bars in a time varying magnetic field.

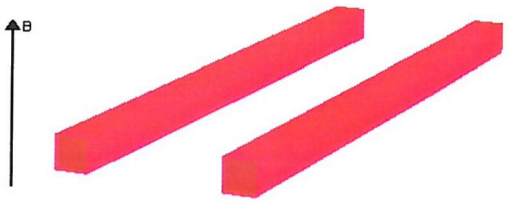

Figure 1.2 Two disconnected conductors

A 2d representation of this system can be used if the bars are very long as in figure 1.3

Figure 1.3 A 2d representation of two disconnected conductors

However, the 2d model can not resolve the difference between the geometry in figure 1.2 and that shown in figure 1.4 where short circuit current flows at the end of the bars.

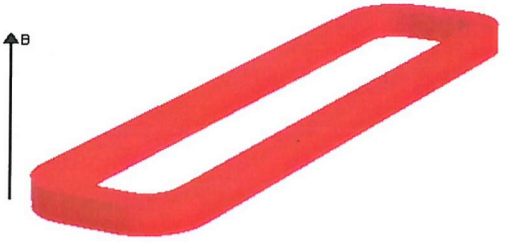

Figure 1.4 Two short-circuited conductors

A simple external circuit is needed to describe the difference between the two similar systems.

The first use of complex circuit equations with external impedances and inductors involved filamentary conductors, for example [29] and [30]. Filamentary conductors are coils wound with many turns of insulated wire such as those used to model motor stator windings or to approximate a superconducting coil. The current density distribution is determined by the arrangements of the filaments in the windings and is therefore known. The wire is assumed to

have a small cross sectional area such that eddy currents and therefore their distribution in the wires can be neglected.

In models which are invariant in the z direction (XY symmetry) and in axi-symmetric models, the current density is defined by the turns density and the current in each turn of the winding. An external voltage is applied to the circuit which results in a current or, if a driving potential is not present, a filamentary circuit can be used to model a secondary coil in a transformer or a pick up coil. Coils consisting of massive conductors can also be formed into circuits by the addition of resistors and inductors [31]. Investigations of both filamentary and eddy current circuits concentrated initially on independent circuit loops where the current in each circuit is isolated from the others. Circuits may be defined using nodal equations or 'mesh loop' equations where 'mesh' refers to the connections of a circuit and is not to be confused with the finite element mesh. The currents in the mesh loops are the unknowns in the circuit equations.

Real external circuits contain arbitrary arrangements of components, where the mesh loops are connected in parallel and in series [32]. It is necessary to identify a set of mesh loops to fully define the circuits, although there will normally be more than one way of choosing the set of mesh loops. An example of an eddy current problem where arbitrary connections are needed is the modelling of rotor bar end winding resistances in a squirrel cage induction motor [33].

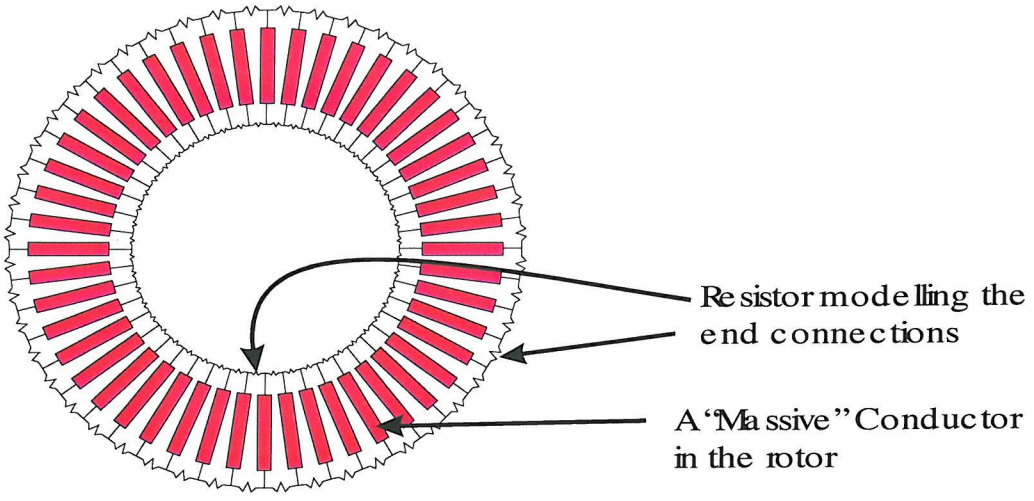

Figure 1.5 Circuit connection of a squirrel cage rotor

Examples of arbitrary connections of filamentary conductors are found in the protection circuits in superconducting coils. If the coils become resistive (quench) the energy is dumped into a set of protection resistors or diodes [34]. There are cases where arbitrary eddy current and filamentary circuits are combined in one model; one application is in asynchronous machines with filamentary circuits in the stator and eddy current circuits in the rotor [35].

1.3.2 Modified nodal analysis

The orthodox approach to modelling circuits and fields is to develop equations describing the current in the voltage driven external circuits with the finite element terms. There is a second approach that uses a Modified Nodal Analysis (MNA) [39]; this does not require the identification and formation of mesh loops. The circuit equations in MNA represent either current sources, voltage sources or components with unknown potential drops across them. The circuit equations can be automatically extracted from a nodally defined circuit with the aid of some graph theory [40] that can be used as a robust way of identifying an optimal set of branches from a circuit. Using a nodally defined circuit rather than a mesh loop approach allows easier coupling to the nodal based information typically generated by schematic circuit capture programs. The disadvantage of MNA is that very simple circuits must be entered in a nodal form even if they only involve one or two components. The approach which has been used in this work is to develop conversion routines which can use nodally defined circuits and produce equivalent mesh loops. This allows the user of the software to define a circuit by identifying the mesh loops or by entering the nodal connections.

The use of MNA has been extended further to represent the circuit conductors explicitly as a controlled voltage source. A controlled voltage source is represented by a circuit element composed of two sub elements. One element has two voltage Degrees Of Freedom (DOF) on its terminals and one has a current DOF [41]. The equations produced by these elements are not symmetric, which is not desirable as solution times and computer memory requirements will be greater than with symmetric equations. The use of controlled voltage sources is however general enough to be used in coupling to 3d finite element models, although the formulation is however significantly more complicated than for the 2d cases considered in this work.

1.3.3 Non-linear circuit components

Most simple external circuits contain resistors, inductors and capacitors, that can be coupled to finite element equations because their impedances are known. In inverter drive circuits, active components such as diodes and thyristers need to be represented [42]. Their impedance is a non-linear function of the current through them or the potential across them. In a full circuit analysis package, the non-linear behaviour of the current and voltage in these devices is usually supplied from libraries. In combined FEA / circuit package the components are typically represented as binary switches, with either a very low or very high value resistance to model the closed and open circuit behaviour [43]. When a device is switched from high to low resistance in a time transient scheme, the instant of switching must be correctly captured, otherwise the resulting discontinuity in currents may lead to unwanted oscillations in the solution. If the time step is adapted so that a time stepping point is used at the moment of switching [44], the oscillations in the solution can be greatly reduced. An alternative approach has been used in simple circuits to model the non-linear behaviour of components such as resistors and capacitors by representing them as 0D and 1D finite elements [45]. The arbitrary variation of the component value has been simulated as a function of time or position allowing the modelling of devices such as switched reluctance motors.

1.3.4 Direct coupling to other effects

Electromechanical devices are an important application of finite simulation tools. In general it is necessary to model the movement of components in the system as well as their connections to external circuits. Rotational motion is required for motors, generators and bearings and linear motion is required for contactors, switches and linear motors. When the finite element model is solved in a directly coupled time transient scheme, it is straightforward to update the position of the moving part of the model at each time step. The motion within the finite element mesh can be achieved by remeshing at each step, special overlapping finite elements [46,47] or by Lagrange multipliers on the moving / stationary interfaces [48]. If rigid body dynamics are also included in the coupling, the position of a moving part can be calculated from the forces derived from the finite element solution [49], either through the virtual work principle [51] or by the use of Maxwell Stress Method (MSM) [50].

In the analysis of an electromechanical device, it may be required to study the thermal properties of the system. All of the coupling techniques previously studied do not preclude coupling to a thermal solution. A thermal solution can take as input the energy losses in a device, calculated from the joule heating or hysteresis losses. A frequency domain or time transient thermal solution can solve for the temperature distribution in a device. The temperature in the device can then be used to update the material properties used in the finite element solution. This is an example of indirect or weak coupling which may be appropriate, although changes of state which pass through the Curie temperature may require careful hand-shaking between simulations.

1.4 Implementation details

The circuit coupling in this work has been developed to complement the existing functions of the Vector Fields Opera-2d package. The circuit coupling options have been implemented in five of the programs which calculate quasi-static electromagnetic fields in the following limits

1. Frequency domain (AC)
2. Time transients (TR)
3. Rotating machines (RM)
4. Linear motion (LM)
5. Demagnetisation rigs (DM)

Coupling to external circuits in these programs was developed in a way that does not appreciably add to the solution times and memory requirements. All pre-existing options within the solvers such as non-linearity and symmetry conditions, either periodic or implied by the boundary conditions, are compatible with the external circuits. The Opera-2d Pre and Post-Processor (PP) has been extended in order to define and edit the external circuits.

1.5 Thesis outline

Chapter 2 begins with a review of Maxwell's equations and introduces the terminology used. Maxwell's equations are developed using the magnetic vector potential to describe the field in a conducting region due to a known current density. The boundary conditions are also presented. The equations are further developed to describe the fields in conductors with eddy currents, in conductors in circuits composed of filamentary conductors and in circuits formed

from massive conductors where eddy currents are significant. The chapter concludes by introducing the circuit network equations needed to describe an external circuit.

Chapter 3 introduces the finite element method as a technique for solving partial differential equations. The governing equations for the conductor introduced in chapter 2 are spatially discretised using the Galerkin method. Matrix notation is used to concisely express the frequency domain (AC) and time transient (TR) solution of the discretised equations. The resulting equations are manipulated to be symmetric and the numerical techniques which are needed to solve the matrices are discussed.

Chapter 4 explains two techniques which can be used to define the external circuits used in this work. The first technique uses an extension to the Opera-2d PP to define the mesh loops and the connections between the mesh loops. The second technique uses files based on the format used by SPICE where all the nodes and components in a circuit are entered in a list which Opera-2d PP then decodes into mesh loops.

Chapter 5 presents a range of results, starting with analytical comparisons for both time harmonic and time transient finite element solvers. When the coupling technique has been proved to be accurate for circuits containing both filamentary and eddy current conductors, a model has been presented for an induction motor. The model of the induction motor uses both filamentary and eddy current circuits in one formulation.

Chapter 6 summarises the work and discusses both limitations in the work and aspects of the work which can be further developed.

2. Formulation of the basic equations

2.1 Introduction

Maxwell's equations will be introduced in this chapter and will be used to formulate equations describing the field in both massive and filamentary conductors, which are either current driven or form part of external voltage driven circuits. Electric circuit equations will be developed which relate the currents and voltages within the 'mesh loops' of a circuit which contains massive and filamentary conductors.

Figure 2.1 shows a representative configuration containing a conducting material Ω_k, with magnetic permeability μ, electric permittivity ε and electric conductivity σ, bounded by a surface Γ_k, contained within a volume of free space Ω bounded by a surface Γ which may be extended to infinity if required [52].

The conducting material may have a prescribed current J_s or be connected with other conductors into a circuit.

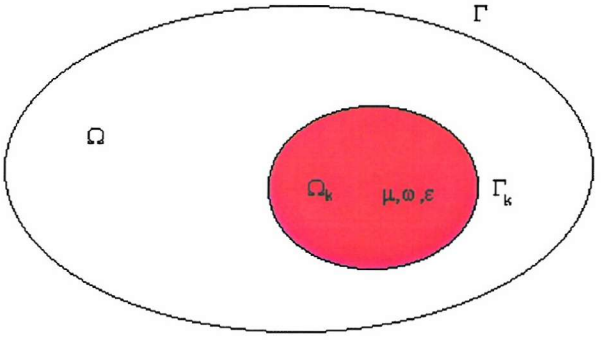

Figure 2.1 Simple model configuration of arbitrary shape

2.2 Maxwell's equations

James Clerk Maxwell's 1892 publication 'A Treatise on Electricity and Magnetism' [1] provides a system of equations which describe electromagnetic fields and forces.

$$\nabla \bullet \mathbf{D} = \rho \tag{2.1}$$

$$\nabla \bullet \mathbf{B} = 0 \tag{2.2}$$

$$\nabla \times \mathbf{E} = -\frac{\partial \mathbf{B}}{\partial t} \tag{2.3}$$

$$\nabla \times \mathbf{H} = \mathbf{J} + \frac{\partial \mathbf{D}}{\partial t} \tag{2.4}$$

where **D** is the electric flux density and **E** is the field strength, **B** is the magnetic flux density and **H** is the magnetic field strength, ρ is the free charge density, **J** is the current conduction density.

These four laws are the unification of previously understood phenomena, i.e. Gauss's law, (equation 2.1) and Faraday's Law (equation 2.3). Maxwell's major contribution was to generalise Ampère's Law (equation 2.4) to include a displacement current

$$\mathbf{J}_D = \frac{\partial \mathbf{D}}{\partial t} \tag{2.5}$$

If the wavelength of any time-varying fields is large compared with the physical dimensions of the problem, this displacement current is negligible compared with the free current density and there is no radiation [2]. All the cases presented in this thesis fall into this category so that the classical field approximation of Ampère's Law (equation 2.4) can be used i.e.

$$\nabla \times \mathbf{H} = \mathbf{J} \tag{2.6}$$

Although this approximation is adequate for this thesis, this can create some anomalies which can only be explained using the full form of the equations [1].

The interface or boundary conditions between regions of different material properties, derivable from equations 2.1-2.4, are

$$(\mathbf{B}_2 - \mathbf{B}_1) \bullet \mathbf{n} = 0 \tag{2.7}$$

$$(\mathbf{D}_2 - \mathbf{D}_1) \bullet \mathbf{n} = \omega_s \tag{2.8}$$

$$(\mathbf{H}_2 - \mathbf{H}_1) \times \mathbf{n} = \mathbf{K} \tag{2.9}$$

$$(\mathbf{E}_2 - \mathbf{E}_1) \times \mathbf{n} = 0 \tag{2.10}$$

where ω_s is the surface charge density, and **K** is the surface current density. Three further final equations are required, the material constitutive equations; these define the relationship between current density and electric field, flux density and field strength.

$$\mathbf{J}_c = \sigma\mathbf{E} \tag{2.11}$$

Equation 2.11 is Ohms Law, where the conductivity σ is in general treated as being frequency independent up to 10^{12} Hz [7]. The two equations relating the fields strength to the flux densities are

$$\mathbf{B} = \mu\mathbf{H} \tag{2.12}$$

$$\mathbf{D} = \varepsilon\mathbf{E} \tag{2.13}$$

where the permeability μ and the permittivity ε are tensors. It is through these constitutive relations that the non-linear properties of materials can be introduced. The permittivity is not relevant in this study of magnetism because the displacement current has been neglected. However, it is essential to model non-linear permeability in magnetic devices.

2.3 Magnetic vector potential

Since the magnetic field vector **B** is solenoidal in nature, as can be seen in equation 2.2, it can be expressed in terms of a 'magnetic vector potential' **A** [39]:

$$\mathbf{B} = \nabla\times\mathbf{A} \tag{2.14}$$

In order to uniquely define the vector potential **A,** the divergence of the vector must also be specified[4]. From equation 2.6 and 2.12

$$\nabla\times\frac{1}{\mu}\nabla\times\mathbf{A} = \mathbf{J} \tag{2.15}$$

Faradays law (equation 2.3) can also be rewritten in terms of the vector potential

$$\nabla\times\left(\mathbf{E} + \frac{\partial\mathbf{A}}{\partial t}\right) = 0 \tag{2.16}$$

and equation 2.16 can then be integrated to give

$$\mathbf{E} = -\left(\frac{\partial \mathbf{A}}{\partial t} + \nabla V\right) \tag{2.17}$$

where V is a scalar potential, and ∇V is the equivalent of a constant of integration. Neither **A** or V are completely defined because a grtadient of an arbitrary scalar function can be added to **A** and the time derivative of the same function can be subtracted from V without affecting **B** and **E**. To uniquely define **A**, a separate condition is specified (called a gauge condition) [2]. The two common gauges are:

$$\nabla \bullet \mathbf{A} = 0 \tag{2.18}$$

called the Coulomb gauge, and

$$\nabla \bullet \mathbf{A} = -\mu\sigma V - \mu\varepsilon\frac{dV}{dt} \tag{2.19}$$

called the Lorentz gauge.

2.4 The 2d limit of the magnetic flux density vector

The magnetic flux density vector can be written in cartesian coordinate systems as

$$\mathbf{B}(x, y, z) \tag{2.20}$$

and in the cylindrical polar coordinate system as

$$\mathbf{B}(r, z, \phi) \tag{2.21}$$

There are two special cases when these fields can be described by a 2d approximation, i.e.

$$\mathbf{B}(x, y) \tag{2.22}$$

when the field is independent of z and

$$\mathbf{B}(r, z) \tag{2.23}$$

when the field is independent of θ.

These lead to a simplification such that only one component of the vector **A** is required to define the fields i.e.

$$\mathbf{B}(x, y) = \nabla \times (0, 0, A_z) \tag{2.24}$$

$$\mathbf{B}(r, z) = \nabla\times(0, 0, A_\phi) \tag{2.25}$$

All the work in this thesis and subsequent formulations of **A** will assume the 2d limit. The Coulomb gauge will be used for **A** (and is a natural choice) as in this 2d limit the scalar potential V in equation 2.17 can be equated to the voltage drop that would be measured across an external circuit [53].

2.5 Conducting regions

It may be convenient to model coils as volumes with prescribed current density and neglect the effect of eddy currents in them. In this case, equation 2.15 becomes

$$\nabla\times\frac{1}{\mu}\nabla\times\mathbf{A} = \mathbf{J}_0 \tag{2.26}$$

where $\mathbf{J}_0$ is the prescribed current density.

In materials where eddy currents are induced and source currents are excited by applied voltages, the fields are again described by equation 2.15

$$\nabla\times\frac{1}{\mu}\nabla\times\mathbf{A} = \mathbf{J} = \sigma\mathbf{E} = -\sigma\left(\frac{\partial\mathbf{A}}{\partial t} + \nabla V\right) = \mathbf{J}_e + \mathbf{J}_s \tag{2.27}$$

$\mathbf{J}_e$ is the eddy current density and $\mathbf{J}_s$ is the source current density. Although the total current density **J** is physically meaningful (and measurable), separating **J** into the two components $\mathbf{J}_e$ and $\mathbf{J}_s$ is not just a matter of notation. In a conducting region where the return path may be considered to be outside of the problem domain (implied by the boundary conditions), the governing equation can be written from equation 2.27 as

$$\nabla\times\frac{1}{\mu}\nabla\times\mathbf{A} + \sigma\frac{\partial\mathbf{A}}{\partial t} = \mathbf{J}_s \tag{2.28}$$

In a conducting region where the eddy currents have a return path within the conducting region (a short-circuited conductor as in figure 2.2) a second equation must be specified for each region.

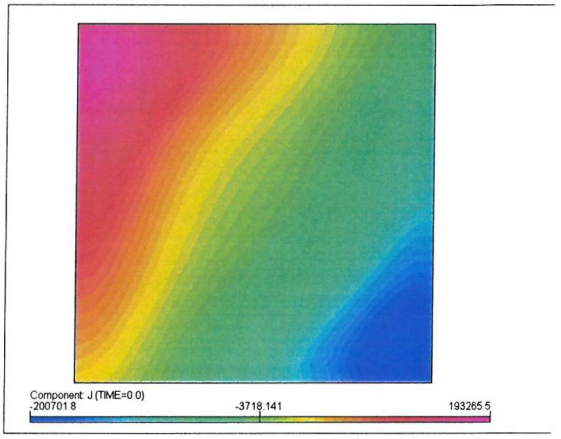

Figure 2.2 Current density in a short circuited conductor with zero total current

An extra equation is also required for each connected set of conducting regions, which may include conductors outside of the model implied by symmetry as in figure 2.3.

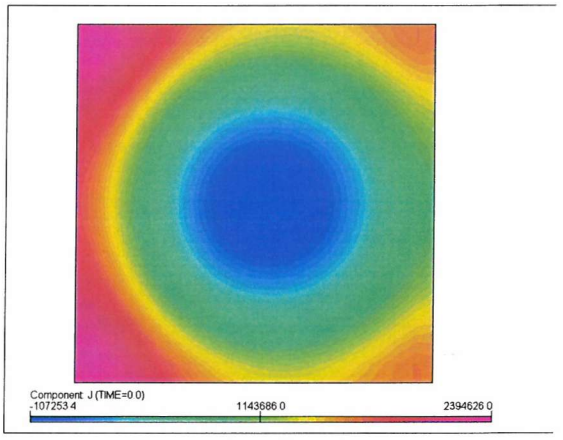

Figure 2.3 Current density in a conductor with its return path outside of the FE model

The total current is fixed by integrating equation 2.27 over just the cross section of the conductor

$$\int_{\Omega k}\left(-\sigma\frac{\partial \mathbf{A}}{\partial t}+\mathbf{J}_s\right) = \int_{\Omega k}\mathbf{J} \tag{2.29}$$

where Ωk is the domain of the conductor k. These extra equations, one per condition, can then be solved together with equation 2.28[27].

2.6 Conductors in external circuits

An external circuit is formed when coils in the finite element model are joined with each other and with other circuit elements such as resistors, inductors and capacitors. Two classes of cols must be considered, those with massive conductors in which eddy currents can flow and those composed of many thin strands or filaments such that the redistribution of current by the eddy currents can be neglected, Figure 2.4.

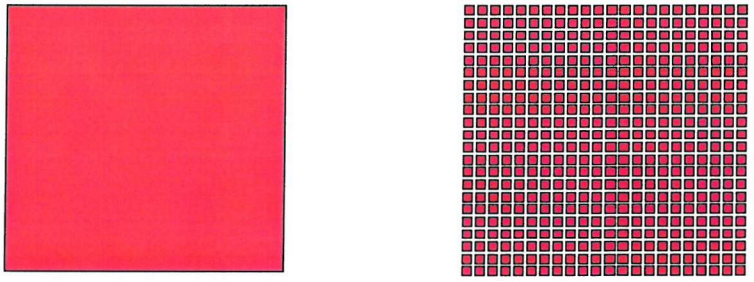

Figure 2.4 A bulk conductor and a filamentary conductor

The treatment of each conductor is very different, and the governing equations for conductors in each type of circuit will be presented in the next two sections.

2.6.1 Circuits with massive conductors

The current in a massive conductor has been described previously in equation 2.27 as

$$\mathbf{J} = \sigma\mathbf{E} = -\sigma\left(\frac{\partial \mathbf{A}}{\partial t}+\nabla V\right) = \mathbf{J}_e+\mathbf{J}_s \tag{2.30}$$

where ∇V represents the voltage drop along the length of the conductor. If V_1 and V_2 are the voltages on the conductor, at the far and near ends respectively, then

$$\mathbf{J}_s = -\sigma\nabla V = \frac{\sigma(V_2 - V_1)}{l} = \frac{\sigma\Delta V}{l} \tag{2.31}$$

where l is the length of the circuit. The convention has been adopted here that a positive voltage drop is in the same direction of positive current. This gives the governing equation of massive conductor in terms of the external circuit parameters l and ΔV as

$$\nabla\times\frac{1}{\mu}\nabla\times\mathbf{A} + \sigma\frac{\partial\mathbf{A}}{\partial t} - \frac{\sigma\Delta V}{l} = 0 \tag{2.32}$$

There is also one additional equation per massive conductor introduced by considering the total current over the cross section of the conductor (equation 2.29)

$$\int_{\Omega k}\left(-\sigma\frac{\partial\mathbf{A}}{\partial t} + \frac{\sigma\Delta V}{l}\right) = I \tag{2.33}$$

where I is the total current in the massive conductor and is an unknown. If it is noted that R_k, the dc resistance of conductor k, can be written as

$$R_k = \frac{l}{\int_{\Omega k}\sigma} \tag{2.34}$$

and then equation 2.33 can be written as

$$\Delta V_k = R_k I_k + R_k\int_{\Omega k}\sigma\frac{\partial\mathbf{A}}{\partial t}d\Omega_k \tag{2.35}$$

Equations 2.32 and 2.35 no longer contain terms of the current density **J**, and have been rewritten in terms of the circuit parameters of voltage and current. Using current rather than current desity allows the equations to be linked the circuit equations which will be developed later in this chapter.

2.6.2 Filamentary conductors in external circuits

Filamentary conductors are composed of many strands of wire wound in series separated by insulation. i.e. figure 2.5.

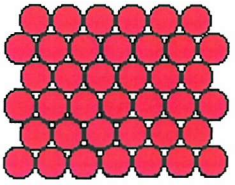

Figure 2.5 Detail of a filamentary conductor

The eddy currents in a conductor decrease exponentially in magnitude as the distance from the surface increases. The decay constant δ is called the eddy current skin depth or penetration depth and is defined for an infinite conducting sheet as [4]

$$\delta = \sqrt{\frac{2}{\omega\sigma\mu_0\mu_r}} \tag{2.36}$$

where ω is the angular frequency of the a.c.current, μ_r is the relative magnetic permeability of the conductor and σ is the conductivity. The equation for the skin depth of an infinite cylindrical conductor is more complicated but is of similar form [56]. The radius of a strand, r, is chosen to be smaller than the skin depth, so that all available material is used to transport current. If r/δ is small then the a.c. and d.c. resistances of a strand are related by the approximation [4]

$$\frac{R_{ac}}{R_{dc}} = 1 + \frac{1}{48}\left(\frac{r}{\delta}\right)^4 \tag{2.37}$$

As r/δ is small, it can be seen that the dc resistance is a good approximation to the ac resistance. There will also be proximity effects as the strands induce currents in their neighbours, but these are small when r is less than δ. In a typical low frequency application of a 50 Hz small motor, a strand will have a radius of about a millimetre, the conductivity will be about $5*10^{-7}$ ohm/metre hence

$$\frac{r}{\delta} = r/\left(\sqrt{\frac{2}{\omega\sigma\mu_0\mu_r}}\right) = \frac{1}{25} \tag{2.38}$$

which satisfies the approximations which have been made about the strands. In such applications it is unnecessary to model the eddy current effects in the strands and all the strands in a conducting region are represented as a conductor with uniform current density i.e.

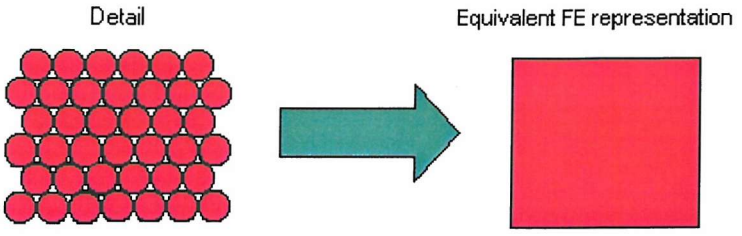

Figure 2.6 Detail of a filamentary conductor

There are applications such as Magnetic Resonance Imagers (MRIs) where this approximation is not adequate for high accuracy calculations - where fields must be calculated to be uniform to the level of 1 part in a million. In order to model the ragged edges of the conductor, the boundary of the FE representation of a conductor has a lower current density applied than the rest of the conductor.

Assuming that each filament carries a current of I amps, the current density in a filament is

$$\mathbf{J} = \frac{I}{S_j} \tag{2.39}$$

where S_j is the area of the j'th filamentary conductor. The second order partial differential equation for **A** obtained from combining equations 2.15 and 2.39 is

$$\nabla\times\frac{1}{\mu}\nabla\times\mathbf{A} = \frac{I}{S_j} \tag{2.40}$$

In order to incorporate the filamentary conductor into an external circuit it is necessary to express the voltage drop along the length of the conductor using equation 2.35 to include all the filaments in a conductor

$$\Delta V_k = \sum\Delta V_j = \sum\left(R_j I_j + R_j\int_{\Omega j}\sigma\frac{\partial\mathbf{A}}{\partial t}d\Omega_j\right) \quad j=1,N \tag{2.41}$$

where Ω_j is the domain of a filament j in conductor k. The resistance of each filament is

$$R_j = \frac{l}{\sigma \int d\Omega_j} = l\Re_j \tag{2.42}$$

where $\Re_j$, the resistance per unit length of conductor k, is a quantity often associated with filamentary circuits. The area of the filament is related to the area of the conductor by

$$S_k = \frac{\lambda S_i}{N} \tag{2.43}$$

where S_k is the area of conductor k and λ is the fill factor [22], i.e. the fraction of the conductor carrying current.

Substitution of equations 2.42 and 2.43 into equation 3.32 gives the quantities ΔV, $\Re_j$ and I_k which can now be expressed in a form which is directly connected with external circuit analysis thus

$$\Delta V_k = Nl\Re_j I_k + \frac{lN}{S_k}\int_{\Omega k} \frac{\partial \mathbf{A}}{\partial t} d\Omega_k \tag{2.44}$$

It is important to note that all quantities are in terms of the domain Ω_k, except for $\Re_j$ which is a property of the constituent filaments.

2.7 Circuit network equations

Circuits are connected networks of devices, each having two or more leads carrying currents. Leads are connected to circuit nodes, each node has an electric potential, or voltage V. Devices can be connected to each other in an arbitrary manner; to completely describe a circuit connectivity a list of the devices and the circuit nodes to which they are attached is needed.

Figure 2.7 A simple circuit element

The aim is to be able to represent any circuit connectivity in a general way. To do this a matrix equation is constructed for the circuit with the currents in the devices and the voltages at the circuit nodes as the unknowns.

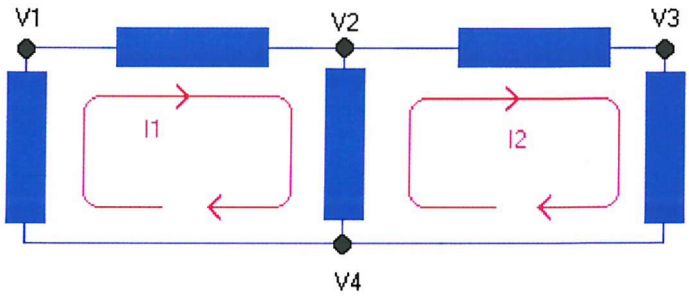

Figure 2.8 A circuit with complex connectivity

A complex circuit, such as figure 2.8, can be analysed by using Kirchoff's' junction rule [22] which states that 'The algebraic sum of the currents entering or leaving a junction is zero' i.e.

$$\sum I = 0 \tag{2.45}$$

The sign of the current leaving the junction is opposite to that for a current entering the junction, so the current in figure 2.9

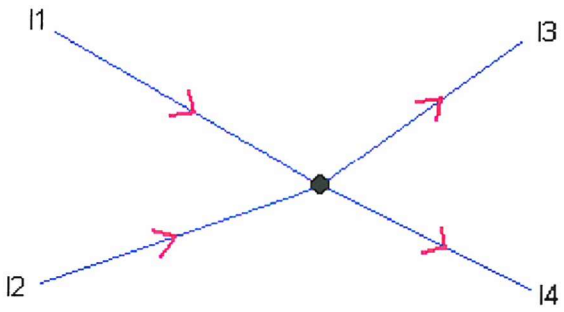

Figure 2.9 Currents at a junction

can be written as

$$I_1 + I_2 + I_3 + I_4 = 0 \tag{2.46}$$

It is more convenient however to use Kirchoff's loop rule which states that 'The algebraic sum of the *changes* in the potential around a closed loop is zero' i.e.

$$\sum \Delta V = 0 \tag{2.47}$$

which is shown for loop I1 in figure

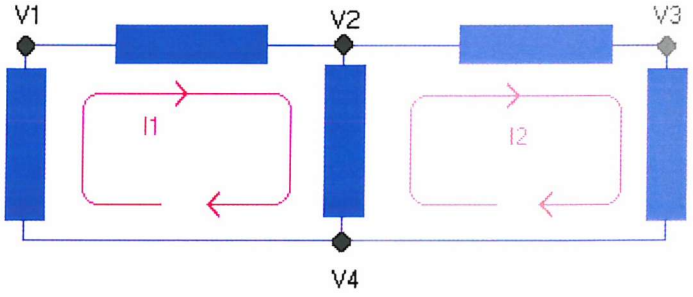

Figure 2.10 A loop composed of circuit components

This is a more convenient approach as a circuit is broken into 'loops' where each element is characterised by the potential difference across it. The potential drops (ΔV)across common components are

Circuit Component	Potential drop ΔV
Resistor	ZI
Inductor	$L\frac{dI}{dt}$
Capacitor	V_c
Voltage source	V_s
Massive circuit conductor	$R_k I_k + \int_{\Omega k} -\sigma \frac{\partial \mathbf{A}}{\partial t}$
Filamentary circuit conductor	$Nl\Re_j I_k + \frac{lN}{S_k}\int_{\Omega k}\frac{\partial \mathbf{A}}{\partial t} d\Omega_k$

TABLE 2.1 The potential drop across circuit elements

where L is the inductance, Z an impedance and V_c is the voltage across the plates of a capacitor. In a time transient solution V_c is given by

$$V_c = \frac{1}{C}(q_0 + \int_0^t I dt) \tag{2.48}$$

where C is the capacitance and q_0 is the initial charge on the capacitor. The voltage drop, V_c, on a capacitor is not known *a priori*, however it can be determined by numerical integration in a time stepping algorithm. In the time harmonic case it will be shown in chapter 3 that capacitors can be treated in the same way as inductors.

The circuit equation (2.47) for a general circuit 'mesh loop' containing many types of components including capacitors can now be written as

$$\sum \Delta V_k + \sum RI + \sum L\frac{dI}{dt} = \sum V_s - \sum V_c = \sum E \tag{2.49}$$

where E is a general voltage source. There will typically be -more than one 'mesh loop' coupled to a finite element model and so there is a matrix of equations, with one equation (2.49) for each loop. i.e.

$$[\mathbf{M}][\Delta \mathbf{V}_k] + [\mathbf{Z}_m][\mathbf{I}]_m + [\mathbf{L}_m]\frac{d\mathbf{I}_m}{dt} = [\mathbf{E}_m] \tag{2.50}$$

$\Delta \mathbf{V}_k$, $\mathbf{E}_m$ and $\mathbf{I}_m$ represent the vectors of voltage drops, voltage sources and currents in a circuit, $\mathbf{Z}_m$ and $\mathbf{L}_m$ represent matrices of impedances and inductances and **M** is a matrix describing the direction of the current in a conductor. Matrices are required to describe the circuit components as one component may be in more than one mesh loop as shown in figure 2.11.

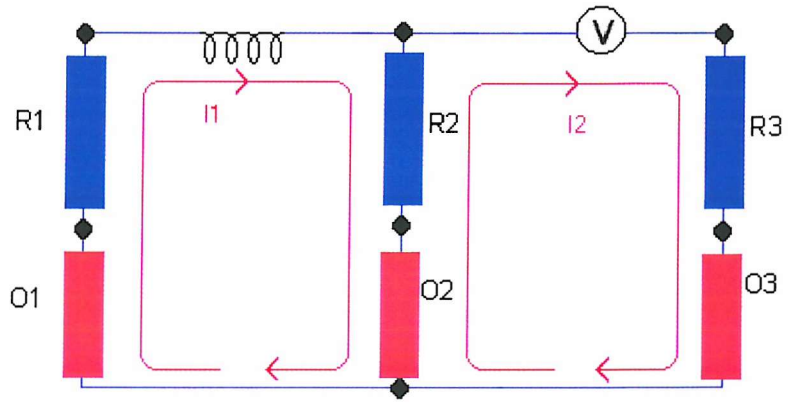

Figure 2.11 A circuit with more than one mesh loop

The components O_n are the conductors represented in a finite element model. It can be seen in figure 2.11 that R2 is in both mesh loop 1 and 2, whereas R1 and R3 are only in one circuit, this is represented in the matrix **Z** by

Term	Meaning
$\mathbf{Z}_{ii}$	Impedance in mesh loop i
$\mathbf{Z}_{ij}$	Impedance in mesh loop i and j

TABLE 2.2 Definition of the impedance matrix

The sign of $\mathbf{Z}_{ij}$ is given by as the sign of the current in the circuit loop$_i$; in figure 2.11 the sign of $\mathbf{Z}_{12}$ will be positive and the sign of $\mathbf{Z}_{21}$ will be negative. The matrix **L** of inductances is treated in a similar way.

It can also be seen in figure 2.11 that conductor O_2 is also in mesh loops 1 and 2. Matrix **M** describes the connectivity, thus

Term	Meaning
$M_{ij}=+1$	Conductor i is the right way in mesh j
$M_{ij}=-1$	Conductor i is the wrong way in mesh j
$M_{ij}=0$	Conductor i does not belong to mesh j

TABLE 2.3 Definition of the connectivity matrix

The meaning of the 'right way' for a conductor in a 2d XY model simply defines a sign convention:

- The direction of a mesh loop for a conductor is into the model and it is named a Go conductor

and the 'wrong way' is

- The direction of a mesh loop for a conductor is out of the model and it is named a Return conductor

Once the currents in the circuits have been calculated, the current density in a conductor is found from the current, the area and the **M** term. It is clear that the direction of a mesh loop is arbitrary and can be reversed without affecting the calculated current density in the conductor. In a normal circuit there will be as many Return as Go conductors, although if only part of a circuit is modelled and symmetry is exploited this may not be true in the insolated part that has been modelled. In a 2d XY model, when one conductor in a mesh loop has been assigned a direction, all of the other conductors are easily identified because a Go conductor is normally connected to a Return conductor.

2.8 Symmetry

In finite element analysis it is normal to try to reduce the number of elements which are required to model a system while retaining the same accuracy. One technique which has already been introduced is to exploit the symmetry of the fields and only model part of the system. The symmetry is implied by the choice of boundary conditions [12], by setting a normal

or tangential flux on the boundary which implies a positive or negative reflection. A more explicit way is to set a periodic condition on the boundary which defines a relationship between the potentials of two nodes $A_i=f(A_j)$. Typically positive ($A_i=A_j$) or negative ($A_i=-A_j$) periodicity is required. Periodic boundary conditions must be used if the flux on the boundary cannot be described as normal or tangential.

If a problem includes external circuits then the symmetry of the problem must also affect the circuit, see figure 2.12

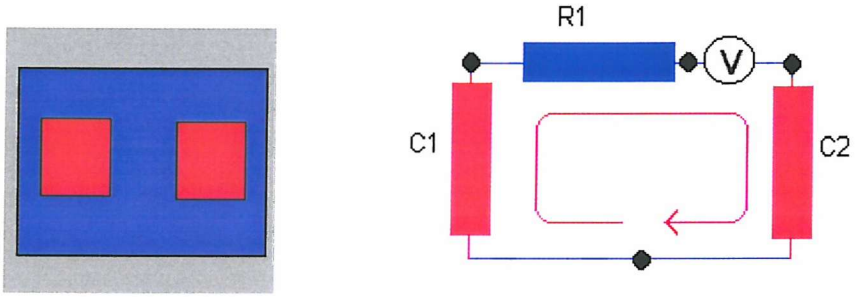

Figure 2.12 A full model and circuit

and the half model in figure 2.13.

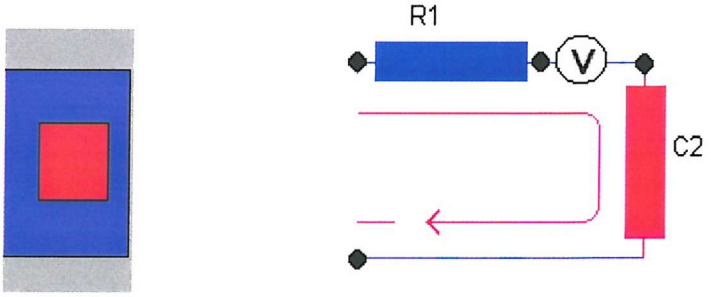

Figure 2.13 Half model and circuit

If the circuit in figure 2.13 is used for the half model it is clear that for the same voltage source the current will be greater than in figure 2.12 as the impedance circuit is lower. One option is to reduce the driving voltage and the external impedances by a factor of two to regain the same current. A simpler approach is to imply the missing component by increasing the effective length of the circuit *l*. This can be done by either the user or within a program by introducing a symmetry factor N_s so the length of a circuit l_s, which is used in the global matrix is

$$l_s = l^* N_s \tag{2.51}$$

where l is the length defined as by the user. The length is a property of a circuit and not of a model as it may be required to define circuits of different lengths within a model.

2.9 Summary

Equations have been developed which link electromagnetic fields and external circuit equations. The circuits are modelled as mesh loops and it has been shown how components can be present in more than one loop. It has been shown that introducing circuits does not remove the ability to exploit the symmetry of the magnetic fields to reduce the number of degrees of freedom of a problem.

3. Finite element method

3.1 Introduction

In this chapter the finite element method will be introduced and will be applied to the field equations developed in chapter 2. The 2d XY vector potential formulation will be fully developed, and the results of axi-symmetry and its associated potentials will be discussed. The equations which are developed will then be coupled to the circuit equations from chapter 2 to give a complete system of equations for both frequency and time domain solutions.

3.2 Nodal and edge finite elements

The finite element method is one approach that can be used to solve partial differential equations. The basic method provides a discrete framework that can be used to interpolate continuous functions characterised by the value of the function at a set of points (or nodes) in space. In the finite element method the points are connected by a contiguous mesh of elements. Within each element the variation of the function is typically described by a low order polynomial.

The traditional finite element approach based on nodal elements is not well adapted to the description of vector functions and in recent years methods of representing vector functions using edge elements have been developed. In these elements the vector fields are interpolated by local vector functions (again low order polynomials) associated with the edges joining the discretisation points.

It is a moot point whether the 2d discretisation of A_z is a nodal or edge method, but in practice for the 2d limit, the two approaches give exactly the same approximation.

3.3 Finite element discretisation

In two dimensions, the geometry is divided into elements, typically triangles as in figure 3.1.

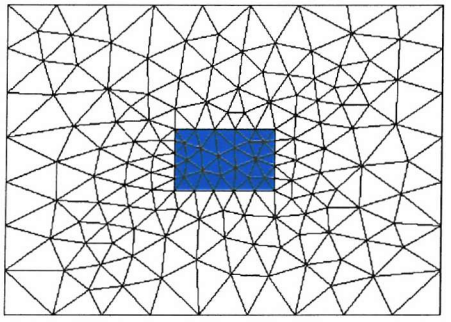

Figure 3.1 A model meshed with triangular elements

An approximate solution to the defining partial differential equation is calculated at the nodes on the discrete finite element representation of the model. Initial values on some of the nodes are known from either boundary conditions or from source current density.

For a single triangular element, using characteristic values at the nodes, the potential within the element is described as

$$\mathbf{A}(x) = \sum N_i(x)\mathbf{a}_i \tag{3.1}$$

where $\mathbf{A}$ is the potential in the element, $\mathbf{a}_i$ is the potential at node i (a trial parameter), and N_i is the local shape function [7]. The shape function, N_i, can be interpreted as the contribution of node i to the potential at a point in the element. In general shape functions can be defined so that

$$N_i(\mathbf{X}_i) = 1 \tag{3.2}$$

$$N_j(\mathbf{X}_j) = 0 \tag{3.3}$$

The shape functions for the nodes used in this work are either linear (first order) or quadratic (second order). It can be shown that the error in the discrete solution depends on the element size (h) and the order of the shape function polynomials. With first order elements

$$Error = O(h^2) \tag{3.4}$$

whereas with second order elements[7]

$$Error = O(h^3) \tag{3.5}$$

The disadvantage of using second order shape functions is that they increase the number of equations which need to be solved and so increase the solution time and memory requirements.

3.4 Forming the matrix contributions for the XY case

In order to solve the partial differential equation (PDE) the finite element approximation to the potential (equation 3.1) is substituted into the field equations. The vector form of Poisson's equation describes the magnetostatic fields, or the time varying fields when there are no eddy currents.

3.4.1 Matrix contributions for a conductor

The z directed vector potential in a 2d problem of a conductor with no eddy currents was described in equation 2.26 as

$$\nabla\times\frac{1}{\mu}\nabla\times\mathbf{A}_z = \mathbf{J}_0 \tag{3.6}$$

where $\mathbf{J}_0$ is the applied current density, which is uniform over the domain. Substituting in equation 3.1 yields

$$\nabla\times\frac{1}{\mu}\nabla\times\sum N_i\mathbf{a}_{zi} - \mathbf{J}_0 = 0 \tag{3.7}$$

The residual can be defined as

$$R = \left(\nabla\times\frac{1}{\mu}\nabla\times\sum N_i\mathbf{a}_{zi} - \mathbf{J}_0\right) = 0 \tag{3.8}$$

where in general, the residual $|R|$, only vanishes when $\mathbf{a}_i$ is an exact solution. This equation can only be solved exactly if it has C_1 continuity [7]. A alternative method [54] is to force the residual to be zero on average over the domain of the problem rather than over each element in the problem. This is expressed as

$$\int_{\Omega} \omega_i R d\Omega = 0 \tag{3.9}$$

where ω_i is a specially chosen function called a weighting function. The integral in equation 3.9 is over all space, however the shape functions N_i are only applicable over an element hence

$$\int_{\Omega} \omega_i R d\Omega \sim \sum_{n = 1, elems} \int_{elem} \omega_i R_n d\Omega \tag{3.10}$$

and the integral is now over the domain of each element.

If the number of weighting functions (ω_i)is chosen to be equal to the number of trial parameters ($\mathbf{a}_i$), a set of linear equations is obtained by substituting equation 3.8 into equation 3.10 thus

$$\sum_{n = 1. elems} \int_{\Omega} \omega_i \nabla \times \frac{1}{\mu} \nabla \times N_i d\Omega \mathbf{a}_{zi} = \sum_{n = 1. elems} \int_{elem} (\omega_i \mathbf{J}_0) d\Omega \tag{3.11}$$

This is simply a set of linear equations of the form

$$K_{ij} \mathbf{a}_{zi} = g_i \tag{3.12}$$

If the trial functions in equation 3.11 are chosen to be the same as the shape functions N_i then the method is called the Galerkin Method [55] i.e.

$$\sum_{n = 1. elems} \int_{elem} N_i \nabla \times \frac{1}{\mu} \nabla \times N_i d\Omega \mathbf{a}_{zi} = \sum_{n = 1. elems} \int_{elem} N_i \mathbf{J}_0 d\Omega \tag{3.13}$$

The shape functions N_i must be valid within each element as required by equation 3.10, but there has not been any requirement imposed on their validity when crossing the boundaries between elements. The shape functions which have been chosen are finite and continuous between elements but the derivatives are discontinuous and finite. The second derivatives are however discontinuous and infinite [39]. This level of continuity is referred to as C_0 [7] and imposes the restriction that the integrand in equation 3.13 cannot contain derivatives higher than the first derivative.

It can be seen that equation 3.13 does contain second derivatives, these can be removed by integrating by parts and applying a vector form of Greens function [56],

$$\int_\Omega \mathbf{F} \cdot \nabla \times \mathbf{G} d\Omega = \int_\Omega \mathbf{G} \cdot \nabla \times \mathbf{F} d\Omega - \int_\Gamma (\mathbf{F} \times \mathbf{G}) \cdot \mathbf{n} d\Gamma \tag{3.14}$$

In order to correctly interpret the surface term that has been introduced, we return to considering the integral over the whole domain before the local shape functions were introduced, rather than considering the problem on an element by element basis. Applying Green's function to the vector potential term in equation 3.9 gives

$$\int_\Omega \omega_j \cdot \nabla \times \frac{1}{\mu} \nabla \times \mathbf{A}_z d\Omega = \int_\Omega \frac{1}{\mu} \nabla \times \mathbf{A}_z \cdot \nabla \times \omega_j d\Omega - \int_\Gamma \omega_j \times \left(\frac{1}{\mu} \nabla \times \mathbf{A}_z \right) \cdot \mathbf{n} d\Gamma \tag{3.15}$$

which can be rearranged as

$$\int_\Omega \omega_j \cdot \nabla \times \frac{1}{\mu} \nabla \times \mathbf{A}_z d\Omega = \int_\Omega \nabla \times \omega_j \cdot \frac{1}{\mu} \nabla \times \mathbf{A}_z d\Omega - \int_\Gamma \omega_j \cdot \mathbf{H} \times \mathbf{n} d\Gamma \tag{3.16}$$

In equation 3.16 the continuity requirement on **A** has decreased, whereas the continuity requirement on ω_j has increased, and this equation is usually referred to as the weaker form of the original expression [7].

A surface term has been created which is related to the continuity of the tangential **H** field in equation 2.9. Continuity in the tangential **H** field therefore implies that this term will be cancelled when summing the two contributions from either side of an element. At the problem boundary this term is zero if the field is normal to the boundary (the default Neuman condition). For potential boundary conditions this term can be made to vanish be setting the weighting function ω_j to be zero at the boundary. Using this new form of this equation, equation 3.17 is written as

$$\sum_{n = 1.\, elems} \int_{elem} \nabla \times N_j \cdot \frac{1}{\mu} \nabla \times N_i d\Omega \mathbf{a}_{zi} = \sum_{n = 1.\, elems} \int_{elem} N_j \mathbf{J}_0 d\Omega \tag{3.17}$$

The terms in this equation are easily evaluated: in linear elements the shape function for node n is [39]

$$N_i = \frac{a_i + b_i x + c_i y}{2A_e} \tag{3.18}$$

where A_e is the area of the element. As the field in an XY model is only z directed, the curl is easily evaluated.

$$\nabla \times N_i = \mathbf{i}\frac{dN_i}{dx} - \mathbf{j}\frac{dN_i}{dx} = \frac{\mathbf{i}c_i - \mathbf{j}b_i}{2A_e} \tag{3.19}$$

In further examples, the equations will be kept in terms of the shape functions N_i as the equations are more compact. Equation 3.17 can be written in a matrix form as

$$[\mathbf{S}][\mathbf{A}] = [\mathbf{J}] \tag{3.20}$$

where for the matrix of S nodes

$$\mathbf{S}_{ij}(S \times S) = \int_\Omega \frac{1}{\mu} \nabla \times N_i \cdot \nabla \times N_j d\Omega \tag{3.21}$$

$$\mathbf{A} = N_j \mathbf{a}_j \tag{3.22}$$

$$\mathbf{J}_j(N) = \int_\Omega N_j \mathbf{J}_j d\Omega \tag{3.23}$$

3.4.2 Matrix contributions for conductors with eddy currents

The two equations which describe the field in conductors with eddy currents are equations 2.28 and 2.29, repeated here for clarity

$$\nabla \times \frac{1}{\mu} \nabla \times \mathbf{A} + \sigma \frac{\partial \mathbf{A}}{\partial t} = \mathbf{J}_s \tag{3.24}$$

$$\int_{\Omega k} \left(-\sigma \frac{\partial \mathbf{A}}{\partial t} + \mathbf{J}_s \right) d\Omega = \int_{\Omega k} \mathbf{J} d\Omega \tag{3.25}$$

The same Galerkin method as introduced in 3.4.1 can be used to discretise equation 3.24, where the only new quantity which has been introduced is the time dependence of the field. $\mathbf{J}_s$ is constant, therefore equation 3.25 is solved with unit weight (i.e. N=1) to give

$$\int_{\Omega k} -\frac{\partial \mathbf{A}}{\partial t} d\Omega + \int_{\Omega k} \frac{\mathbf{J}}{\sigma} d\Omega = \int_{\Omega k} \frac{\mathbf{J}_s}{\sigma} d\Omega \tag{3.26}$$

Using unit weight and dividing through by σ retains the symmetry which was present in the equations before they were coupled i.e.

$$\begin{bmatrix} [\mathbf{S}] & 0 \\ 0 & 0 \end{bmatrix} \begin{bmatrix} \mathbf{A} \\ \mathbf{F} \end{bmatrix} + \begin{bmatrix} -[\mathbf{G}] & -[\mathbf{P}]^T \\ -[\mathbf{P}] & [\mathbf{H}] \end{bmatrix} \begin{bmatrix} \frac{\partial \mathbf{A}}{\partial t} \\ \mathbf{J} \end{bmatrix} = \begin{bmatrix} \mathbf{J}_s \\ \frac{\mathbf{J}_s}{\sigma} \end{bmatrix} \tag{3.27}$$

where **S**, **A** and **J** have the same meaning as before and **F** is the time integral of **J**. Other new terms are

$$\mathbf{G}_{ij}(N \times N) = \sigma \int_{\Omega} N_i N_j d\Omega \tag{3.28}$$

$$\mathbf{P}_j(E) = \int_{\Omega} N_j d\Omega \tag{3.29}$$

$$\mathbf{H}_{jj}(E \times E) = \int_{\Omega} \mathbf{J}_j d\Omega \tag{3.30}$$

where **P** is a vector and **H** is a diagonal matrix. The terms **P** and **H** are only included if an eddy current conductor has its return path within the domain of the model. There are E eddy current conductors of this type. The eddy current conductors may consist of more than one isolated domain and there is just one equation per eddy conductor not one equation per conducting domain.

This formulation does not yield the current density as solution vector, only the time integral of the current density. In order to get the current density, **F** must be numerically differentiated to get **J** and added to the applied current density $\mathbf{J}_S$.

3.4.3 Matrix equations for massive conductors in circuits

The three governing equations for massive conductors and circuits which were introduced in chapter 2 are

$$\nabla \times \frac{1}{\mu} \nabla \times \mathbf{A} + \sigma \frac{\partial \mathbf{A}}{\partial t} - \frac{\sigma \Delta V}{l} = 0 \tag{3.31}$$

$$\Delta V_k = R_k I_k + R_k \int_{\Omega k} \sigma \frac{\partial \mathbf{A}}{\partial t} d\Omega_k \tag{3.32}$$

$$[\mathbf{M}][\Delta \mathbf{V}_k] + [\mathbf{Z}_m][\mathbf{I}]_m + [\mathbf{L}_m]\frac{d\mathbf{I}_m}{dt} = [\mathbf{E}_m] \tag{3.33}$$

The Galerkin procedure applied to equation 3.31 and 3.32 produces the two element based equations:

$$\sum \int_{elem} \frac{1}{\mu} \nabla \times N_j \cdot \nabla \times N_i d\Omega \mathbf{a}_{zi} - \sum \int_{elem} \sigma N_j \frac{\sigma \Delta V}{l} d\Omega \frac{d\mathbf{a}_{zi}}{dt} - \sum \int_{elem} N_j \frac{\sigma}{l} d\Omega = 0 \tag{3.34}$$

$$\sum \int_{\Omega k} \sigma N_i d\Omega \Delta V_k - \sum \int_{\Omega k} \sigma N_i d\Omega \frac{d\mathbf{a}_{zi}}{dt} - R_k I_k = 0 \tag{3.35}$$

which are summations over all the elements in the massive conductors. A final set of equations is produced which is nearly symmetric by dividing equation 3.32 and equation 3.33 by the length of conductor, hence.

$$\begin{bmatrix} [\mathbf{S}] & -\frac{[\mathbf{C}]}{l} & 0 \\ 0 & \frac{[\mathbf{R}^{-1}]}{l} & -\frac{[\mathbf{D}]}{l} \\ 0 & \frac{-[\mathbf{D}]^T}{l} & -\frac{[\mathbf{Z}]}{l} \end{bmatrix} \begin{bmatrix} \mathbf{A} \\ \nabla \mathbf{V} \\ \mathbf{I} \end{bmatrix} + \begin{bmatrix} [-\mathbf{G}] & 0 & 0 \\ -\frac{[\mathbf{C}]^T}{l} & 0 & 0 \\ 0 & 0 & -\frac{[\mathbf{L}]}{l} \end{bmatrix} \frac{\partial}{\partial t} \begin{bmatrix} \mathbf{A} \\ \nabla \mathbf{V} \\ \mathbf{I} \end{bmatrix} = \begin{bmatrix} 0 \\ 0 \\ -\frac{[\mathbf{E}]}{l} \end{bmatrix} \tag{3.36}$$

Where **C** is defined as

$$\mathbf{C}_{ij}(K \times S) = \int_c \sigma \nabla N_i dS \tag{3.37}$$

K is the number of massive circuit conductors and **D** is a vector length K which describes which conductor is in which circuit and whether these conductors are the 'go' or 'return' sections (previously referred to in a general way as **M**). This matrix equation is not yet symmetrical, but will be made symmetric later when a solution scheme is considered.

3.4.4 Matrix equations for filamentary conductors in circuits

The three equations which were developed for this system in chapter 2 were

$$\nabla\times\frac{1}{\mu}\nabla\times\mathbf{A} = \frac{I}{S_j} \tag{3.38}$$

$$\Delta V_k = Nl\Re_j I_k + \frac{lN}{S_k}\int_{\Omega k}\frac{\partial \mathbf{A}}{\partial t}d\Omega_k \tag{3.39}$$

$$[\mathbf{M}'][\Delta \mathbf{V}_k] + [\mathbf{Z}_m][\mathbf{I}]_m + [\mathbf{L}_m]\frac{d\mathbf{I}_m}{dt} = [\mathbf{E}_m] \tag{3.40}$$

The potential drop ΔV_k can be eliminated by substituting equation 3.39 into equation 3.40.

The Galerkin procedure is used on the resulting two equations to give summations over the elements in the filamentary conductors thus

$$\sum\int_\Omega \nabla\times N_j\cdot\frac{1}{\mu}\nabla\times N_i d\Omega \mathbf{a}_{zi} - [\mathbf{D}']^T\frac{lN}{S_k}\sum\int_\Omega d\Omega I_k = 0 \tag{3.41}$$

$$[\mathbf{D}']\frac{lN}{S_k}\sum\int_{\Omega k}\frac{\partial \mathbf{A}}{\partial t}d\Omega_k + (([\mathbf{Z}_m] + [\mathbf{D}']Nl\Re_k) + [\mathbf{I}_m]) + [\mathbf{L}_m]\frac{d\mathbf{I}_m}{dt} = [\mathbf{E}_m] \tag{3.42}$$

where $\mathbf{D}'$ is the vector which describes which circuit each filamentary conductor is in and whether it is the right or wrong way. If the circuit equation 3.42 is multiplied by -1 then the final system of equations is almost symmetric, thus:

$$\begin{bmatrix} [\mathbf{G}] & -[\mathbf{D}']^T[\mathbf{C}'] \\ 0 & -\frac{[\mathbf{Z}']}{l} \end{bmatrix}\begin{bmatrix}\mathbf{A}\\ \mathbf{I}\end{bmatrix} + \begin{bmatrix} 0 & 0 \\ -[\mathbf{D}'][\mathbf{C}']^T & \frac{-[\mathbf{L}]}{l} \end{bmatrix}\frac{d}{dt}\begin{bmatrix}\mathbf{A}\\ \mathbf{I}\end{bmatrix} = \begin{bmatrix} 0 \\ -\frac{[\mathbf{E}]}{l}\end{bmatrix} \tag{3.43}$$

where

$$\mathbf{C}' = \frac{N}{S_k}\int_\Omega d\Omega \tag{3.44}$$

$$\mathbf{Z}' = \mathbf{Z} + Nl\Re_k \tag{3.45}$$

One of the degrees of freedom was eliminated to obtain the final matrix. This has the advantage that there is no longer a term for the resistance of an individual conductor - the resistance of all the conductors are lumped together in the in $\mathbf{Z}'$ term. This flexibility allows an easier interface to the software as the total measured resistance of a circuit can be entered rather than having to define the resistance for each conductor. The interface developed in the software still allows the user to define the resistance of each winding, but sums them together into the $\mathbf{Z}'$ term.

3.4.5 Full matrix

All the contributions from all the conductors in eddy current circuits, filamentary circuits and ones which are short circuited can be combined into one large system of equations thus

$$\begin{bmatrix} [\mathbf{S}] & 0 & \frac{-[\mathbf{C}]}{l} & -[\mathbf{C}'][\mathbf{D}'] \\ 0 & 0 & 0 & 0 \\ 0 & 0 & \frac{[\mathbf{R}^{-1}]}{l} & \frac{-[\mathbf{D}]^T}{l} \\ 0 & 0 & -\frac{[\mathbf{D}]}{l} & \frac{[\mathbf{Z}]}{l} \end{bmatrix} \begin{bmatrix} \mathbf{A} \\ \mathbf{F} \\ \nabla\mathbf{V} \\ \mathbf{I} \end{bmatrix} + \begin{bmatrix} -[\mathbf{G}] & [\mathbf{P}]^T & 0 & 0 \\ [\mathbf{P}] & [\mathbf{H}] & 0 & 0 \\ \frac{-[\mathbf{C}]^T}{l} & & 0 & 0 \\ -\frac{[\mathbf{D}'][\mathbf{C}']^T}{l} & 0 & 0 & \frac{[\mathbf{L}]}{l} \end{bmatrix} \frac{d}{dt} \begin{bmatrix} \mathbf{A} \\ \mathbf{F} \\ \nabla\mathbf{V} \\ \mathbf{I} \end{bmatrix} = \begin{bmatrix} \mathbf{J}_s \\ \frac{\mathbf{J}_s}{\sigma} \\ 0 \\ -\frac{[\mathbf{E}]}{l} \end{bmatrix} \tag{3.46}$$

Even though this final system is not symmetric, it can be made to be symmetric when the equations are solved. Before considering solution strategies the other 2d case, axi-symmetry, will be introduced.

3.5 The axi-symmetric case

The equivalent rotationally symmetric system to the XY system that has been described, will have only R and Z components of field, which can be represented by a vector potential with only an azimuthal component. Using a one component vector potential

$$B_r = \frac{dA_\phi}{dz} \quad \text{and} \quad B_z = -\frac{1}{r}\frac{d}{dr}(rA_\phi) \tag{3.47}$$

The equations that were developed in section 3.4 for the XY case can be developed for the vector potential A_ϕ by using the cylindrical polar version of the curl operator. One difference in the formulation is that the length of the circuit l is not an independent variable but is simply $2\pi r$.

When examining the matrix terms and considering the equation 3.47 it is noticed that rather than solving for A_ϕ it is more natural to solve for the magnetic flux Φ [39], where

$$\Phi = rA_\phi \tag{3.48}$$

One problem which is encountered when using both these potential types is that there is a singularity at r=0, as some of the matrix terms contain r as a denominator. However the integrals are finite and the vector potential must be zero on axis. The integrals can be evaluated by numerical quadrature providing points on axis are avoided. When recovering the fields on the z axis it can be seen from equation 3.47 does not define B_z at r=0 and other techniques are used to recover the field.

For some geometries the solution varies as ln(r) close to r=0. In these cases convergence of the A and rA formulations is poor. The problem can be avoided by solving in a transformed space [66] i.e.

$$\Phi = rA_\phi \quad \text{and} \quad r^2 = s \tag{3.49}$$

Now that the matrix equations have been defined, the next two sections show how they are implemented in frequency domain and time transient solutions.

3.6 Frequency domain solutions

A frequency domain solution is one where the field is varying in a time harmonic way. This can be represented in two dimensions as

$$\mathbf{A} = \mathbf{A}^c \exp(j\omega t) \tag{3.50}$$

where $\mathbf{A}^c$ is a complex representation of $\mathbf{A}$ and ω is the angular frequency of the field. In a linear problem, all other field quantities will have similar relationships. The time derivative of the field can be seen to be

$$\frac{d\mathbf{A}}{dt} = j\omega \mathbf{A}^c \exp(j\omega t) = j\omega \mathbf{A} \tag{3.51}$$

This relationship can be substituted into equation 3.46 to give a single solvable matrix. Two rows in the matrix have been divided by ω to obtain symmetry yielding

$$\begin{bmatrix} [\mathbf{S}] - j\omega[\mathbf{G}] & j\omega[\mathbf{P}]^T & \frac{-[\mathbf{C}]}{l} & -[\mathbf{C}'][\mathbf{D}'] \\ j\omega[\mathbf{P}] & \omega[\mathbf{H}] & 0 & 0 \\ \frac{-[\mathbf{C}]^T}{l} & 0 & \frac{[\mathbf{R}^{-1}]}{j\omega l} & \frac{-[\mathbf{D}]^T}{j\omega l} \\ -\frac{[\mathbf{D}'][\mathbf{C}']^T}{l} & 0 & -\frac{[\mathbf{D}]}{j\omega l} & -\frac{[\mathbf{Z}]}{j\omega l} - \frac{[\mathbf{L}]}{l} \end{bmatrix} \begin{bmatrix} \mathbf{A} \\ \mathbf{F} \\ \nabla \mathbf{V} \\ \mathbf{I} \end{bmatrix} = \begin{bmatrix} \mathbf{J}_s \\ \frac{\mathbf{J}_s}{\sigma} \\ 0 \\ -\frac{[\mathbf{E}]}{j\omega l} \end{bmatrix} \tag{3.52}$$

Examining this final matrix, it is now clear what conditions must hold to provide a solution. The massive conductors in the circuits must have a non zero resistance whereas the circuits involving filamentary conductors must have some impedance in their circuits. If either of these conditions are not met the matrix will have a zero on the diagonal and be singular. Another consideration is that the frequency must not be zero or the resistance terms will be infinite and the diagonal term for the short-circuited conductors will be zero. If a zero frequency solution is required, the currents in the circuit equations can be calculated independently. The calculated currents can then be entered as specified current densities.

Equation 3.52 has complex coefficients and will have a complex solution. A complex conjugate gradient method with an incomplete Cholesky preconditioning [63] (CICCG) has proved reliable after scaling the contributions. It is necessary to scale, or normalise, the contributions as they are very different in magnitude because they represent different physical quantities. Scaling is performed by multiplying out the rows and columns so that the magnitude of the diagonals is 1. Symmetry can be retained by operating on the columns as well as the rows. Other preconditioners, such as the Quasi-Minimal-Residual (QMR) system, have been reported to be very effective in reducing the time taken to solve the matrix equations [64]. Very recent work on algabraic multigrid methods [65], which have been adapted to cope with dense blocks in sparse matrices, are reported to be good preconditioners for a wide variety of problems.

The effect of capacitors in the circuit equations has been neglected until now in the formulation of the final frequency domain matrix. Let us consider the impedance of a capacitor and the impedance of an inductor in an AC circuit,

$$Z_L = j\omega L \quad \text{and} \quad Z_C = \frac{1}{j\omega C} \tag{3.53}$$

where Z_L and Z_C are the impedances of an inductor and capacitor respectively. It is clear by inspecting 3.52 equation that it is only the impedance of the device which is needed. An extra term can be added to the impedance terms in the matrix to include the impedance of a capacitor such that the total impedance term after symmetry-retaining operations is

$$\mathbf{Z}' = -\frac{[\mathbf{Z}]}{j\omega l} - \frac{[\mathbf{L}]}{l} + \frac{[\mathbf{C}^{-1}]}{l\omega^2} \tag{3.54}$$

The simple time harmonic substitution used in equation 3.50 assumes that the material characteristics are constant and do not therefore vary with time, flux density or current. Non-linear magnetic properties, where μ is dependant on the field, are likely to have some effect in a real application. The effect can be seen in a real application when a perfect sinusoidal voltage is applied. The currents generated will contain higher order harmonics of the fundamental frequency as well as the fundamental.

A first order approximation for non-linear permeability is to use average permeability, but this is still restricted to only looking at the fundamental frequency. Higher order harmonics can be calculated at the expense of solving larger systems of equations [67].

3.7 Transient solutions

3.7.1 Models requiring transient solutions

The time harmonic solution is not always adequate to model eddy current problems. There are many classes of problems which require a full transient solution where a solution is evaluated as a function of time. Problems which need transient solutions usually involve one or more of the following:

- Drives which are not time harmonic

- Capacitive discharge.
- Motion
- Non-linear materials
- Permanent magnets

Non time harmonic drives can be used to model the energising of a circuit (switch on) as well as a fault condition (switch off). Capacitive discharge can be modelled [58] by placing a charge on a capacitor when conventional drives are not present. When a problem includes motion, the matrix contributions for the elements in the air gap between the moving and stationary parts must be recalculated for each position [60]. A time transient solution is therefore required for each position. In order to fully model the non-linear magnetic behaviour of permeable regions including permanent magnets, the transient solver is used to recalculate the permeability from the field as a function of time.

3.7.2 A time marching scheme

The coupled electromagnetic and external circuit system described in equation 3.46 can be written compactly as

$$\mathbf{RX} + \mathbf{S}\frac{\partial \mathbf{X}}{\partial t} = \mathbf{B} \tag{3.55}$$

where **R** and **S** are matrices, **X** is the vector of unknowns and **B** is the vector of 'right hand sides'. This equation is solved by dividing the time into finite domains and performing a calculation to progress the solution through time starting with some initial condition. The right hand sides are recalculated at each time step. The time domain can be discretised using a weighted residual approach [7] giving a time discretised form of equation 3.55 as

$$\left[\mathbf{R}\theta - \frac{\mathbf{S}}{\delta t}\right]\mathbf{x}_{n+1} = -\left[\mathbf{R}(1-\theta) - \frac{\mathbf{S}}{\delta t}\right]\mathbf{x}_n - \mathbf{b}_n + (1-\theta) + \mathbf{b}_n\theta \tag{3.56}$$

where $\mathbf{x}_n$ is the matrix for step n, $\mathbf{b}_n$ is the right hand side term for step n and θ is a factor between 0 and 1. This approach is immediately extendable to adaptive time integration. The solution at time $t+\delta t$ can be compared with different sizes of time steps and since the accuracy should vary as $O(\delta t^2)$ the expected accuracy can be calculated.

The choice of the factor θ changes equations 3.56 to be similar to other well known schemes, shown in table 3.1.

θ	**Scheme**
0	Euler (explicit)
1/2	Crank-Nicholson
2/3	Central Difference
1	Backward difference (fully implicit)

TABLE 3.1 Different theta schemes.

When time marching just the electromagnetic equations it is found that the Crank-Nicholson scheme is stable, but when coupling to the circuit equations, θ must be at least 0.5 as the Crank-Nicholson scheme generates undamped or even divergent oscillations [60]. It has been found that θ=2/3 is reliable. When coupling to mechanical equations it is convenient to use θ=1 because this easily incorporates changes to the mesh and equation system during the time marching.

Equation 3.56 can only be solved if an external impedance is present in filamentary circuits, and conductors in eddy current circuits have non zero resistances. The external impedance terms, which form the diagonal elements in the matrix, are negative so a complex linear algebra solver is used.

A time marching process must begin from specified initial conditions. The initial condition may have to be determined by first solving a static field, given calculated currents from the driving circuits.

3.7.3 Capacitors in the transient solution.

In the solution of a frequency domain problem it was shown that a capacitor could be treated in the same manner as inductors, i.e. as another impedance term in the circuit equations. However, in the transient solution the full transient behaviour of the capacitor must be modelled. From equation 2.48 the voltage drop across the plates of a capacitor can be written as

$$V_{n+1} = V_n + \int_{t1}^{t2} I dt \qquad (3.57)$$

where V_n is the voltage across the capacitor at time step n, t1 is the time at the start of step n and t2 the time at the end of step n. The voltage across the capacitor is used as a right hand side term. The matrix is solved for step n, between time t1 and t2, and the resulting current is used to calculate a new value of the voltage across the capacitor. The voltage drop V_0 across the capacitor must be known when the time marching scheme starts at t=0. If V_0 is non zero it may be used to drive the whole problem.

3.8 Discussion

In this chapter, three different sets of extra equations were formulated in addition to the field in a conducting region:

1. Eddy current conductors with the return path inside the model,
2. Massive conductors in a circuit
3. Filamentary conductors in a circuit.

If the equations for (1) and (2) are compared there can be seen a great deal of similarity. If we compare a single region of (1) with a circuit of type (2) which has no applied voltage and only contains one massive conductor, the extra equations are

$$\int_{\Omega k}\left(-\sigma\frac{\partial \mathbf{A}}{\partial t}+\mathbf{J}_s\right)d\Omega \;=\; \int_{\Omega k}\mathbf{J}\,d\Omega \tag{3.58}$$

and

$$\int_{\Omega k}-\sigma\frac{\partial \mathbf{A}}{\partial t}d\Omega - R_k I_k \;=\; \int_{\Omega k}\sigma\Delta V_k\,d\Omega \tag{3.59}$$

Its is now clear that the extra equation for (1) could have been written as

$$\int_{\Omega k}-\sigma\frac{\partial \mathbf{A}}{\partial t}d\Omega - \int_{\Omega k}\sigma\nabla V d\Omega \;=\; \int_{\Omega k}\sigma\nabla V_s\,d\Omega \tag{3.60}$$

where ∇V_s is the source term - $\mathbf{J}_s/\sigma$. The matrix of equations could have then be written as

$$\begin{bmatrix} \mathbf{S} & -[\mathbf{C}]^T \\ -[\mathbf{C}] & \mathbf{H} \end{bmatrix} \begin{bmatrix} \mathbf{A} \\ \sigma\nabla V \end{bmatrix} + \begin{bmatrix} [\mathbf{G}] & 0 \\ -[\mathbf{C}]^T & 0 \end{bmatrix} \frac{\partial}{\partial t} \begin{bmatrix} \mathbf{A} \\ \sigma\nabla V \end{bmatrix} = \begin{bmatrix} \mathbf{J}_s \\ -\sigma\nabla V_s \end{bmatrix} \tag{3.61}$$

This matrix equation is not symmetric, but can be made to be symmetric by applying row and column scaling as used for the circuit equations. These are more natural equations than the ones first proposed in [27] as the unknowns are **A** and $\sigma\nabla V$, which give directly -**J**, unlike equation 3.27 where **J** is recovered from the time derivative of **F**. If we go one stage further and add an imaginary circuit equation for this isolated conductor we get

$$\begin{bmatrix} [\mathbf{S}] & -[\mathbf{C}] & 0 \\ 0 & [\mathbf{R}^{-1}] & -[\mathbf{D}] \\ 0 & -[\mathbf{D}]^T & -\mathbf{Z} \end{bmatrix} \begin{bmatrix} \mathbf{A} \\ \nabla V \\ \mathbf{I} \end{bmatrix} + \begin{bmatrix} [\mathbf{G}] & 0 & 0 \\ -[\mathbf{C}]^T & 0 & 0 \\ 0 & 0 & 0 \end{bmatrix} \frac{\partial}{\partial t} \begin{bmatrix} \mathbf{A} \\ \nabla V \\ \mathbf{I} \end{bmatrix} = \begin{bmatrix} 0 \\ 0 \\ -\nabla V_s \end{bmatrix} \tag{3.62}$$

where **R** is a diagonal matrix of the resistances of all conductors, **Z** is the sum of the resistances of all the conducting regions which make up the conductor and **D** is a diagonal matrix of 1's. This matrix can be now directly compared to equation 3.36 and it is seen to be identical for a unit problem length. There is no great advantage in using this formulation in 3.62, but it shows that the two types of conductors can be treated in the same way. The advantage of using equation 3.61 over 3.27 is that there is no need to introduce the time integral of **J**.

3.9 Conclusion

The equations which describe coupled finite element and external circuit analysis have been fully formulated for the frequency domain and time transient systems. A time stepping procedure has been outlined which uses adaptive time stepping able to control the time stepping errors. It has been noted that special attention is required at the start of the time stepping process to prevent large transients. Restrictions of the external circuits, i.e. an external impedance being required, have been investigated by examining the final system of equations.

These methods were implemented in the Opera-2d software. The next chapter describes the implementation.

4. Defining the external circuit

4.1 Overview

Coupling between finite elements and circuits was implemented in the Opera-2d software. The combined Pre and Post-processor was extended to allow the definition, editing and listing of external circuit mesh loops.

Two different ways have been developed to enter the definition of a circuit. The most natural definition for the software is for the user to enter a mesh loop as a list of resistors, inductors, capacitors and finite element conductors. For more complex circuits, where components appear in more than one mesh loop, it may be non trivial to identify the independent mesh loops. The alternative technique to enter the definition of the circuits is to simply identify each component and to which circuit nodes it is connected. This definition can then be converted to the mesh loop format by an automated procedure.

4.2 Defining the mesh loops.

In order to identify a finite element conductor which is to be used within an external circuit it is given a label, the 'conductor number'. One or more regions may be assigned the same conductor number. Assigning the same conductor number to many regions implies that they are joined at the ends of the model. The conductor numbers are also used to define the regions which are eddy current conductors and have the return path of the current within the conductor. The main menu for the external circuits is shown in figure 4.1

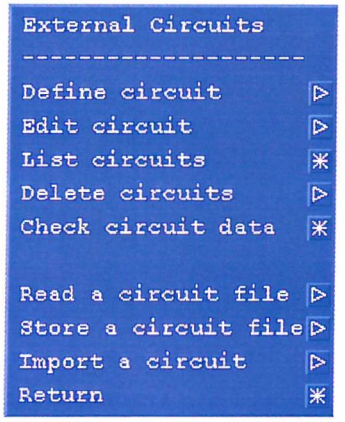

Figure 4.1 Main circuit menu

The definition of each mesh loop is divided into two sections.The first one describes the global circuit parameters such as the external resistance, inductance and capacitance and the second section defines the characteristic of each conductor. Figure 4.2 shows the entry dialogue for the global parameters.

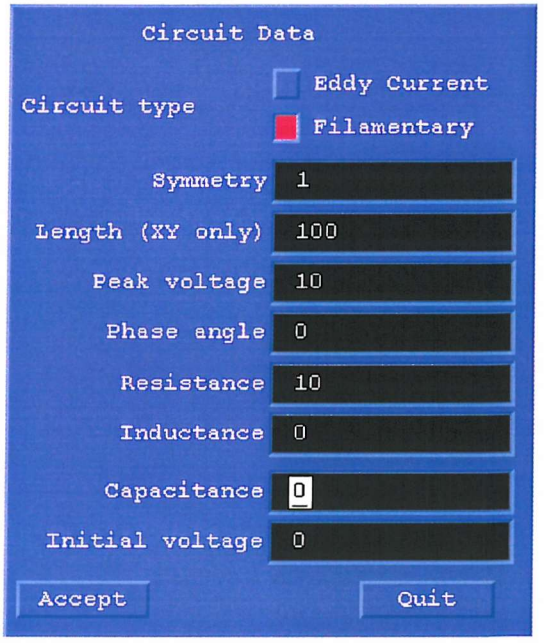

Figure 4.2 Global circuit parameters

It can be seen that the user must select whether the circuit is based on eddy current (massive) conductors or on filamentary conductors. This is required so that the circuit equations can be set up correctly and the circuit data checked. One example is that the eddy current circuits require an external impedance. If there is more than one resistor, capacitor or inductor in the circuit, these must be summed by the user and only the total value entered. The resistance and inductance fields are also used to describe the internal impedances of the voltage source if necessary.

In order to correcly define each mesh loop, the current is considerd to flow in one prescribed direction. If the current in the conductor provides a positive potential drop along the conductor, the 'sense' of the conductor is 'go' if the potential drop is negative the sense is 'return'. If the current direction is reversed, the sign of the calculated current is also reversed. The application of the 'sense' of conductors in a mesh loop is equivalent to applying positive and negative current density in a current driven model.

When the global parameters have been specified, the individual conductor must be added to the circuit. In an eddy current circuit, only the conductor sense must be specified (whether it is a go or return conductor), i.e. figure 4.3.

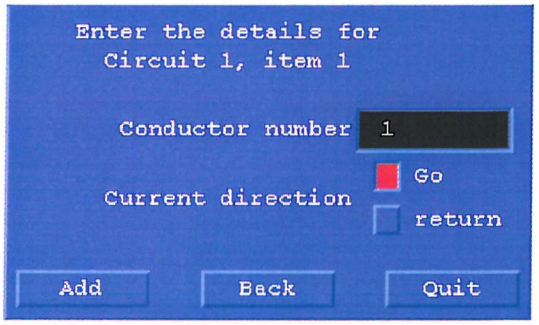

Figure 4.3 Eddy current conductor parameters

For a filamentary conductor the number of turns and the resistance per unit length of the wire must also be described. If the resistance of the wires is combined into the global resistance, the resistance per unit length can be set to be 0. The definition of a filamentary conductor is shown in figure 4.4.

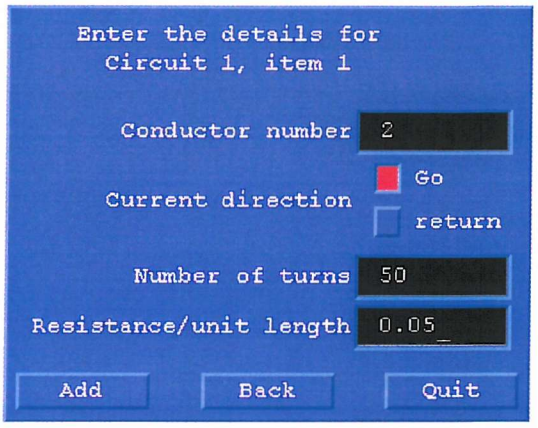

Figure 4.4 Filamentary conductor parameters

Once more than one circuit has been defined, the edit menu can be selected to add the components which appear in more than one circuit, the 'shared' components (figure 4.5).

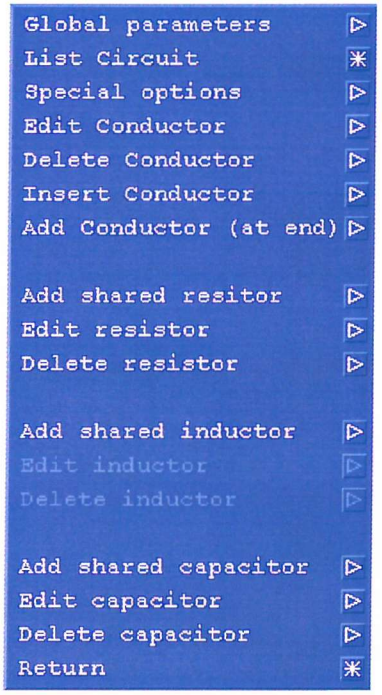

Figure 4.5 The edit menu

The edit menu also allows any other parameter in the circuit to be modified and conductors to be added, inserted or removed from the circuit.

The main circuit menu also allows circuits to be saved or loaded to a file so that different finite element models can use the same circuits.

4.3 SPICE like circuits

The mesh loop entry technique provides an easy to use interface allowing the user to input circuits into the software, but it requires the user to analyse the circuits and identify independent mesh loops. A more natural way to describe a circuit is to define the connections between the nodes of the circuit. There are many circuit analysis tools which can take a nodal data file as input and analyse the behaviour of the circuit. Many of these tools are based on Berkely labs SPICE, although the commercial packages far exceed the capabilities of the original 'freeware' program. The format of the input data files for SPICE are a very simple and convenient way to describe our circuits and they form the basis of the second circuit entry technique.

4.3.1 Format of the SPICE like file

The SPICE like file contains many lines of descriptions. Each line describes a component and its connection to its neighbouring nodes. A general line is written thus

XN i j Pe

where X is the component type, N the number of the component, i and j are the two nodes that are joined by the component. P is the value of the component and e is the exponent of the value. An example is

R1 3 4 10k

This describes a 10k ohm resistor between node 3 and 4 which has the label R1. The types of components currently decoded are shown in table 4.1

Component	Label
Resistor	R
Inductor	L
Voltage Source	V
Capacitor	C
OPERA Conductor	O

TABLE 4.1 SPICE like circuit components

where the OPERA conductor value is the conductor number. An OPERA conductor number is a label applied by a user to identify a conductor in a model. There are some properties of the circuit which cannot be described using normal SPICE notation. These are embedded in comment lines, which start with a * and affect the circuit properties from that line onward;, examples are shown in table 4.2.

Comment line	Meaning
LEN	Circuit length
SYMMETRY	Circuit symmetry
TYPE	Circuit type (filamentary or eddy)
SENSE	Conductor sense
PHASEANGLE	Phase angle of an AC drive
TURNSPERCOIL	Turns of a filamentary conductor
RESISTPERLEN	Resistance per unit length of a filamentary conductor
INITIALVOLTAGE	Initial voltage of a capacitor in transient analysis

TABLE 4.2 Additional circuit parameters using comments

Most of the comment factors need to be described only once per file, even if the file describes many circuits. The sense parameter can be defined for each independent circuit, so that the current direction upon analysis appears in the expected direction. The sense of other conductors in a circuit is calculated automatically because adjacent OPERA conductors in a mesh loop must have opposite senses.

An example of a circuit and its SPICE like representation is presented in figures 4.6 and table 4.3.

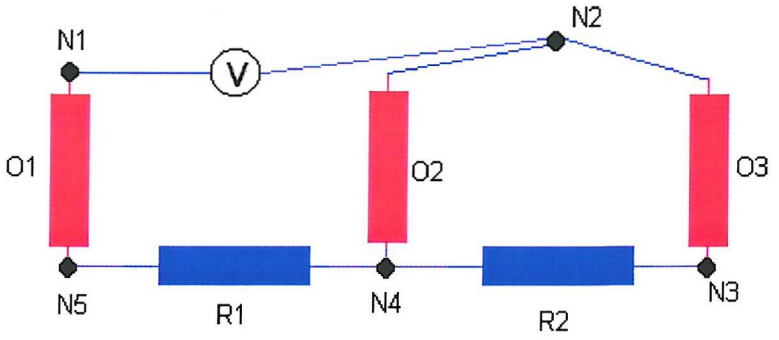

Figure 4.6 An example circuit

* TYPE EDDY
* LEN 1
SENSE GO
V1 1 2 10
O2 2 4
O1 5 1
O3 2 3
R1 3 4 2k
R2 4 5 2k

TABLE 4.3 An example SPICE type file

4.3.2 Creating mesh loops from SPICE like files

In order to convert the nodal SPICE like file into mesh loops two processes are needed:

1. A text interpreter to break the lines down into meaningful components
2. An analyser to convert a nodal description to a loop description.

The text interpreter is a straightforward program which splits up each line into tokens which are then loaded into compound arrays. In order to obtain loops from a nodal analysis, simple graph theory is used to break the nodal connections into a 'spanning tree'. A tree is a collection

of branches (lines joining the vertices of a graph) which do not connect to each other and form closed loops. A spanning tree is a tree which contains all the vertices of the original graph.

In order to describe the spanning tree of a circuit, consider the graph of the circuit in figure 4.6, where each component has been replaced by a line, and connecting wires have been removed.

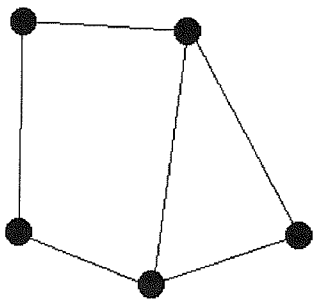

Figure 4.7 Graph of circuit

There are many spanning trees for the graph in figure 4.7, two examples are shown in figure 4.8

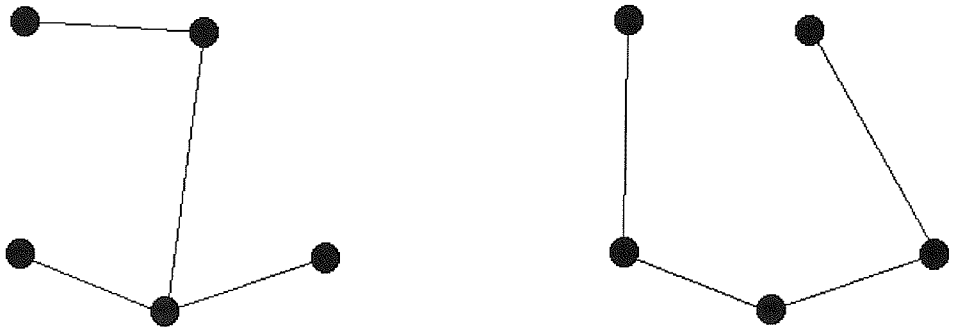

Figure 4.8 Two spanning trees from the same graph

The co-trees, which are the gaps between the nodes, define each independent loop. To obtain the loop, a co-tree is closed and then a loop can use the branches which define a closed

loop. The loops from the first of the spanning trees in figure 4.8 can be drawn as shown in figure 4.9

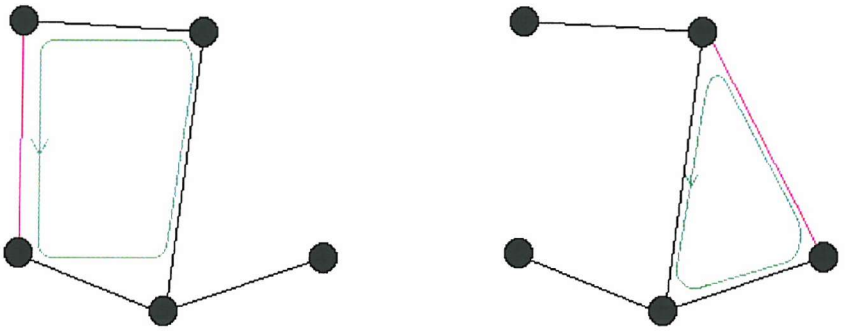

Figure 4.9 The two loops formed from the spanning tree

The direction of the arrows in the loops are not important. Choosing the opposite direction for the mesh loop will produce an equal and opposite current in the circuit. The sense of each loop is defined by the connection between the first and second nodes identified in the loop.

There are many ways to find the spanning tree of a graph, the simple technique employed here is

1. Pick a starting node A,
2. Find an adjacent node B, and mark it as visited, mark the edge A-B as visited.
3. Move to another adjacent node C, unless it has been visited before
4. If a node C has been visited before, find an unvisited node D and start at 1.
5. Continue process until all nodes have been defined.

The loops are identified by,

1. Scan the edge list an unvisited edge E-F (a co-tree)
2. find the shortest path between node E and F (which is not the co-tree), this is a loop.
3. Mark the edge E-F visited
4. Go back to step 1, until there are no longer any unvisited edges.

Once all the loops have been identified, the impedance components (resistors, inductor and capacitors) are placed back in the loops. The impedance which is not shared with other loops is summed to be the external impedance. The loops are then compared to find the total impedance and these are entered into a matrix of impedances. Conductors are identified which are shared with another loop. The final step is to place the conductors in the loops. Unless flagged otherwise it is assumed that adjacent conductors have the opposite sense.

4.3.3 Problems identifying the spanning tree and loops

It is possible that a SPICE file supplied by a user may not correctly define a set of mesh loops. The spanning tree generated from the graph analysis of a SPICE file is checked to see if mesh loops can be formed. These checks include identifying

1. Incomplete loops, where components are not part of a closed loop
2. Nodes connected to themselves without components
3. Impedance components are in a parallel circuits

The first two conditions may indicate an error in the input from a user and a warning is issued. The last condition occurs very often in circuits and causes a problem in the loop generation algorithm as the circuit is stored in a compressed node-node matrix. This matrix can only contain one entry for each pair of nodes A and B. To overcome this limitation a 'virtual impedance' or a zero resistance piece of wire is inserted in one of the loops. The original components now have connectivity A-B and A-C-B.

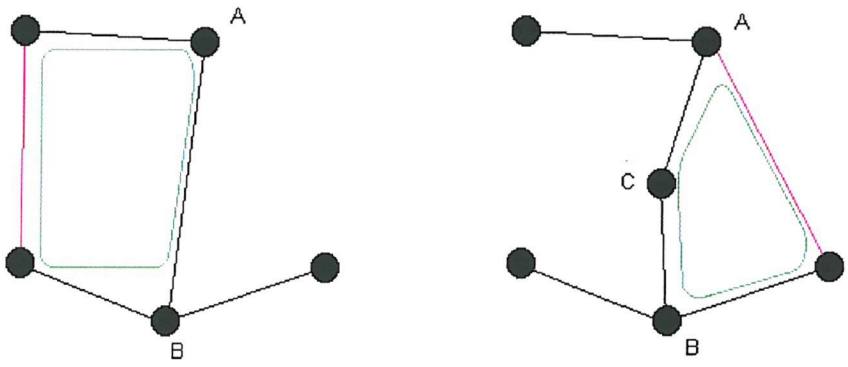

Figure 4.10 Insertion of a zero impedance wire into a loop

When the final loops are checked for shared impedances, both loops are still identified as containing the same components.

4.4 Discussion

In this chapter two techniques have been presented which allow a user to enter the data associated with external voltage driven circuits. The first technique involves the user identifying the mesh loops in a circuit and using the graphical user interface (GUI) to enter the components. The second technique involves the user listing the connectivity of a circuit in a SPICE type file, describing the nodes in a circuit and the components in them. The analysis of the SPICE type file produces mesh loops automatically. The first technique requires very little data handling by the program, whereas the SPICE type file analysis requires a lot of calculations. These are however so fast that the user is not aware that a process is happening.

The mesh loop entry technique is best suited to small simple circuits, whereas the SPICE type file allows complicated arrangements to be entered with less chance of data entry error.

There is a limitation with the SPICE type file entry technique: currently if a circuit is created which does not contain a conductor, the circuit is invalid. If a circuit without any conductors is created, the graph analysis can be restarted with a different starting node. Restarting the analysis may produce a different spanning tree where the loops which are produced contain conductors. A circuit without any conductors is valid in circuit analysis, it is just a limitation of the implementation in Opera-2d which requires that each loop contains a conductor. The routines which build the finite element matrix contributions have been written expecting all circuits to contain a conductor and if there are no conductors present the circuit does not get entered into the matrix.

5. Results

5.1 Introduction

In this chapter, a range of results will be presented which demonstrate both the accuracy and the flexibility of the algorithm which has been used to couple external circuits to finite element analysis.

The first case considered is a simple circuit using filamentary conductors which will be compared to analytical results. Secondly, a circuit involving massive conductors will be compared to known solutions of disconnected connectors. An analytical example will then be presented which contains more than one circuit, where the mutual inductance between the two circuits will be taken into account. The chapter will conclude with a motor manufacturer's model of an induction motor. The model contains circuits which contain both massive and filamentary conductors.

5.2 Circuits with filamentary conductors

5.2.1 Time harmonic analysis of a finite element model for a single circuit

A simple model is proposed in order to compare computed results with analytical results. A straightforward finite element model is one which does not contain

- Eddy currents
- Inhomogenous magnetic materials
- Symmetry

The model in figure 5.1 is such a model and represents the cross section through a long filamentary coil. The coil is surrounded by free space.

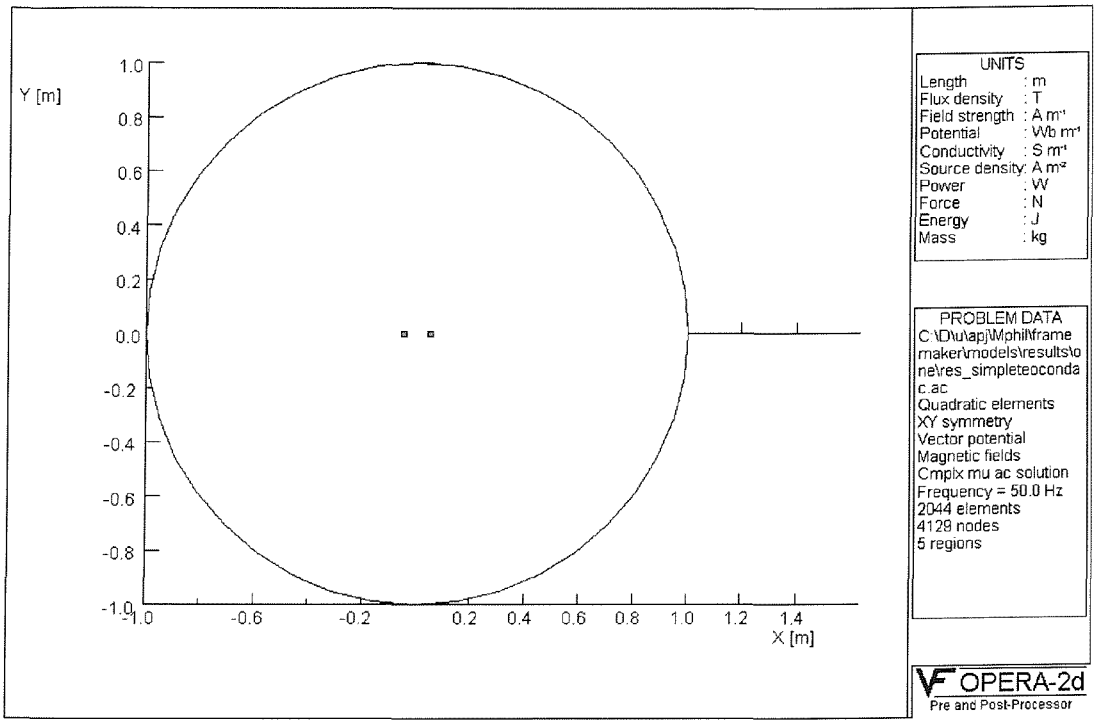

Figure 5.1 Two infinitely long filamentary conductor

The model information on the right hand side of the picture shows the total number of elements and nodes in the model and that the model is to be solved with second order shape functions (quadratic elements). The detail of the finite element mesh in and around the conductors can be seen in figure 5.2

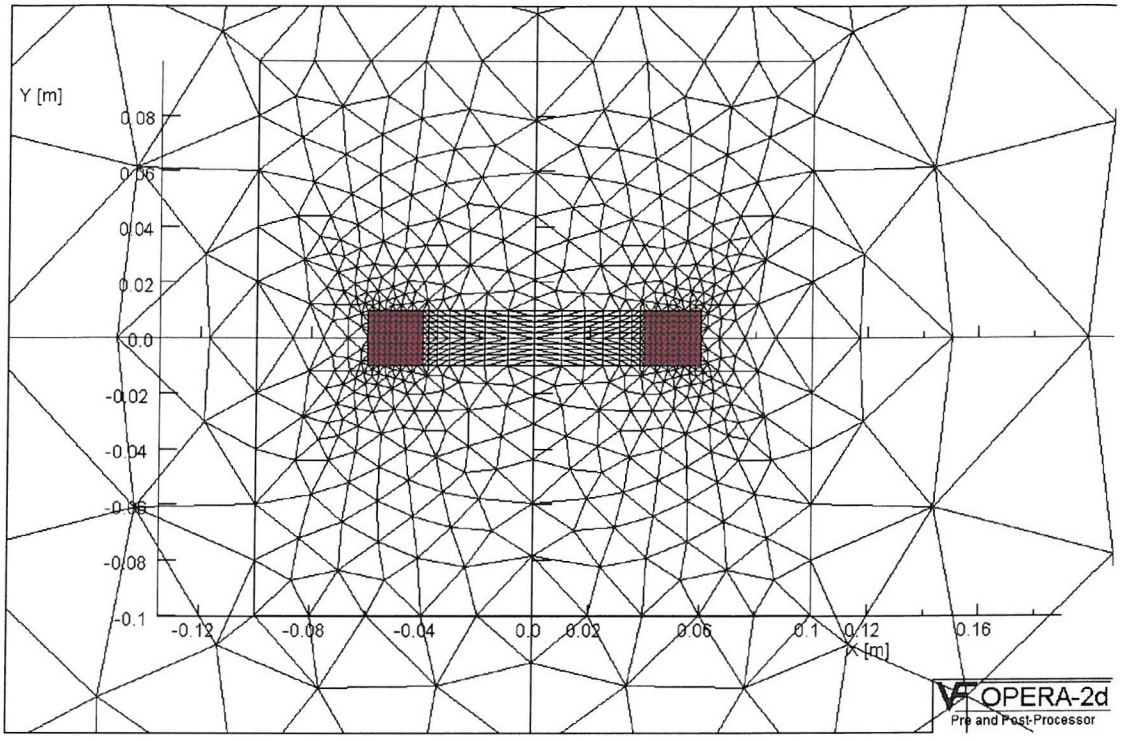

Figure 5.2 Detail of the finite element mesh

The external circuit is composed of the two conductors in series, connected by a voltage source and an external resistance. A schematic of the circuit can be seen in figure 5.3.

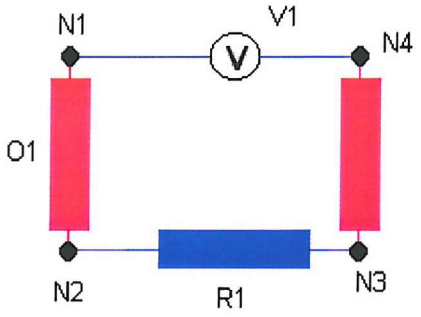

Figure 5.3 A simple external circuit with 2 filamentary conductors

The external resistance can be used to represent the internal resistance of the voltage supply, the resistances in the end windings or the resistance in connecting wires.

The circuit is entered into the program using the SPICE type definition, table 5.1

* TYPE FILA
* LEN 1
V1 1 4 240
R1 2 3 1E-6
* TURNS 200
* RESIST 0.017
O1 1 2
O2 3 4
.END

TABLE 5.1 An example SPICE type file

For clarity, the components are described in table 5.2

Component	**Label**	**Property**	**Value**
Opera Filamentary conductor	O1	Conductor label	1
	O2	Conductor label	2
		Turns	200
		Length	1 metre
		Resistance per unit metre	0.017 Ohms
Resistor	R1	Impedance	1E-6 Ohms
Voltage source	V1	Voltage	240 Volts

TABLE 5.2 Properties of the circuit components

When the circuit is imported into the Opera Preprocessor, a single 'loop' is formed and reported by the pre-processor in figure 5.4

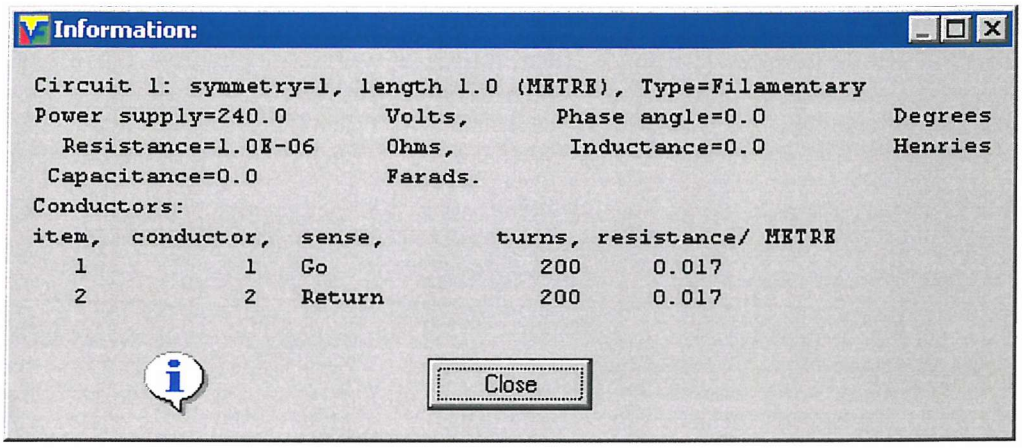

Figure 5.4 The loop formed from the SPICE like data file

The problem is solved with the time harmonic solver (AC solver) at 50 Hz and the potential distribution in figure 5.5 is obtained. Although the absolute values of the two dimensional vector potential **A** are hard to interpret, a contour plot of **A** represents flux lines.

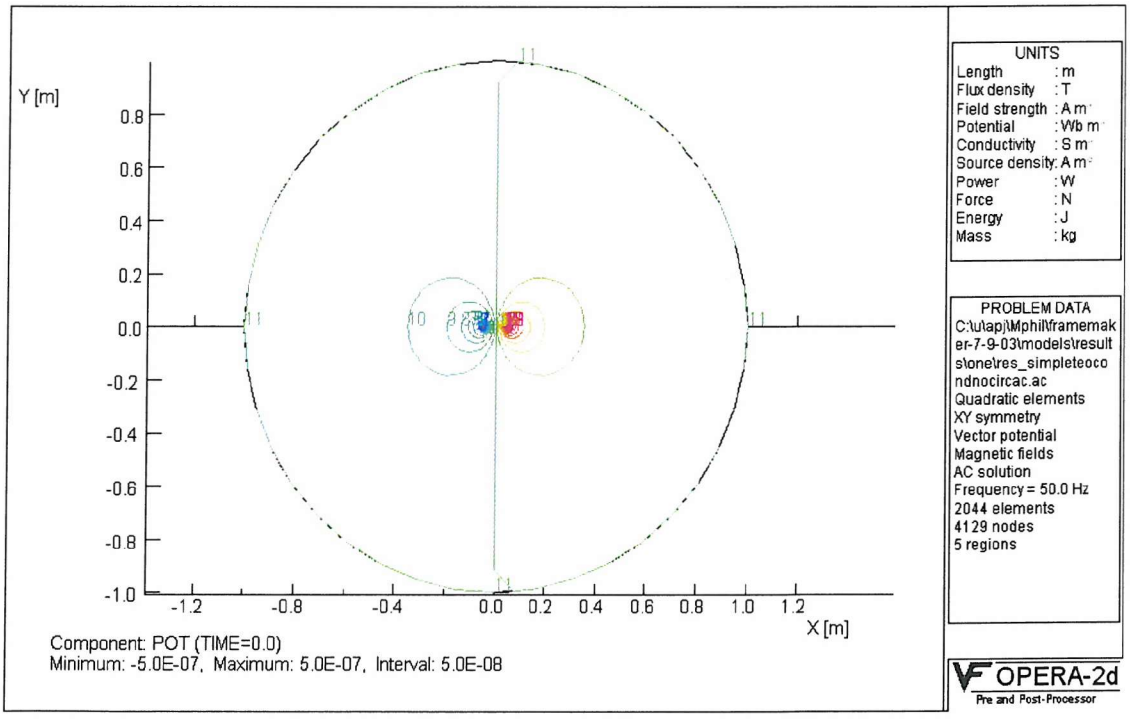

Figure 5.5 The potential contour plot from the time harmonic solver

In figure 5.6 it can be seen the current density is uniform across the domain of the conductors.

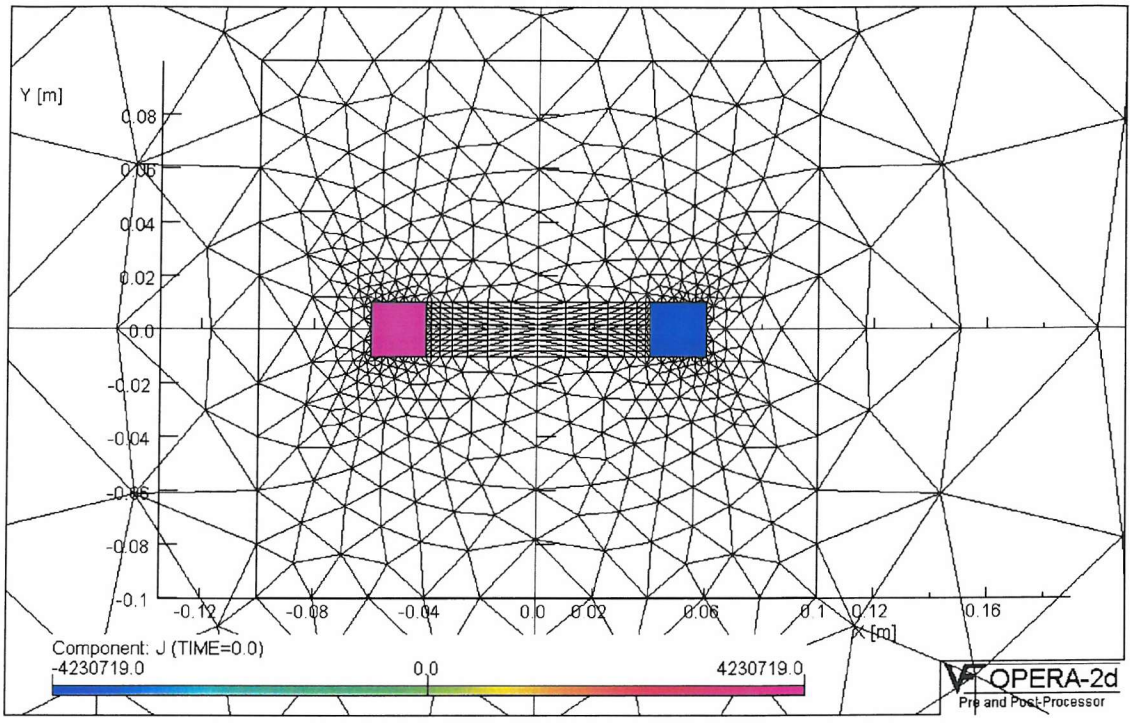

Figure 5.6 Current density in the conductor

The filamentary conductor in this example is assumed to have a constant turns density, the current density is therefore constant over the cross section. The current density in each element of the conductor is

$$J = \frac{\text{circuit current*turns}}{\text{element area}} \tag{5.1}$$

Hence if the post-processor is used to calculate the integral of the current density over the domain of a conductor it will yield the amp-turns of the circuit not the current.

5.2.2 The analytical model

The expected value of the time harmonic solution can be calculated by solving circuit equations for the circuit in figure 5.3. The inductance of the conductors in a system with constant permeability and no eddy currents is a static quantity related to its geometry. This can be calcu-

lated by solving a static magnetic field model with a known current density. The inductance can then be found from the energy in the model from:

$$\text{Energy} = \frac{1}{2}\int LI^2 \tag{5.2}$$

where the integral is over the whole of the model. I is the current in the conductor and L is the unknown inductance. The current in this equation refers to the current in the circuit - not the current density in the conducting region. If the conductor is representing a multi-turn coil then, from equation 5.1, the current is

$$I = \left(\int_{\text{conductor}} \mathbf{J}\,dS \right) / \text{turns} \tag{5.3}$$

The energy can be obtain from the built in integral calculations in the post processor i.e.

$$\text{Energy per unit length} = \int_{\text{model}} \mathbf{A} \bullet \mathbf{J}\,dS \tag{5.4}$$

where **A** is the vector potential (the solution variable) and **J** is the current density in an element. As **J** is only non zero in the conductor in this model, the energy integral can be carried out in just a conductor hence

$$\text{Inductance per unit length} = \frac{\int \mathbf{A} \bullet \mathbf{J}\,d\Omega}{\int \mathbf{J}\,d\Omega / (\text{turns})^2} \tag{5.5}$$

where Ω is the domain of one of the conductors.

The post processor can be used to calculate the integral over one conductor, figure 5.7

UNIVERSITY OF SOUTHAMPTON LIBRARY

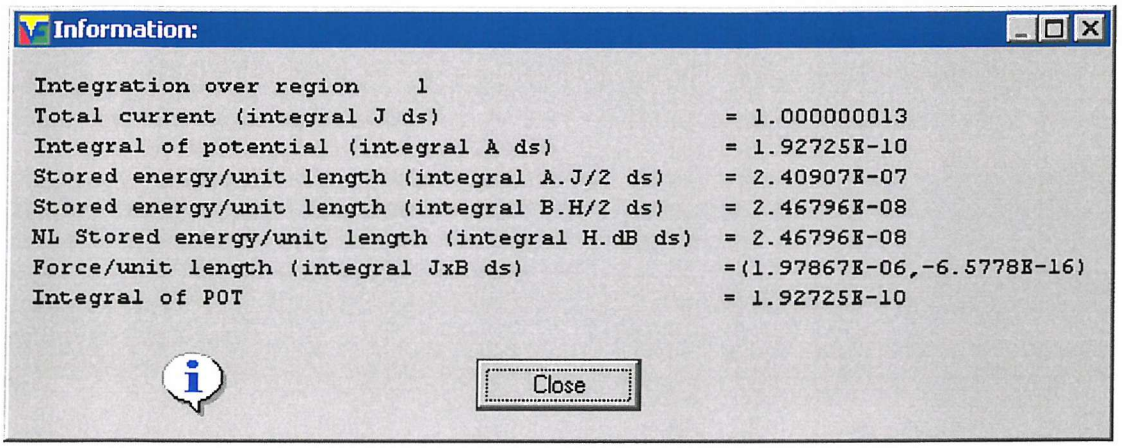

Figure 5.7 The results of the built in integrals over the domain of one of the conductors

The inductance of the circuit can be calculated from the built in integrals using the expression

```
$para #inductance 4*energy/((current/200)**2)
```

The same model can also be solved with quadratic shape functions elements, the two results are shown in table 5.3.

Finite elements	Inductance
Quadratic	0.03854508
Linear	0.03792655

TABLE 5.3 Comparison of the inductance using quadratic and linear elements

The difference between the two values is about one percent, the quadratic element results will be more accurate because they are able to better represent the field when it is changing rapidly. The finite element result for the inductance will converge towards the correct value when smaller elements are used. However, the accuracy of the calculated inductance is not important in this test. The circuit model is coupled to the finite element model, and it is the inductance of the finite element model that will be used to determine the analytic solution.

The values of inductance can now be used in the circuit analysis. Kirchoff's laws are applied to the circuit in figure 5.3 giving

$$L\frac{d}{dt}i(t) + Ri(t) = V_m e^{j\omega t} \tag{5.6}$$

where the voltage varies sinusoidally with time and has the angular frequency ω. The solution to this equation is [68]

$$i(t) = \frac{V_m}{R + j\omega L} e^{j\omega t} \tag{5.7}$$

The maximum amplitude of the current is given by

$$I_m = \frac{V_m}{\sqrt{R^2 + (\omega L)^2}} \tag{5.8}$$

and the phase lag between the current and the driving voltage is

$$\theta = \text{atan}\left(\frac{\omega L}{R}\right) \tag{5.9}$$

The time harmonic finite element solution reports the circuit current as the real component (in phase) and the imaginary component (90 degrees out of phase) which are

$$\frac{V_m R}{R^2 + (\omega L)^2} \quad \text{and} \quad \frac{-V_m \omega L}{R^2 + (\omega L)^2} \tag{5.10}$$

using the Opera-2d preprocessor this can be expressed as

```
$para #react    (freq*PI*2*#Inductance)
$para #RealVal (240*#Res)/(#Res**2+#react**2)
$para #ImigVal -((240*#Omega)/(#Res**2+#react**2))
```

Where `#res` is the total circuit resistance, `freq` is the solution frequency and `#RealVal` and `#ImigVal` are the real and imaginary components respectively.

Table 5.4 shows calculated current from the circuit equations and the computed current from the time harmonic solver.

Circuit current	Real	Imaginary
Circuit equations	8.46143892	-15.0679470
Time harmonic solver	8.46143545	-15.0679474

TABLE 5.4 Comparison of calculated and computed current, quadratic elements

	Real Current	Imaginary
Circuit equations	8.67131655	-15.1939030
Time harmonic solver	8.67131655	-15.1939032

TABLE 5.5 Comparison of calculated and computed current, linear elements

There is very good agreement in the solutions as expected. The solution with linear elements shows an error of about 1e-9 and quadratic elements 1e-7. The tolerance on the equation solutions of the linear algebra solver in time harmonic solver is 1e-7, so a better agreement than this is not expected.

5.2.3 The Time Transient solution

The model can be similarly analysed in the time transient solver. If the driving function in the transient circuit is set to a 50Hz Cosine, the solution should be the same as the in the time harmonic case once the initial transients have subsided. A simulation was run with linear elements and an adaptive time step with a tolerance of 0.001.

The current in the circuit is shown as a function of time in figure 5.8

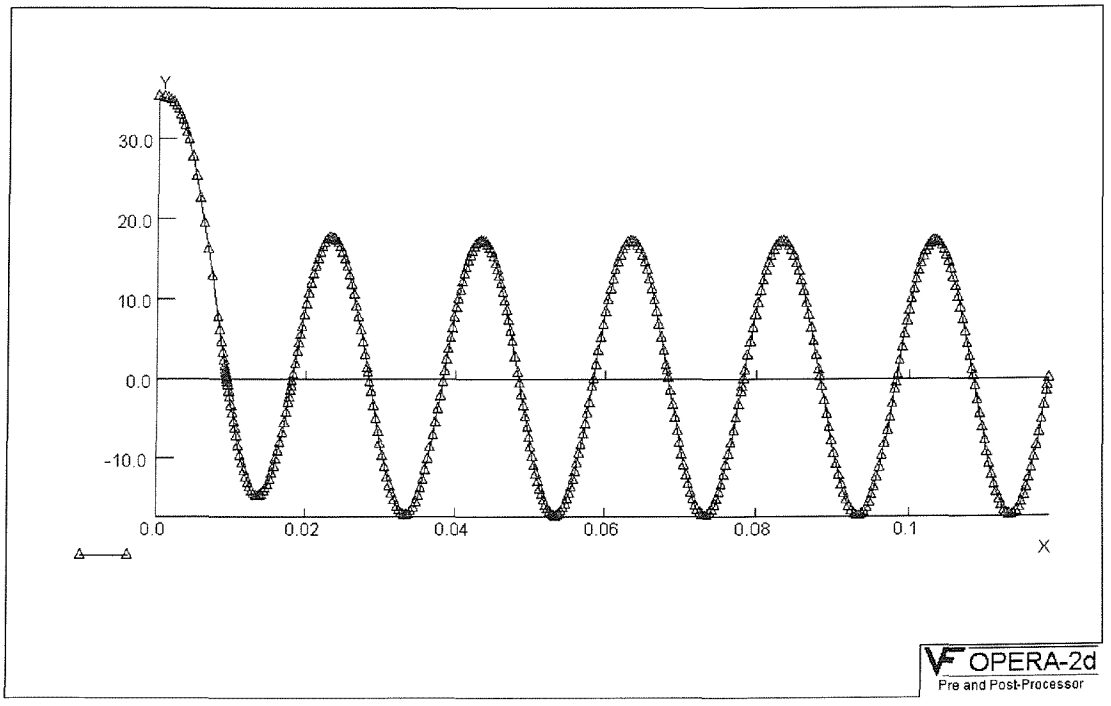

Figure 5.8 Current in the circuit in amps as a function of time

The adaptive time stepping uses an average time step of 0.0025 seconds which equates to 80 time points for each AC cycle.

There is an initial transient which has a time constant of about 0.03 seconds. The initial current is much higher than the magnitude of the time harmonic solution because a DC current is calculated at time zero. The initial DC current is reported by the program as 35.294112456748 Amps, which can be calculated from the circuit equations, thus

$$I = \frac{V}{R} = \frac{240}{2 \times (200 \times 0.017) + 1e-6} = 35.294112 \tag{5.11}$$

It can be seen that these values agree exactly. In initial testing the result only agreed to 1e-8, on investigation it was discovered that the element coefficient routines were only calculating the area of elements to an accuracy of 1e-8. The area of an element is used in the circuit calculation as the total resistance of the wires is calculated from

$$\sum_{elements} \frac{\text{turns}}{\text{coil area}} * \int_{element} dS \tag{5.12}$$

The area of the elements are calculated using guassian quadrature, and it was found that the gaussian weights for quadratic elements were only defined to eight significant figures. This level of accuracy is not required for real models and was only noticed because there was an analytical example available for comparison. The results reported by the program are normally only displayed to 8 or 9 significant figures. Results which have been presented with higher precision are just for illustration and were obtain by making temporary modification to the programs.

After many cycles, the current settles down to a regular harmonic solution which should be the same as the analytical solution. A comparison is shown in table 5.6, where one cycle at 50Hz is 0.02 seconds.

Time transient solution with tolerance 0.001 (linear solution)	Current, time t	Current time t+0.005
0.02	9.45886652	-15.3902712
0.2	8.73691705	-15.1026068
2	8.74165455	-15.1042648
Circuit equations	8.67131655	-15.0679470

TABLE 5.6 The circuit current as a function of solution time

It can be seen that the inaccuracy in the circuit equation after 2 seconds is about 1 percent, yet the requested tolerance was 0.1%. The 'tolerance' is calculated in the solver as the relative difference between two field solutions - this does not necessarily mean that the same accuracy in the circuit solution is achieved. Secondly, the errors in a time stepping scheme generally become larger as time stepping progresses because errors compound when the initial values for the next step contain the errors of the last step. A greater accuracy in the circuit solution can be obtained by using small time steps, which is achieved by using a smaller tolerance, or selecting a short fixed the time step.

Time transient solution (linear solutions)	time =0.2s	time =2s
Circuit equations	8.67131655	8.67131655
100 steps per cycle	8.74797711	8.74797687
1000 steps per cycle	8.67936617	8.67936592
10000 steps per cycle	8.67212537	8.67212512
100000 steps per cycle	8.67139751	
1000000 steps per cycle	8.67132723	

TABLE 5.7 The effect of the time step upon circuit current

It can be seen in table 5.7 that when sufficient time steps are used the analytical result is achieved. If a log-log scale is used to plot the error between the calculated and analytic values and the time steps per cycle a correlation can be seen, Figure 5.9

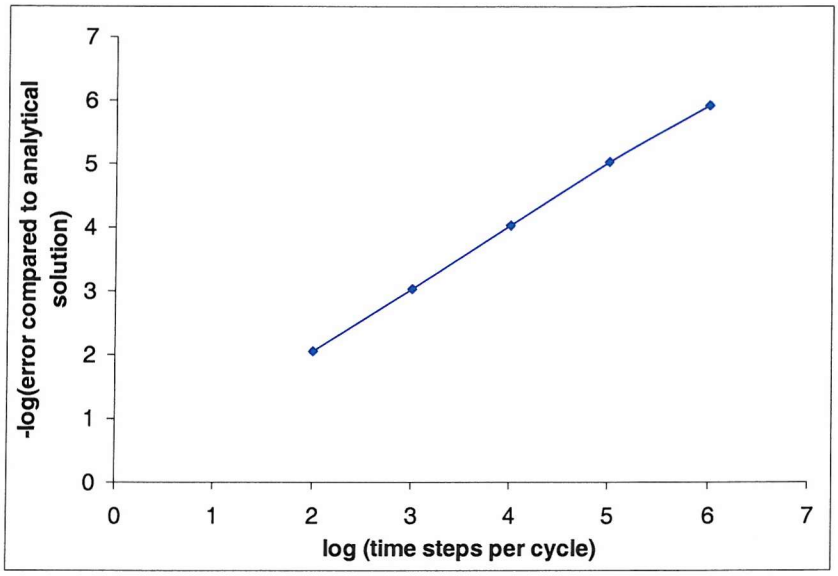

Figure 5.9 The relationship between error and the number of time steps

As the number of time steps increases the result tends towards the analytical value; this demonstrates that the formulation and implementation are both correct. Using the very small time steps is not practical for real models and adaptive steps are generally used with the corresponding reduction in circuit solution accuracy.

5.3 Eddy current circuits

A simple circuit is proposed to check the validity of the eddy current circuits. The circuit contains two massive conductors and an external resistor. This model is compared to a current driven eddy current model. The errors in finite element approximation will be the same for both the current and voltage driven case, so by comparing the voltage and current driven solutions any errors in the circuit calculations can be investigated. The finite element model is similar to the previous example but the conductors are solid pieces of copper. The conducting regions are assigned a conductivity of 5e7 S/m from which the program calculates the resistance. The circuit represents 'bus bars' carrying large currents and is shown in figure 5.10

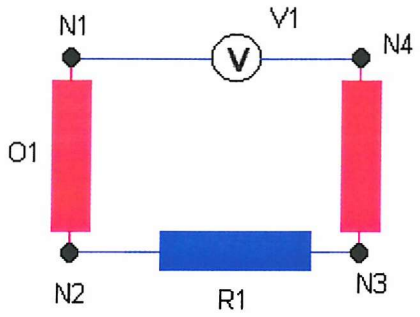

Figure 5.10 A simple external circuit with two massive conductors

and described in the SPICE format thus

* TYPE EDDY
* LEN 100
V1 1 4 12
R1 2 3 1E-8
O1 1 2
O2 3 4
.END

TABLE 5.8 SPICE type file for a simple circuit

When the circuit is solved at 50 Hz the following distribution of current is obtained in the conductors

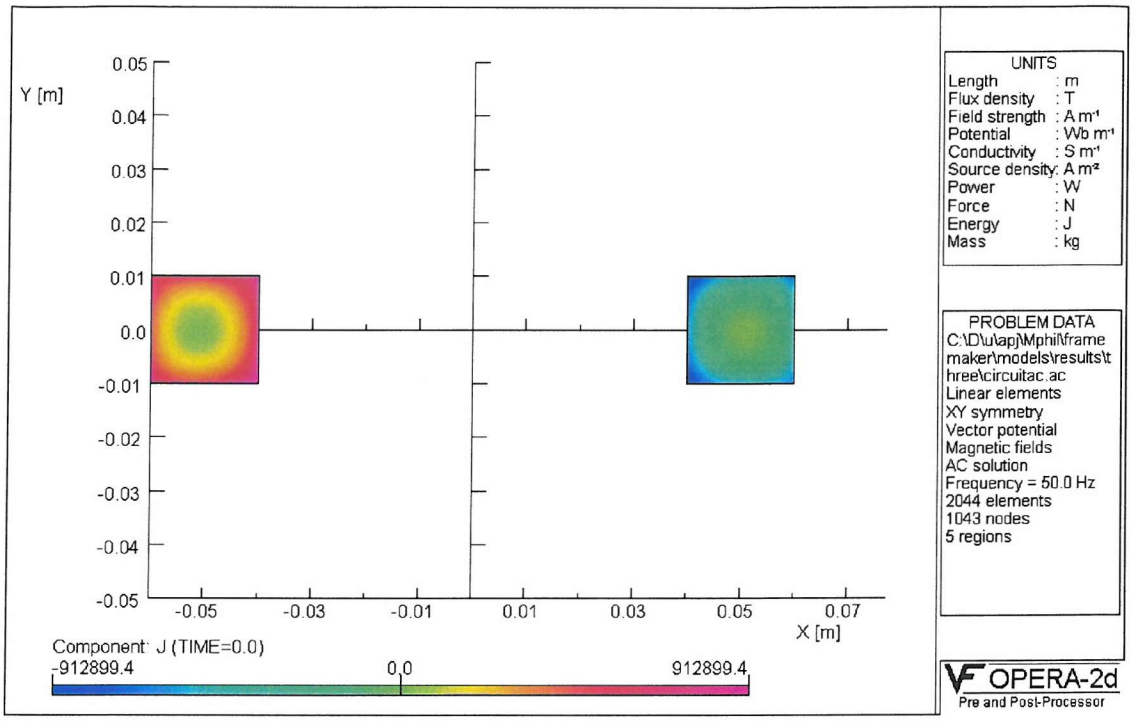

Figure 5.11 Current density in the circuit conductors

The eddy currents can be clearly seen in the conductors. The current has a maximum value at the edges of the conductor and decays in intensity in the centre of the conductor as expected.

The value of the skin depth from equation 2.36 should be about 1 cm. If the current density is plotted in the conductor as a function of position the following result is obtained.

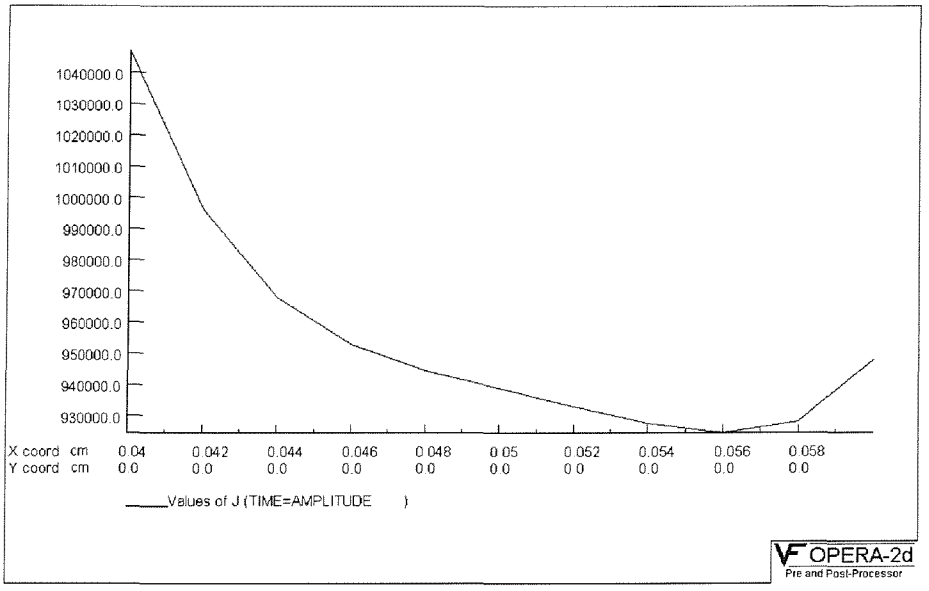

Figure 5.12 Graph of the amplitude of the current density as a function of position

The decrease in current with distance implies a skin depth of a few cm. This is greater than the predicted skin depth for an infinite plane as the fields penetrate from all sides of the conductor, eddy currents are also induced from the field in the other conductor. It is important that the skin effect is captured by the finite elements, which is achieved by ensuring that there are at least a few finite elements per skin depth.

The current in the circuit is

Real current (amps)	Imaginary current (amps)
126.047 Amps	-359.684 Amps

TABLE 5.9 Current in the circuit

This is the same as a peak current of 381.131 with phase angle of 70.68 degrees

When there is no applied voltage, at phase 90 degrees, a contour plot of the current density shows the out of phase component of the current.

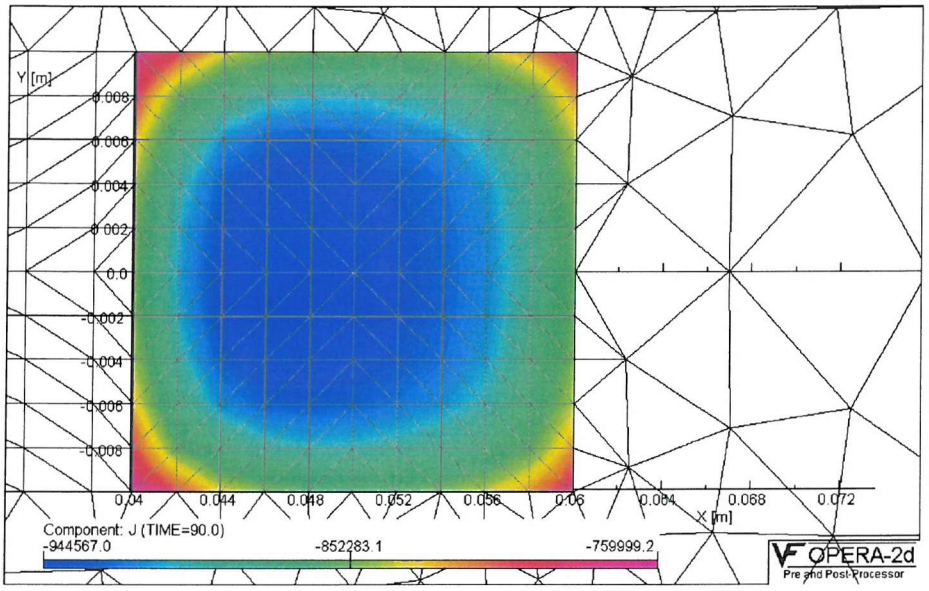

Figure 5.13 Out of phase current density in a conductor

It can be seen that the maximum value of the current density is no longer at the surface of the conductor. Rather than comparing this model to an analytical solution, the model is compared to a current driven version of the model.

The simplest current driven model is a half model, figure 5.14, where the supplied current magnitude and phase are taken from the results of the circuit analysis.

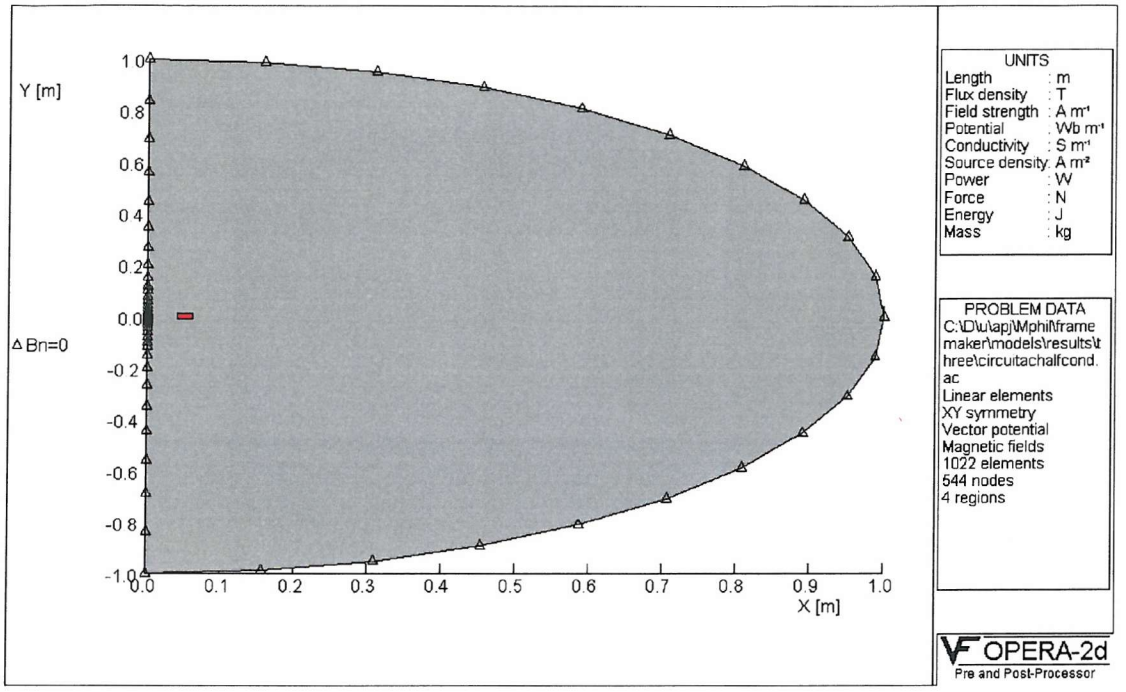

Figure 5.14 The half model with boundary conditions

The current density is fixed in the conductor by applying an extra equation per conductor as described in section 2.5. The field patterns and current densities of the two solutions are idential. figure 5.15 shows the potential distribution in and around the conductor in the two models

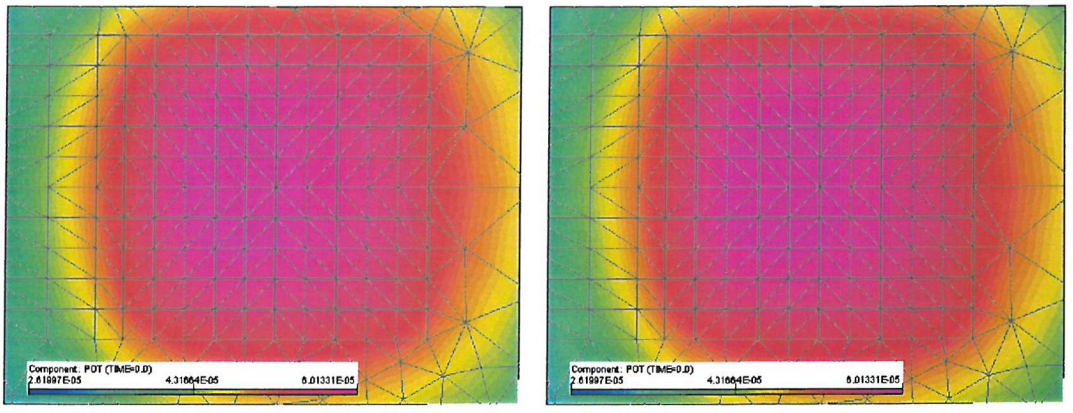

Figure 5.15 Potential in the conductor for current (left) and circuit (right) driven models

If the voltage driven model is solved in the time transient program with a sinusoidal drive and an a adaptive tolerance of 0.001, the potential distribution after 100 cycles can be seen in figure 5.16

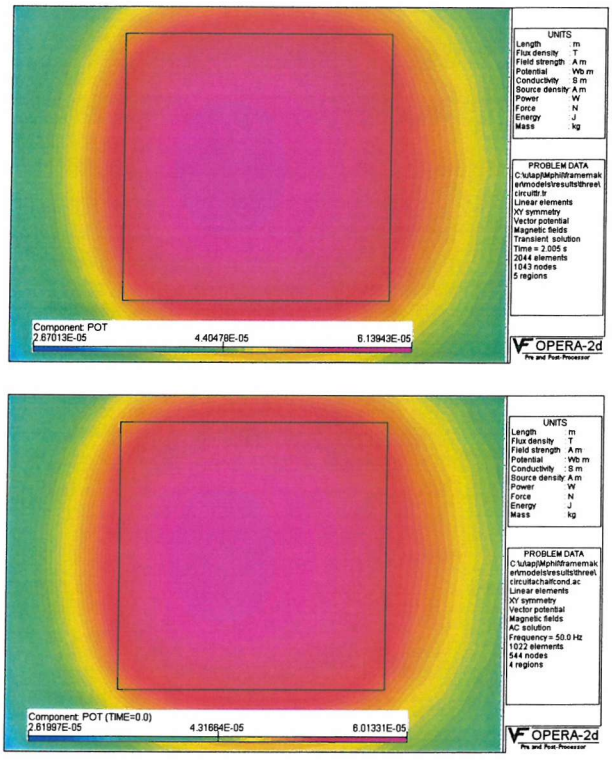

Figure 5.16 Potentials in a voltage driven (top) and current driven models

Although the potential and current densities are very similar, the values differ by a few percent. After the initial transient has decayed, the total circuit current can be compared to the time harmonic solver.

Model	Current (amps)
Time harmonic	126.047
Time transient (100 cycles)	128.520

TABLE 5.10 Current in the circuit

The accuracy in the value of the circuit current is similar to the transient solution of a filamentary circuit. A time stepping tolerance of 0.001 in the field solution yields an absolute accuracy in the circuit current of 1 percent.

Figure 5.17 shows the comparison of the current in a circuit as a function of time, when the initial sinusoidal voltage is phase of 0^o and a phase of 90^o.

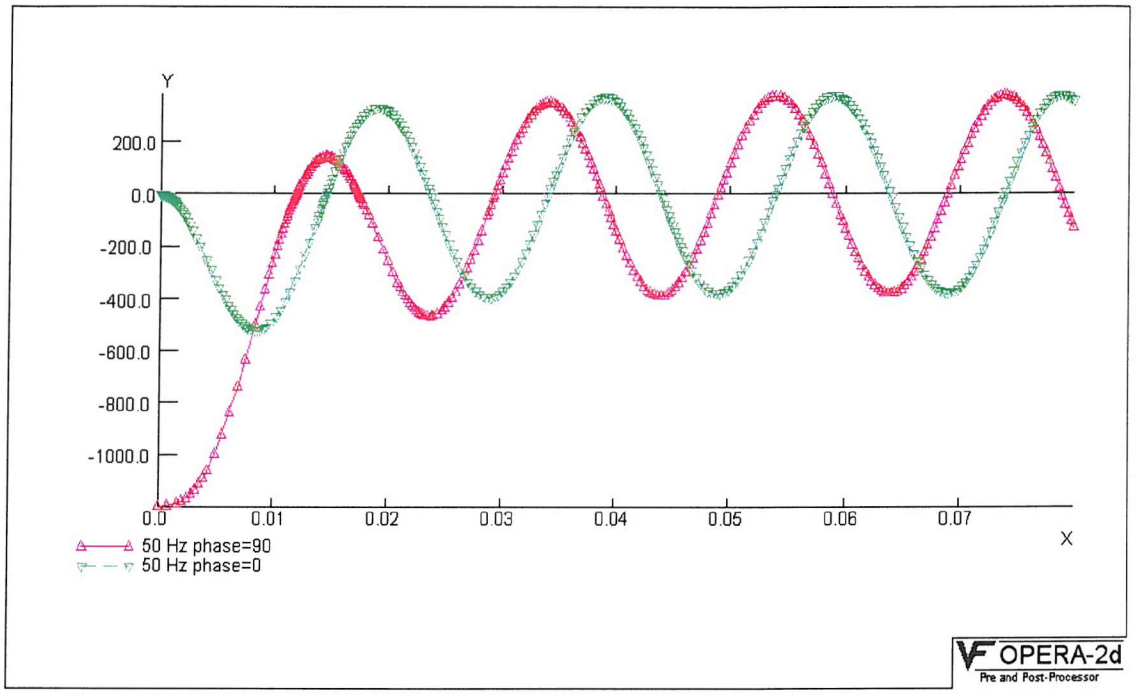

Figure 5.17 Transient analysis of the voltage driven circuit.

It can be seen that when the drive voltage starts at a maximum, the current is very large (-1199.9988 amps) compared to the AC solution, and is consistent with the expected DC current i.e.

$$I = \frac{V}{R} = \frac{V}{R_{ext} + R_{cond}} = \frac{V}{1e-8+2\times 0.005} = \frac{12}{0.01000001} = 1199.9988 \quad (5.13)$$

If the initial voltage is a minimum at t=0 it can be seen the time stepping algorithm requires small steps to cope with a rapidly changing solution driven by large changes in supply voltages. Turning on the voltage when it is at its minimum is required in devices to minimise large transient currents.

5.4 Multiple Circuit example

An example is presented which contains two filamentary circuits. One circuit has an applied voltage and the other does not, figure 5.18.

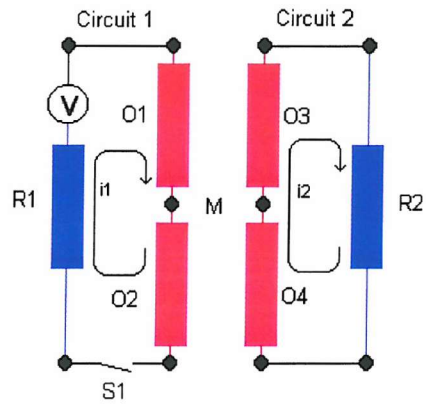

Figure 5.18 Two inductively coupled circuits

The connection between the two circuits is by the magnetic field of one circuit linking the second. The finite element model's geometry is shown in figure 5.19.

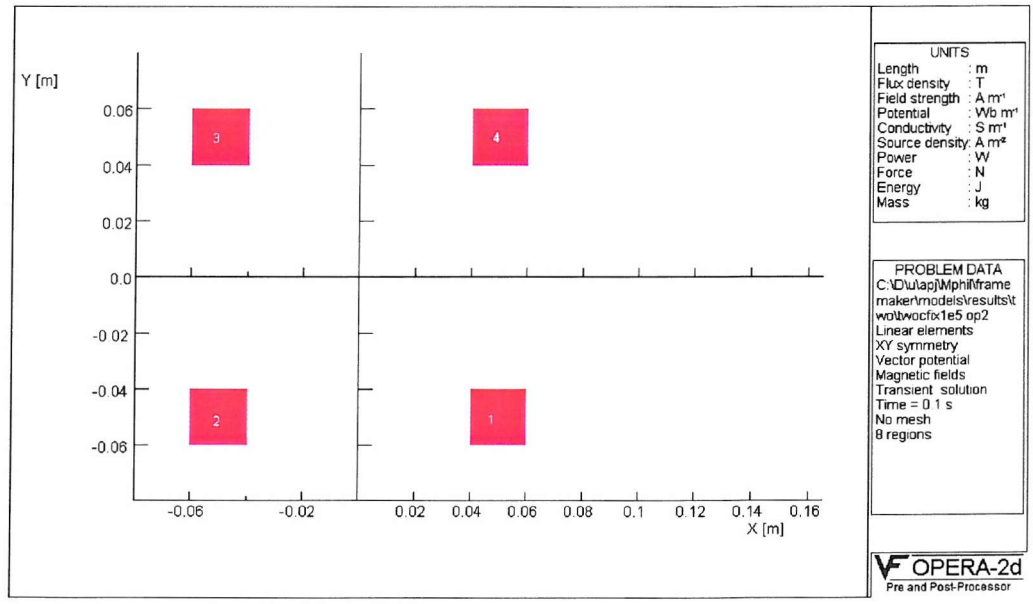

Figure 5.19 Orientation of the 4 circuit conductors

Each circuit has the same properties as the earlier filamentary example in table 5.2. The switch is initially open in circuit one and current does not flow in either circuit. At time=0 the switch

is closed, this is achieved in the software by applying a step function scaling to the drive in circuit one. The step function scaling is f(t)=0 when t<0 and f(t)=1 when t>=0.

The analytical analysis of this system requires both the self inductances of the circuits and the mutual inductance between them. The model is symmetrical so the self inductance of circuit 1, L1 is the same as L2. The self inductance is found using equation 5.5 by applying current in one circuit and calculating the energy of the whole model; this is found to be 0.03778807 Henries.

The mutual inductance is found by applying the current in one circuit and calculating the flux linked by the other. The flux linked from one circuit, a, to another, b, is

$$\varnothing_b = M_{ab} I_a = \int n \mathrm{A}_{b1} d\Omega_{b1} - \int n \mathrm{A}_{b2} d\Omega_{b2} \tag{5.14}$$

where M is the mutual inductance, A_{b1} is the vector potential in conductor 1 of circuit b, n is the turns density in the coil and Ω is the domain of a conductor.

The mutual inductance evaluates to 0.005408678 Henries, an order of magnitude less than the self inductance.

The analytical solution of this model is described an Appendix A which gives the current in the circuits as

$$i_1 = \frac{V}{R}\left(1 - e^{-\alpha t}\left(\frac{\cosh(\beta t) + (\alpha^2 + \beta^2)L - \alpha R}{\beta R} + \sinh(\beta t)\right)\right) \tag{5.15}$$

$$i_2 = \frac{(\alpha^2 + \beta^2)MV}{\beta R^2} e^{-\alpha t} \sinh(\beta t) \tag{5.16}$$

$$\text{where} \quad \alpha = \frac{LR}{L^2 - M^2} \quad \text{and} \quad \beta = \frac{MR}{L^2 - M^2} \tag{5.17}$$

Figure 5.20 shows a comparison of the calculated and analytical results for the current in circuit one

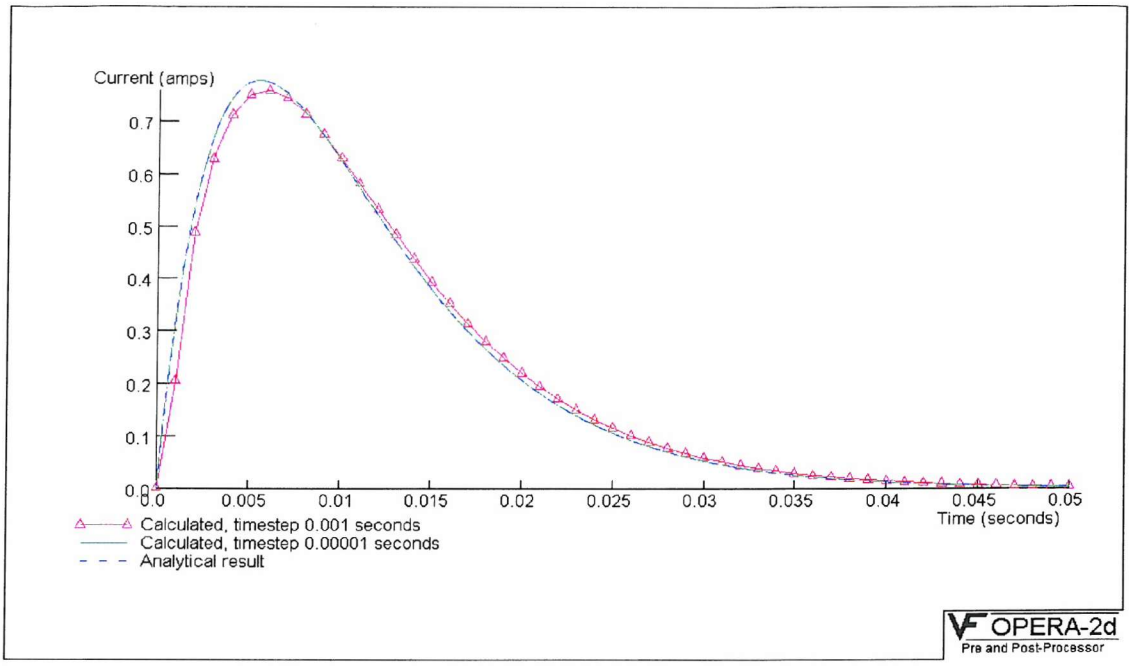

Figure 5.20 Comparison of calculated and measured current in circuit 2

It can be seen that there is excellent agreement when the time step is 0.000001 seconds.

When a 0.0001 time step is used the error in the solution is about 5 percent, this error is due to the time-stepping technique. The time-stepping is only able to model a linear or quadratic change in the solution variable exactly, however using a shorter time step reduces this error (the time stepping error is $O(\delta t^2)$). Adaptive time stepping could not be used to analyse this model as the adaptive scheme did not have a criterion to evaluate a 'minimum time step'. A minimum time step is required so that when large errors are found in the time stepping process, typically in a step change in a drive function or at the start of the time stepping process, the time step does not reduce to an unrealistically small value. An unrealistic value is hard to define, but when the steps get small, the effect of adding the conducting matrix (the S matrix) to the stiffness matrix (R matrix) is just a perturbation and the time stepping system stalls. Unfortunately this model does not have any conducting regions and the minimum time step defaults to the maximum time step. The maximum time step is not defined in this model, it is normally set to make sure that discontinuities in the driving functions are captured. Therefore in this model, time steps are evaluated only at the time output points. A real model will typi-

cally have at least one region of conducting material and a value for the minimum time step would be correctly evaluated.

5.5 An induction motor

A three phase induction motor has been modelled by a manufacturer [70]. It has circuits consisting of filamentary conductors in the stator and circuits consisting of massive conductors in the rotor, figure 5.21

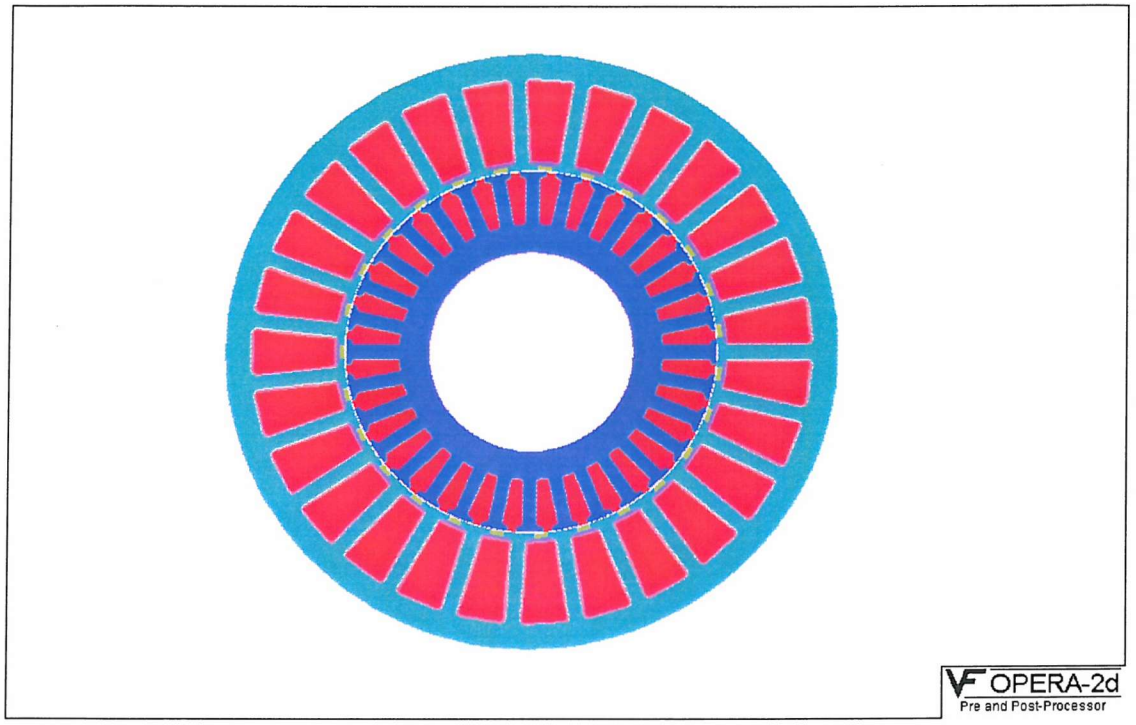

Figure 5.21 Finite element model of an induction motor

The circuits in the rotor represent the connectivity of the rotor bars and the end windings in a squirrel cage, as was previously explained in figure 1.5. The filamentary circuits are used to represent the three voltage driven phases in the stator. There are two sets of circuits, one half is in the upper half of the slot and the second in the lower half.

The fully time transient analysis of a rotating machine is a computationally intensive process which can take many hours or days to run [49]. If the rotor is considered to be in a stationary frame of reference, it can be considered to be in the rotating magnetic field of the stator. This can be approximated by applying a rotating field at this 'slip' frequency. The system can then

be analysed by time harmonic analysis at the slip frequency after other variables, such as length, are adjusted to comply with the technique [69].

The magnetic field in the permeable material and the current density in the conductors can be seen in figure 5.22.

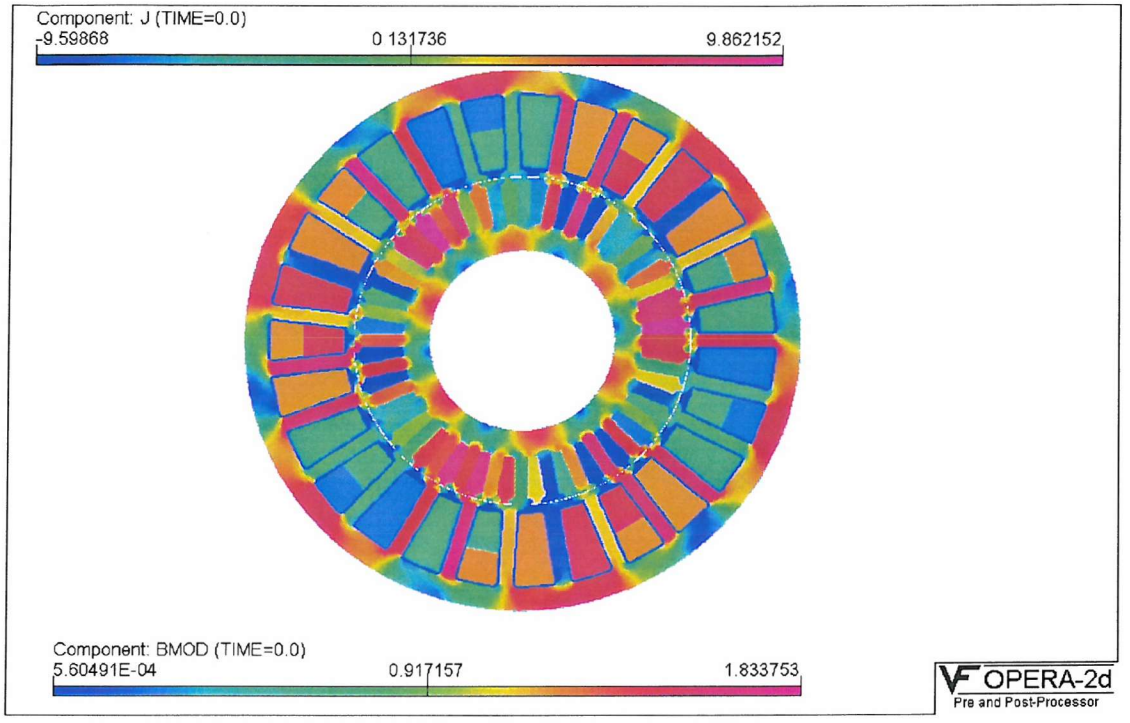

Figure 5.22 Magnetic field and current density in an induction motor

The torque can be calculated from this model using the Maxwell stress method [69]. This solution represents only one position of the rotor but the solution is obviously dependant upon the relative position of the rotor and the stator. A number of different solutions are calculated at different rotor positions so that an average value of torque can be calculated. When results from this model are compared to measured values an agreement to within ten percent has been achieved. This is a long way from the 1e-7 agreement of the analytical example. There are many sources of errors including

- The model is a 2d slice of a skewed rotor. Many 2d slices or a full 3d model are needed to better represent the real device.
- A 3d model is required to correctly model the end inductances of the circuits.

- The use of time harmonic analysis to approximate a time transient problem means that only one frequency has been considered. There are many harmonics of the solution frequency which need to be considered - which is most accurately achieved with full time harmonic analysis of a rotating model.
- The material modelling in the finite element model may not accurately represent the real materials. A hysteresis model has not been included in the non linear behaviour so iron losses have not been accounted for. The material properties will also be temperature dependant and do not currently reflect the temperature distribution in the model.
- A single frequency time harmonic analysis cannot represent the effect of non-linear magnetic materials. A time transient solution is needed to represent the permeability change as a function of time.

The errors listed are not unique in circuit driven problems, they are just as applicable to current driven problems.

5.6 Summary

The results which have been presented in this chapter demonstrate the accuracy or the direct coupling technique for circuits composed of both filamentary and massive conductors. When real devices are analysed, the technique has been shown to be useful in modelling both the external connections of conductors as well as the primary voltage driven circuits.

6. Conclusions

6.1 Summary

The project aimed at extending existing finite element analysis programs to include external circuit connections and components. This has been achieved by the use of direct coupling between the circuit and finite element equations. Two different techniques have been presented to describe the circuit data in the finite element program, a network loop approach and a node-node technique using the SPICE net list format.

Coupling of an external circuit to the finite element model allows a better representation of an electrical system than can be achieved with current density applied to the elements. One use of an external circuit is to model the power supply of a device. The power supply's voltage, internal impedance and the impedances of any connecting wires can be coupled to the finite element model. The external circuit can also be used to describe the connectivity of domains in a 2d model along with circuit components which join the domains. An example has been shown where the connectivity of the rotor bars in a squirrel cage rotor, along with the resistances which joins the bars, has been described as interconnected circuit network loops.

The direct coupling approach has been shown to be straightforward in implementation and flexible in use. The use of adaptive time stepping in transient analysis has been shown to be a useful technique to control the errors in the solution potentials. The errors in the solution are related to the length of the time step in a time marching scheme, reducing the time step reduces the error in both the field and circuit equations. When the same circuit equations are used in time harmonic analysis, the currents in the circuits have been shown to agree with analytical results.

Two different techniques have been presented to enter the circuit data into the pre-processor. The first technique directly interfaces with the internal storage structure of the circuits as network loops. Once the loops have been entered, any connectivity between the different loops are specified. Loop entry allows for rapid entry of simple circuits. More complicated circuit networks can benefit by being defined by nodal connectivity, which is easily identified from circuit diagrams. The nodal definition file has been based on the SPICE data format as this is a

common format used by circuit designers. The pre-processor converts the SPICE data format into the native loop format.

The external circuit implementation is compatible with mesh motion and is suited to the analysis of rotating or linear machines where finite elements are coupled to both circuits and motion. Rotating machines such as generators or motors can be analysed to calculate the field distributions and torque.

6.2 Further work

6.2.1 The finite element solvers

This implementation of circuit coupling is available within the two dimensional time harmonic and time transient solvers available from Vector Fields. There are two areas where the work can proceed further; the inclusion of more non-linear components, where the impedance of a device is not constant, and allowing circuit loops which do not include any conducting regions to be included.

The only non-linear components currently modelled are inductors and capacitors. The time transient solvers could be extended to include non-linear circuit components such as diodes, thyristers and switches. At each step in a time marching scheme the impedance of a non-linear device must be recalculated and the circuit equations updated with the new value.

Switches can be modelled as resistors with zero or 'very high' resistances or by recalculating the circuit equations when a switch opens or closes; opening a switch removes an equation. Neither of these two models are currently possible in the software as the circuit matrix contributions are calculated once, before the time marching scheme starts. At present, switches are modelled by stopping the solver when switching occurs, the circuit equations are then rebuilt and the program restarted. Another approximation which is used is to set the drive to be a function of time, or as a function of a position in a machine. The function has the value one when the switch is closed and zero when it is open.

Diodes, thyristers and similar devices can also be considered as switches. A first order representation of a diode is as a switch, with the switch being controlled by the direction of current through the diode. A better approximation is to use a look up table of the current / voltage characteristic of a diode to give its impedance. A real model of a diode should however also include

other properties such as its capacitance and recovery time. For any approach to be applied to the current software, restructuring is required to allow quick rebuilding of the circuit matrix coefficients at each time step. If switching happens at a non predetermined time, then a robust technique will need to be developed to capture the time of switching to reduce the oscillations in the solutions which are associated with discontinuities in the current [43].

The restriction that a circuit must have a conductor in it, is due to the algorithm which has been used to assemble the coupled matrix. The coupling coefficients are calculated by iterating through all the conductors in all the circuits. If a circuit does not contain any conductors, then the global parameters of the circuit (such as resistance, voltage and inductance) do not get entered into the global matrix. If a circuit is composed from inter-connecting loops then one valid (although unlikely) set of network loops may have a loop without a conductor in it. These conductor-less loops can be produced when importing SPICE import files. When the program was originally designed it was not clear that loops without any conductors in them would be useful and there was no provision to allow conductor-less loops. There is an alternative way of assembling the coupled matrix which would allow for loops without conductors which could be used.

6.2.2 Circuit definition

Two techniques have been presented to enter circuit data, either as network loops or using SPICE like files. It would be easier for users of the software if an interactive drawing package was used to view and edit the circuit data as well as the current option of viewing the circuits as a list of components.

Schematic capture is one name given to the technique where circuit components and wires are drawn in a graphics program and then automatically converted into circuits. Schematic capture could be implemented by converting a graphical circuit to a SPICE like file. This conversion is straightforward as both sets of data are stored as node-node connections. Creating a graphics package is not trivial and beyond the scope of this work, especially if the circuit diagram is to be overlaid on top of the picture of the finite element model.

6.2.3 Three dimensions

The three dimensional edge potential finite element software which Vector Fields has developed also uses applied current densities in conductors. The conductors are not however included as conducting regions within a finite element mesh, they are converted to potentials on the interfaces between the domains which contain conductors and the domains which do not. Work is ongoing to include external circuits by using the circuit representation of a conductor as a continuous set of filaments through a conductor. The filaments are then included as part of the finite element mesh. Although the work completed in this thesis has not been extended to three dimensions, work carried out here has helped to solve problems in the three dimensional implementation i.e. how to retain a symmetric matrix. This work has also clarified that it is best to consider non-linear components during the initial design phase rather than as a later enhancement - allowing the circuit equations to be easily rebuilt at each time step.

References

[1] Maxwell, J. C., *A Treatise on Electricity and Magnetism*, 2 Vols, Clarendon Press, Oxford (1982).

[2] Stratton, J.A., *Electromagnetic Theory*, McGraw-Hill, New York, 1941.

[3] R. F. Harrington, *Time-Harmonic Electromagnetic Fields*, New York, McGraw-hill, 1961.

[4] Hammond, P., *Applied electromagnetism*, Pergamon Press, 1971.

[5] H. C. Lai, P. J. Leonard, D.Rodgers and N.Allen, *3D Finite element Simulation of Electrical Machines Coupled to External circuits,* IEEE Trans. Magn., Vol 33, No.2, 1997.

[6] C. R. I. Emson et al, *Modelling Eddy Currents in Rotating System*, Submitted to COMPUMAG '97 Conference, Rio de Janeiro, Brazil, November 1997. FIND

[7] O. C. Zienkiewicz and K. Morgan, *Finite Elements and Approximation Methods.* New York: Wiley (1983).

[8] Jianming Jin, *The Finite Element Method in ~Electromagnetics*, Wiley, (1993).

[9] C. A. Brebbia, *The Boundary Element Thehod for Engineers*, Printec Press, 2nd edition (1980).

[10] J. Kaisjoki, K. Forsman, A. Koski, L. Kettunen, *Implementation of a hybrid method for eddy current problems*, COMPEL: Int J for Computation and Maths. in Electrical and Electronic Eng, Vol. 18 No.3 pp. 398 - 409, 1999.

[11] I. A. Tsukerman, A. Konrad, G Meunier and J. C. Sabonnadiére, *Coupled field-circuit problems: Trends and accomplishments*, IEEE Trans. Magn., Vol. 29, pp. 1701-1704, 1993.

[12] P. P. Silvester and R. L. Ferrari, *Finite elements for electrical engineers*, Cambridge University Press (1990)

[13] D. O'Kelly, *Performance and control of Electrical Machines,* McGraw Hill, 1991.

[14] A. Demenko, *Equivalent RC Networks with Mutual Capacitances for Electromagnetic Field Simulation of Electrical Machine Transients*, IEEE Trans. Magn., 28(2), pp. 1406-1409, 1992.

[15] PC-IMD, SPEED Consortium, Dept. of Electronics & Electrical Engineering, University of Glasgow.

[16] M. Feliziani, *Circuit-oriented FEM: Solution of circuit-field coupled problems by circuit Equations,* IEEE Trans. Magn.,38 (2),pp. 965-968, 2002.

[17] P. I. Kolterman, J. P. A. Bastos, S. R. Arruda, *A Model For Dynamic Analysis of AC Contactor*, IEEE Trans. Magn. Vol. 28, No. 2, 1992.

[18] T. E. McDermott, P. Zhou and John Gilmore, *Electromechanical System Simulation with Models Generated from Finite Element Solutions*, IEEE Trans. Magn., Vol. 33, No.2, 1997.

[19] H. A. Mantooth and M. Vlach, *Beyond SPICE with Saber and MAST,* Analogy white paper MP-0161, Beaverton, Oregon.

[20] L. W. Nagel, *SPICE2: a computer program to simulate semiconductor circuits*, Memo UCB/ERL, M530, Electronics Research Laboratory, University of California, CA, 1975.

[21] J. Väänänen, *Theoretical Approach to Couple Two-Dimensional Finite Element Models with External Circuit Equations*, IEEE Trans. Magn., Vol. 32, pp. 400-409, 1996.

[22] G. Bedrosian, *New method for coupling Finite Element Field Solutions with external Circuits and Kinematics*, IEEE Trans. Magn., Vol 29, pp. 1664-1668, 1993.H.Benson, University Physics, Wiley, page 546, 1991.

[23] C. F. Gerald, P. O. Wheatley, Applied Numerical Analysis, Addison-Wesley, 1984.

[24] N. M. Abe and J. R. Cardoso, *Coupling Electric Circuit and 2D-FEM Model with Dommel's approach for transient analysis*, IEEE Trans. Magn.,34 (5),pp. 3487-3490, 1998.

[25] A. Y. Hannalla and D. C. Macdonald, *Numerical analysis of transient magnetic field problems in electrical machines*, Proc. IEE, 123(9), pp.893-898,1976.

[26] Ph.G. Potter and G. K. Campbrell, *A combined finite element and loop analysis for non-linearly interacting magnetic fields and circuits*, IEEE Trans Magn., 19(6),pp 2352-2355, 1983.

[27] C.S. Biddlecombe, J. Simkin, *Enhancements to the PE2d package*, IEEE Trans. Magn., Vol. Mag-19, No. 6, November 1983.

[28] A. Konrad, *The numerical solution of steady-state skin effect problems - an integrodifferential approach*, IEEE Trans. Magn., 17, pp.1148-1152, 1981.

[29] F. Pirou and A. Razek, *Coupling of saturated electromagnetic systems to non-linear power electronic devices*, IEEE Trans. Magn., 24(1), pp. 274-277, 1988.

[30] F. Hecht and A. Marocco, *A finite element simulation of an alternator connected to a non linear external circuit*, IEEE Trans. Magn., 26(2), pp.964-967, 1990.

[31] J. Weiss and V.K. Garg, *Steady state eddy current analysis in multiply -excited magnetic systems with arbitrary terminal conditions*, IEEE Trans. Magn., 24(6), pp.2676-2678, 1988.

[32] I.A. Tsukerman, A. Konrad and J.D. Lavers, *A method for circuit connections in time-dependant eddy current problems*, IEEE Trans. Magn., 28(2), pp.1299-1302, 1992.

[33] D. Shen, G. Meunier, J.L. Coulomb and J.C. Sabonnadiere, *Solution of magnetic fields and electrical circuits combined problems*, IEEE Trans. Magn., 21(6), pp.2288-2291, 1985.

[34] M. Wilson, Superconducting magnets, Oxford University Press 1987.

[35] C.S.Biddlecombe, J.Simkin, A.P.Jay, J.K.Sykulski, S.Lepaul, *Transient Electromagnetic Analysis Coupled to Electric Circuits and Motion*, IEEE. Trans Magn.34(5), pp. 3182 - 3185,1998.

[36] P. Lombard, G. Meunier, *A general method for the electric and magnetic coupled problem in 2d and magnetomagentic domain*, IEEE Trans. Magn., Vol.28 (2), pp. 1291-1294, 1992.

[37] M. V. K. Chari and P.P. Silvester, *Finite element analysis of magnetically saturated dc machines*, IEEE Trans. P AS, 90, 2362 (1971).

[38] Robert E. Collin, Field Theory of Guided waves, pages 9-10. IEEE Press 1991.

[39] M. C. Costa, S. I. Nabeta and J. R. Cardoso, *Modified Nodal Analysis Applied to Electric Coupled with FEM in the Simulation of a Universal Motor*, IEEE Trans. Magn.,36 (4), pp. 1431-1434, 2000.

[40] H. De Gersen, R. Mertens, U. Pahner, R. Belhams and Kay Hayemer, *A topological method used for Field-Circuit Coupling*, IEEE Trans. Magn., 34 (5), pp. 3190-3193, 1998.

[41] J. Wang, *A Nodal Analysis Approach for 2d and 3d Magnetic-Circuit Coupled problems*, IEEE. Trans Magn., 32, pp.1074-1077, 1996.

[42] J. F. Charpentier, Y. Lefevre and H. Piquet, *An Original and Natural Method of Coupling Electromagnetic Field Equations with Circuit Equations Put in a State Form*, IEEE Trans. Magn. Vol. 34, No. 5, 1998.

[43] P. Kuo-Peng, N. Sadowski, N. J. Batistela and J. P. A. Bastos, *Coupled Field Circuit Analysis Considering the Electromagnetic Device Motion*, IEEE Trans. Magn., Vol 36, No.4, 2000.

[44] P. Dular and P. Kuo-Peng, *An Efficient Time Discretisation Procedure for Finite Element - Electronic Circuit Equation Coupling*, IEEE Trans. Magn., Vol36, No.4, pp1293-1299, July 2000.

[45] J. R. Brauer, *Time-Varying Resistors, Capacitors, and Inductors in Nonlinear Transient Finite Element Models*, IEEE Trans. Magn., Vol. 34, No.5, 1998.

[46] I. A. Tsukerman, *Overlapping finite elements for problems with movement*, IEEE Trans. Magn., Vol. 28, No.5 pp. 2247-2249, 1992.

[47] S. Lepaul, J.K.Sykulski, C.S.Biddlecombe, A. P. Jay and J.Simkin, *Coupling of Motion and Circuits with Electromagnetic Analysis*, IEEE Trans. Magn., Vol. 35, No.3, pp. 1602-1605, 1999.

[48] D. Rodger, H. C. Lai , P. J. Leonard, *Coupled Elements for Problems Involving Movement,* IEEE Trans. Mag,. Vol. 26, No. 2, pp. 546-550, 1990.

[49] S. Lepaul, C. S. Biddlecombe, J. Simkin, A. P. Jay and J. K. Sykulski, *Transient Electromagnetic Analysis Coupled to Electric Circuits and Mechanical Systems*, in Proceedings of the 4th International Workshop on Electric and Magnetic Fields, Marseille, May 1998, pp. 237-242.

[50] M. Trlep, A. Hamler, B. Hribernik, *Various Approaches to Torque Calculations by FEM and BEM*, in Proceedings of 7th International IGTE Symposium, pp. 416-419, 1996,

[51] J. L. Coulomb and G. Meunier, *Finite Element Implementation of Virtual Work Principal for Magnetic Forces, Torques and Stiffness*, IEEE Trans. Magn., Vol. MAG-20, No.5, pp.1894-1898, 1984.

[52] K.J. Binns, P. J. Lawrenson, and C.W. Trowbridge. *The Analytical and Numerical Solution of Electric and Magnetic Fields*, Wiley, 1992.

[53] C.J.Carpenter, *Comparison of alternative formulation of 3-Dimensional Magnetic Field and Eddy current problems at power frequencies*, IEE Proc., Vol 124, No.11, November 1977, pp. 1026-1034.

[54] B.A. Finlayson, *The Method of Weighted Residuals and Variational Principals.* New York Academic Press (1972).

[55] B. G. Galerkin, *Series solution of some problems of elastic equilibrium of rods and plates,* Vestn. Inyh. Tech., 19, 897 (1915)

[56] M. R. Spiegel, *Theory and problems of vector analysis*, McGraw-Hill (1987).

[57] G. Rizzoni, *Principles and Applications of Electrical Engineering*, Irwin (1996)

[58] *OPERA-2d reference manual,* Vector Fields, 24 Bankside, Kidlington, Oxfordshire, OX5 1JE.

[59] W. R. Smythe, *Static and Dynamic Electricity,* The Maple Press (1950)

[60] I. Tsukerman, *A Stability Paradox for Times-Stepping Schemes in coupled Field-Circuit Problems*, IEEE Trans. Magn., Vol. 31, No. 3, November 1995.

[61] A. Gibbons, Algorithmic Graph Theory, Cambridge University Press (1987).

[62] A. H. Stroud and D. Secrest, *Gaussian Quadrature Formulas*, Englewood Cliffs, N. J. Prentice-Hill (1966).

[63] J. A. Maijerink and H.A. van de Vorst, *An iterative solution omethod for systems of which the coefficient matrix is a symmetrix M-matrix*, Maths. Comp., Vol. 31, 148-162, (1977)

[64] H. De. Gersem, R. Mertens, D. Lahaye, S. Vandevalle and K. Hameyer, Solution strategies for Transient, Field-Circuit Coupled Systems, IEEE Trans. Magn. Vol. 35, No.4, (2000)

[65] D. Lahaye, S.Vandewalle and K. Hameyer, *An Algebraic Multigrid Preconditioner for Field-Circuit Coupled Problems*, IEEE Trans. Magn, Vol. 38,No. 2, 2002.

[66] H. Melissen and J. Simkin, *A new coordinate transformation for the finite element solution of axi-symmetric problems in magnetostatics*, Compumag conference on the Computation of Electromagnetic Fields. Tokyo, September 1989 Proceedings, MAG=26(2), March, 391-394 (1990).

[67] J. Gynselinck, P. Dular, C. Geuzaine, ans Willy Legros, *Harmonic-Balance Finite Modeling of Electromagnetic Devices: A Novel Approach,* IEEE Trans. Magn., Vol. 38, No. 2, 2002, pp521-524, 2002.

[68] J. A. Edminster, *Theory and problems of Electric circuits,*McGraw Hill (1972)

[69] *OPERA-2d user guide manual,* Vector Fields, 24 Bankside, Kidlington, Oxfordshire, OX5 1JE.

[70] Private communications with D. Griffith, FR-HiTemp Limited, Abbey Work, Titchfield, Fareham, Hampshire.

Appendix A: Currents in circuits with mutual inductance

The analytical solution of two circuits composed of filamentary conductors is reproduced from Smythe [51]. The two circuits are coupled by their mutual inductance M, as shown in figure A.1

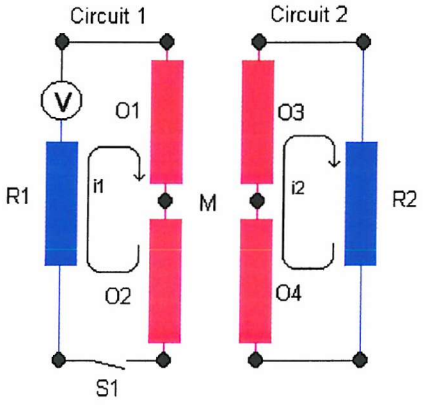

Figure A.1 Two inductively coupled circuits.

Applying Kirchoff's law for the two circuits gives

$$L_1\frac{di_1}{dt} + M\frac{di_2}{dt} + R_1 i_1 = V \tag{A.1}$$

$$L_2\frac{di_2}{dt} + M\frac{di_1}{dt} + R_2 i_2 = 0 \tag{A.2}$$

Solving equation A.1 for di_2/dt, substituting in equation A.2, solving for R_2i_2 and then multiplying by M gives

$$-MR_2 i_2 = (L_1L_2 - M^2)\frac{di_1}{dt} + L_2R_1 i_1 - L_2V \tag{A.3}$$

This is differentiated with respect to t, substituted into equation A.1 and multiplied by R_2 to give

$$(L_1L_2 - M^2)\frac{\partial^2 i_1}{\partial t^2} + (R_1L_2 + R_2L_1)\frac{di_1}{dt} + R_1R_2 i_1 = R_2V \tag{A.4}$$

The right hand side can made to be zero by adding the steady state solution $i_1=V/R_1$. The general solution of equation A.4 is

$$i_1 = C_1 e^{k1t} + C_2 e^{k2t} + \frac{V_1}{R_1} = e^{-\alpha t}(A\cosh(\beta t) + B\sinh(\beta t)) + \frac{V_1}{R_1} \qquad \text{(A.5)}$$

where the constants α and β are

$$\alpha = \frac{R_1L_2 + R_2L_1}{2(L_1L_2 - M^2)} \quad \text{and} \quad \beta = \frac{\sqrt{((R_1L_2 - R_2L_1)^2 + 4M^2R_1R_2)}}{2(L_1L_2 - M^2)} \qquad \text{(A.6)}$$

and A and B are found from the initial conditions. When t = 0, $i_1=0$ so that $A=-V/R_1$.

The transient solutions of A.1 and A.2 are similar, except the steady state solution for i_2 is $i_2=0$. The solution for i_2 is therefore

$$i_2 = e^{-\alpha t}(C\cosh(\beta t) + D\sinh(\beta t)) \qquad \text{(A.7)}$$

The initial conditions when t = 0 is $i_1=0$, so that C=0. Putting the values found from A and C into A.5 and A.7 and substituting into A.2, and then dividing out by $e^{-\alpha t}$ gives,

$$P\sinh(\beta t) + Q\cosh(\beta t) = 0 \qquad \text{(A.8)}$$

where

$$P = (M\alpha R_1B + \beta V) + DR_1(R_2 - \alpha L_2) \qquad \text{(A.9)}$$

and

$$Q = -(M\alpha R_1B + \beta V) + DR_1\beta L_2 \qquad \text{(A.10)}$$

Since A.2 is satisfied for all values of *t*, P and Q can be equated to zero separately. Doing this, and solving for A.9 and A.10 for B and D, and substituting for A, B, C, and D in A.5 and A.7 gives

$$i_1 = \frac{V}{R_1}\left(1 - e^{-\alpha t}\left(\frac{\cosh(\beta t) + (\alpha^2 + \beta^2)L_2 - \alpha R_2}{\beta R_2} + \sinh(\beta t)\right)\right) \tag{A.11}$$

$$i_2 = \frac{(\alpha^2 + \beta^2)MV}{\beta R_1 R_2} e^{-\alpha t} \sinh(\beta t) \tag{A.12}$$

Appendix B: List of publications

Two peer refereed papers have been published as a result of the work described in this report. A further three papers have been presented at workshops and discussion meetings. The references for the published papers are:

[1] C.S.Biddlecombe, J.Simkin, A.P.Jay, J.K.Sykulski, S.Lepaul, *Transient Electromagnetic Analysis Coupled to Electric Circuits and Motion*, IEEE. Trans Magn.34(5), pp. 3182 - 3185,1998.

[2] S. Lepaul, J.K.Sykulski, C.S.Biddlecombe, A. P. Jay and J.Simkin, *Coupling of Motion and Circuits with Electromagnetic Analysis*, IEEE Trans. Magn., Vol. 35, No.3, pp. 1602-1605, 1999.

Transient Electromagnetic Analysis Coupled to Electric Circuits and Motion

C.S.Biddlecombe, J.Simkin
Vector Fields Ltd., 24 Bankside, Kidlington, Oxford, OX5 1JE, UK.

A.P.Jay, J.K.Sykulski, S.Lepaul
Department of Electrical Engineering, University of Southampton, SO17 1BJ, UK.

Abstract -**This paper presents implementation details of coupling circuit equations and motion with two dimensional finite element models for transient magnetic analysis. Finite elements with incomplete shape functions are used in a novel way to handle the interface between the moving and stationary parts of the mesh. The final system of equations can then be solved using adaptive time stepping.**

Two examples are presented, a generator, which is coupled to motion and a motor, which is coupled to external circuits.

Index terms–**Electromagnetic fields, electromagnetic analysis, finite element methods, eddy currents**

I. Introduction

Electromechanical machines can be coupled to motion and external circuits.

In this paper will present schemes which

- Efficiently model the slip region between the stationary and moving parts
- Use an efficient time stepping algorithm to allow arbitrary exciting functions and reasonable solution times
- Preserve the sparseness and symmetry of the finite element matrix.
- Couple to complex and arbitrary circuits

II. Coupling to Motion

For a 2D material problem including induced currents, a fully time transient solution is required. The magnetic vector potential formulation **A** satisfies the equation

$$\nabla \times \nu \nabla \times \mathbf{A} = -\sigma \frac{d\mathbf{A}}{dt} + \mathbf{J}_S \qquad (1)$$

where ν is the reluctance $1/\mu$, $\mathbf{J}_S$ is the source current density, and **A** is the magnetic vector potential.

For a moving material problem with a constant velocity **u**, a motion term must be included

$$\frac{d\mathbf{A}}{dt} = \frac{\partial \mathbf{A}}{\partial t} + (\mathbf{u}.\nabla)\mathbf{A} = \frac{\partial \mathbf{A}}{\partial t} - \mathbf{u} \times \mathbf{B} \qquad (2)$$

However this is only valid if the cross section of the moving media is invariant normal to the direction of motion.

Manuscript received November 3, 1997.

This work was partly supported by the Department of Trade and Industry Teaching Company Scheme between Vector Fields Ltd and Southampton University.

There are two approaches to the solution of this new system.

- The extra source term is included and an asymmetric matrix is solved (referred to in this paper as a 'velocity' solver).
- The moving and stationary meshes in the problem are solved in their own rest frames and are coupled through the elements on their interfaces.

The novel finite elements presented in this paper can be classified in the second approach, called the pseudo-static formulation.

In this formulation, the extra source terms are not needed since the independent meshes are evaluated in their own local co-ordinate system and the coupling between the meshes occurs through an air interface, where there are no sources.

The pseudo-static formulation can be achieved in using number of different schemes, each having advantages and disadvantages.

A. Lockstep mesh:

The elements on the slip surface have a constant subtended angle therefore the mesh size is determined by the smallest feature. The time step is fixed by the time taken to rotate from one mesh alignment to the next [1,2]

B. Lagrange multipliers:

This scheme involves the use of a general slip surface between two disconnected meshes [3]. Continuity of the field components is ensured using Lagrange multipliers.

The matrix arising from this formulation is singular and not well conditioned.

C. Mesh Regeneration:

The simplest method is to re-mesh a slip region at each time step [4]. Potential mesh quality problems occur, as elements with large aspect ratios can be produced. As connections are broken and remade, there can be sudden transitions in the sizes of the matrix coefficients. However this method does allow for arbitrary shaped slip regions.

D. Boundary elements methods:

A dense sub-matrix is produced from all the nodes on the slip surface, this needs to be re-evaluated at each time step. In

small gap problems the integrals are difficult to evaluate, as the integrands can become singular.

E. Novel use of finite elements with incomplete shape functions:

The mesh in the slip region is formed from a variable number of quadrilateral elements whose matrix contributions are recalculated at each time step. The flexibility of the slip region's mesh must be emphasised. The mesh size can be different on the rotor and on the stator interfaces and need not be uniform. The time integration step length can be completely independent of the interface mesh sizes.

III. The Use of Incomplete Shape Functions

We have chosen to develop the use of incomplete shape functions because of the benefits of adaptive time stepping and a well conditioned matrix.

We will demonstrate how the incomplete shape functions can be used to mesh the a 'slip region' found in a motor model between a rotor and a stator, (Fig 1.).

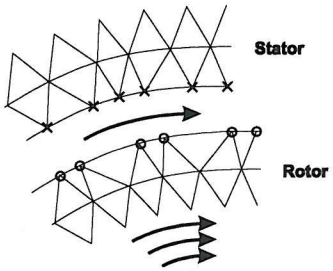

Fig.1 The detail of the mesh: The region between the Rotor and the Stator is meshed using incomplete shape functions.

A. Details about using Incomplete Shape Functions

- The nodes on the stator and rotor are placed in an ordered list according to their angle around the rotation axis.
- An integration sector is defined by two adjacent nodes in the ordered list
- There is one integration sector per node
- The integration of the incomplete shape functions is carried out for all the sectors

B. Details of the integration sectors

Figure 2 shows a typical integration sector in the slip region between the rotor and the stator.

The integration of this sector follows the path; node 1, projection of 3 on the rotor, 3, projection of 1 on the stator and back to 1.

If the first side in the integration path is considered, (from node 1 to the projection of node 3) it can be clearly seen that only part of the domain of the shape function from node 1 contributes to the integration path.

Special cases which arise when, for example, the position of node 1 is coincident with the projection of 4, or the projection of node 3 and 4 lie between node 1 and 2 are all catered for by one general algorithm.

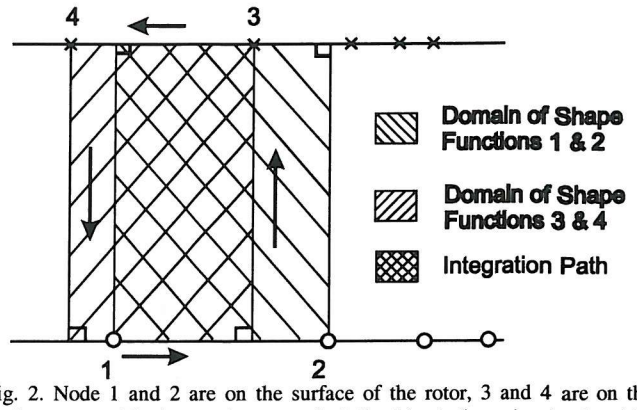

Fig. 2. Node 1 and 2 are on the surface of the rotor, 3 and 4 are on the stationary part. The integration sector is defined by 'adjacent' nodes 1 and 3.

IV. Results For Rotating Motion

The new method was validated by comparing the results from incomplete shape functions with the solution of (1) and (2), by the 'velocity' solver. Figure 3 shows the solution of a rotating disk. The solutions are not identical because the incomplete shape function solution has been extracted before all the transient effects have decayed away, whereas the velocity solver produces a static solution.

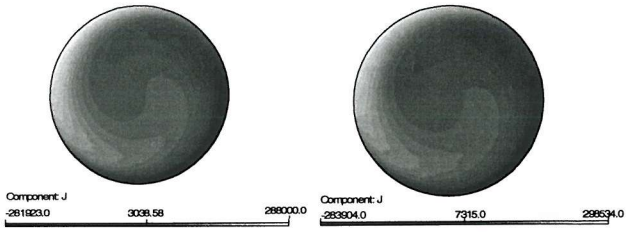

Fig. 3 Eddy currents in a rotating disc calculated by incomplete shape functions (left) and by the velocity solver (right)

A moving generator model has also been solved, where the velocity solver could not have been used, and the equi-potentials can be seen in figure 4.

Fig. 4. The field in a generator example, after a rotation of 483 degrees

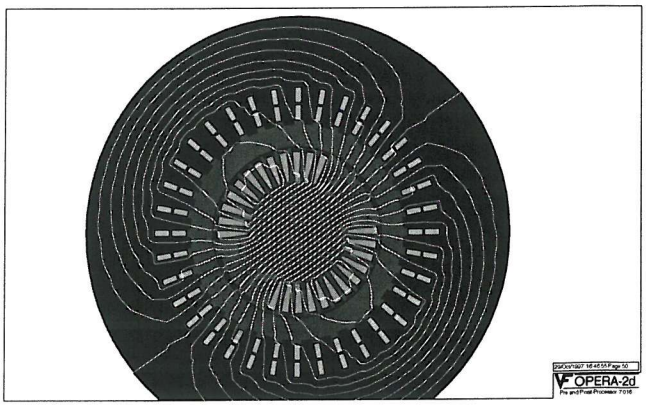

V. Coupling to Circuits

The coupling of electric circuit analysis with finite-element magnetic modelling may be achieved in three ways:

- by developing an integrated code where the two systems of equations are solved simultaneously, with either the FE and circuit models forming a single system of equations (direct coupling), or the FE part handled as a separate system which communicates with the circuit model by means of coupling coefficients (indirect coupling),
- by running a circuit simulation package in parallel with field software (under multitasking environment) with the two programs continuously exchanging information
- by first using the FE modelling to establish an equivalent circuit of a device and then feeding that circuit (in a form of a table, characteristic or equation) into a circuit analysis program.

The last of the above methods offers obvious advantages as computing times are likely to be short and thus the approach is particularly suitable for design purposes. However, it assumes that an equivalent circuit of the device exists and is sufficiently accurate - which often is not the case, especially if the element forms a major part of the system. Simultaneous execution of field and circuit packages has some attractions as coupled systems can be solved using existing commercial packages, with necessary modifications to allow for exchange of information. Highly complex problems, for both the field and circuit part, could be solved, but computing times are likely to be long. The fully integrated approach is usually the preferred option, although as it is normally achieved as an extension to an existing FE code it is often rather limited in terms of the complexity of the circuit which it can handle. Using indirect coupling offers an advantage of preserving the good properties of the FE coefficient matrix, whereas direct coupling leads to very efficient and reliable codes. There ready exists quite extensive literature on the topic, e.g. [5] and [6], and all three approaches continue to be areas of active research world-wide. This paper describes some implementation aspects of a system, which uses direct coupling. Two cases are considered - both important from the practical point of view - of stranded coils (filamentary problem) and massive conductors (eddy current problem).

VI. Formulation of the Basic Equations

The magnetic vector potential formulation **A** and current density J only have z-components, which satisfy the equation

$$\nabla \times \nu \nabla \times \mathrm{A} = J \tag{3}$$

where ν is the reluctance $1/\mu$. The current density in a conducting region is

$$J = -\sigma \frac{\partial \mathrm{A}}{\partial t} - \sigma \frac{\Delta V}{l} \tag{4}$$

where ΔV is the potential difference along the length of the conductor, σ is electrical conductivity, t is time and l is the length of the conductor. The total current flowing in the conductor is

$$I = -\int_S \sigma \left(\frac{\partial \mathrm{A}}{\partial t} + \Delta V \right) dS \tag{5}$$

Combining (3) and (4) gives,

$$\nabla \times \nu \nabla \times \mathrm{A} + \sigma \frac{\partial \mathrm{A}}{\partial t} + \sigma \frac{\Delta V}{l} = 0 \tag{6}$$

which is used in massive conductors, where the skin effect is calculated. In Filamentary conductors the current density is uniform over the conductor and is a function of the number of filaments N, the cross section of the conductor and the current flowing in a filament.

$$J = \frac{NI}{S} \tag{7}$$

The voltage ΔV at the terminals of the filamentary conductor is

$$\Delta \mathrm{V} = \frac{Nl}{S} \int_S \frac{\partial A}{\partial t} dS + NRI \tag{8}$$

where R is the resistance of a single filament. Combining (3) and (7) gives the field in the filamentary conductor defined by

$$\nabla \times \nu \nabla \times \mathrm{A} = \frac{NI}{S} \tag{9}$$

Circuit Network Equations: A matrix is used to represent a general circuit which has Voltage sources (E), impedances (Z) and inductances (L), where

$$[\mathrm{E}] = [\mathrm{Z}][\mathrm{I}] + [\mathrm{L}] \frac{dI}{dt} \tag{10}$$

There is one network equation per network 'loop' and a component may be a member of more than one loop.

Combining the equations: The final system of equations is formed from the field equations (6) and (9), the total current integral equation (5) and the circuit network equation (10). After applying a standard Galerkin procedure, a finite element block Matrix equation is produced

$$\begin{bmatrix} \mathbf{G} & \mathbf{H} & \mathbf{0} \\ \mathbf{0} & \mathbf{W} & \mathbf{D} \\ \mathbf{0} & \mathbf{D}^{\mathrm{T}} & -\mathbf{Z} \end{bmatrix} \begin{bmatrix} \mathbf{A} \\ \Delta \mathbf{V} \\ \mathbf{i} \end{bmatrix} + \begin{bmatrix} \mathbf{Q} & \mathbf{0} & \mathbf{0} \\ \mathbf{H}^{\mathrm{T}} & \mathbf{0} & \mathbf{0} \\ \mathbf{0} & \mathbf{0} & -\mathbf{L} \end{bmatrix} \frac{\partial}{\partial t} \begin{bmatrix} \mathbf{A} \\ \Delta \mathbf{V} \\ \mathbf{i} \end{bmatrix} = \begin{bmatrix} \mathbf{J} \\ \mathbf{0} \\ -\mathbf{E} \end{bmatrix} \tag{11}$$

where

$$\mathbf{G}_{ij} = \int \nu \nabla N_i \nabla N_j dS, \qquad \mathbf{H}_{ij} = \int_k \sigma N_i dS, \qquad \mathbf{W}_{kk} = \int_k \sigma dS,$$

$$\mathbf{Q}_{ij} = \int \sigma N_i N_j dS, \qquad \mathbf{J}_i = \int J_0 N_i dS$$

The integration of **G**, **Q** and **J** is carried out over the whole model, whereas for **W** and **H** it is over the conductor 'k'. **Z** and **L** are diagonal matrices of resistance and inductance respectively. **D** is sparse matrix, where an entry of +1 and -1 represents the direction of current flow in a conductor.

The matrix equation (11) can be conveniently written as

$$\mathbf{RX} + \mathbf{S}\frac{\partial \mathbf{X}}{\partial t} = \mathbf{B} \qquad (12)$$

which can then be solved by an appropriate numerical method.

VII. Numerical Solution

To allow for arbitrary excitation and variable time steps, the matrix equation is solved with a 'theta method' time marching scheme, which has been shown to be stable for θ=2/3 [7].

$$\left[\mathbf{R}(1-\theta) - \frac{\mathbf{S}}{\delta t}\right]\mathbf{a}_n + \left[\mathbf{R}\theta + \frac{\mathbf{S}}{\delta t}\right]\mathbf{a}_{n+1} = \mathbf{b}_n(1-\theta) + \mathbf{b}_{n+1}\theta \quad (13)$$

δt is the time between step n and n+1.

If the circuit equations are multiplied by $\theta\delta$t, the $\mathbf{a}_{n+1}$ matrix coefficients remain symmetrical, allowing for efficient storage and solution. The Matrix is not positive definite so it is solved by scaled incomplete Gauss conjugate gradients (CNJLUG).

The length of the time step δt is controlled to keep the error below a user supplied tolerance. This is achieved by comparing the results after one time step δt, with the value after two steps δt/2. If the solution is not sufficiently accurately the time step is halved and the solution is re-evaluated. When an adequate solution is achieved the next time step is evaluated. Subsequent steps are evaluated using step lengths which are longer or shorter than the previous time steps in order to maintain the error less than the user supplied tolerance while allowing the time stepping to proceed as quickly as possible.

VIII. Results for Circuit Coupling

The coupled equations have been applied to the simulation of a three phase induction motor. Massive conductors with eddy currents (Figure 5) represented the rotor circuits. The stator circuit was represented by voltage driven three phase windings, which were modelled by filamentary conductors.

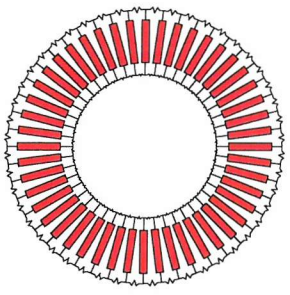

Fig. 4. The Circuit Diagram for the rotor. The solid blocks represent the eddy current conductors and the lines represent the resistors, which are used to model the resistances of connections

The fields plots, induced currents in the rotor bars and the detail of the finite element mesh can been seen in figure5.

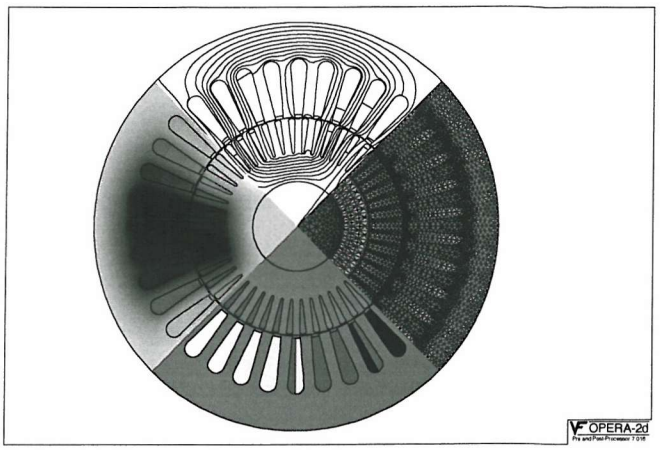

Fig. 5. The equipotentials, top and left, the induced current, bottom, and the mesh detail in the induction motor test problem.

IX. Conclusions

Rotational and motion and arbitrary external circuits can be coupled to two dimensional finite element analysis. The solution time is minimised by using incomplete shape function which allow for motion without reconstructing the finite element matrices and adaptive time stepping which only uses short time steps when the solution is changing rapidly.

The inclusion of kinematic terms and the extension of the use of incomplete shape functions in 3d systems [8] will be needed to provide a complete solution of the electrical motor problem.

References

[1] T. Preston et al, "Induction motor analysis by time stepping techniques," IEEE Trans. Magn, vol 24, pp 471-4, Jan 1988.

[2] D. Rodger, H. C. Lai , P. J. Leonard, "Coupled Elements for Problems Involving Movement", IEEE Trans. Mag. Vol. 26 NO. 2, pp. 546-550, 1990

[3] P. Lombard, G. Meunier "A general Purpose Method for Electric and Magnetic Combined Problems for 2D, Axisymmetry and Transient Systems," IEEE Trans. Magn., Vol.29, pp 1737-1740, 1993.

[4] G. Bedrosian, "A new method for coupling finite element field solutions with external circuits and kinematics," IEEE Trans. Magn., Vol.29, pp. 1664-1668, 1993.

[5] J. Väänänen, "Theoretical Approach to Couple Two-Dimensional Finite Element Models with External Circuit Equations," IEEE Trans. Magn., Vol. 32, pp. 400-409, 1996.

[6] I. A. Tsukerman, A. Konrad, G. Meunier and J. C. Sabonnadiére, "Coupled field-circuit problems: Trends and accomplishments," IEEE Trans. Magn., Vol. 29, pp. 1701-1704, 1993.

[7] O. C. Zienkiewicz and K. Morgan, Finite Elements and Approximation Methods. New York: Wiley (1983)

[8] C. R. I. Emson et al "Modelling Eddy Currents in Rotating Systems", Submitted to COMPUMAG '97 Conference, Rio de Janeiro, Brazil, November 1997.

Coupling of Motion and Circuits with Electromagnetic Analysis

S. Lepaul and J.K.Sykulski
Department of Electrical Engineering, University of Southampton, UK.

C.S.Biddlecombe, A. P. Jay, J.Simkin
Vector Fields Ltd., Kidlington, Oxford, UK.

Abstract–**The paper presents details of coupling circuit equations and motion with two dimensional transient magnetic analysis. Finite elements with overlapping shape functions are used to model the interface between moving and stationary parts of the mesh. The mechanical equation of movement is solved independently to estimate velocity of the rotating component.**

Index terms– **Coupled fields, transient analysis, motional effects, external circuits**

I. Introduction

A magnetic vector potential formulation **A** is used

$$\nabla\times\nu\nabla\times\mathbf{A}=-\sigma\frac{d\mathbf{A}}{dt}+\mathbf{J}_S \qquad (1)$$

where ν is the reluctance and $\mathbf{J}_S$ is the source current density. For a moving material problem with a constant velocity **u**, a motion term must be included

$$\frac{\mathrm{dA}}{\mathrm{dt}}=\frac{\partial\mathbf{A}}{\partial\mathrm{t}}+(\mathbf{u}.\nabla)\mathbf{A}=\frac{\partial\mathbf{A}}{\partial\mathrm{t}}-\mathbf{u}\times\mathbf{B} \qquad (2)$$

However, in the so-called pseudo-static formulation, where the moving and stationary meshes are solved in their own rest frames and are coupled through the elements on the interface, the extra source terms are not needed. The velocity of the moving part will either be known (e.g. for a generator problem) or needs to be estimated by solving the mechanical equation of movement (3), for example for an electric motor.

$$\frac{\mathrm{d}^2\theta}{\mathrm{d}t^2}=\frac{T}{\xi} \qquad (3)$$

ξ is the moment of inertia and T is the torque. At each time step the torque T is estimated from the field solution and, together with the latest values of θ and ω, the angular velocity, provides initial conditions for solving (3) to evaluate a new position of the rotor at the time $t+\Delta t$, where Δt is a variable time step in the transient finite-element scheme.

The effect of external circuits is included by solving

$$\nabla\times\nu\nabla\times\mathbf{A}\ +\sigma\frac{\partial\mathbf{A}}{\partial t}+\sigma\frac{\Delta V}{l}=0 \qquad (4)$$

in massive conductors (in order to include skin effect), or

$$\nabla\times\nu\nabla\times\mathbf{A}=\frac{NI}{S} \qquad (5)$$

Manuscript received June 1, 1998.
J. K. Sykulski, jks@soton.ac.uk, Vecto Fields, info@vectorfields.co.uk.

in filamentary conductors, where ΔV is the potential difference along the length of the conductor, σ is electrical conductivity, l is the length of the conductor, N is the number of filaments and S a conductor cross-section. After applying a standard Galerkin procedure, a finite element block matrix equation is produced [3], (a more general nodal analysis can be developed [4]).

$$\begin{bmatrix}\mathbf{G}&\mathbf{H}&\mathbf{0}\\ \mathbf{0}&\mathbf{W}&\mathbf{D}\\ \mathbf{0}&\mathbf{D}^{\mathrm{T}}&-\mathbf{Z}\end{bmatrix}\begin{bmatrix}\mathbf{A}\\ \Delta\mathbf{V}\\ \mathbf{i}\end{bmatrix}+\begin{bmatrix}\mathbf{Q}&\mathbf{0}&\mathbf{0}\\ \mathbf{H}^{\mathrm{T}}&\mathbf{0}&\mathbf{0}\\ \mathbf{0}&\mathbf{0}&-\mathbf{L}\end{bmatrix}\frac{\partial}{\partial t}\begin{bmatrix}\mathbf{A}\\ \Delta\mathbf{V}\\ \mathbf{i}\end{bmatrix}=\begin{bmatrix}\mathbf{J}\\ \mathbf{0}\\ -\mathbf{E}\end{bmatrix} \qquad (6)$$

where

$$\mathbf{G}_{ij}=\int\nu\nabla N_i\nabla N_j dS\,,\qquad \mathbf{H}_{ij}=\int_k\sigma N_i dS\,,\qquad \mathbf{W}_{kk}=\int_k\sigma dS,$$
$$\mathbf{Q}_{ij}=\int\sigma N_i N_j dS\,,\qquad \mathbf{J}_i=\int J_0 N_i dS$$

Our approach to the solution of this coupled system relies on the use of overlapping shape functions to model the slip region between the stationary and moving parts in the finite element formulation. This procedure is described in the second section. In the third section, we justify the use of Maxwell Stress Method (MSM) for the calculation of the torque. In the fourth section, we describe some methods to solve the mechanical equation (3). Finally, we present some numerical results.

II. Use of Overlapping Shape Functions

The use of elements with overlapping shape functions was proposed in [1]. The space between two surfaces is filled with two sets of elements that extend from one surface to the other, and have no degrees of freedom except on the surface they extend from. Such elements satisfy all the requirements necessary for a finite element approximation.

In the application considered in this paper, that of a rotating device, a slip region or super-element is formed between the rotor and the stator, consisting of two sets of overlapping elements. The first set extends from the rotor slip surface to the stator slip surface; the second set from the stator slip surface to the rotor slip surface. Using this approach, the meshes on the rotor and stator slip surfaces become completely independent and the time integration steps are unrestricted.

We have chosen to develop the use of overlapping shape functions because of the benefits of adaptive time stepping and a well-conditioned matrix. In addition, the technique does

not require the rotor and stator slip surfaces to be concentric, thus rotor vibration can also be included in the motion analysis.

A. Details of the Overlapping Shape Function Technique

Consider the 'slip' region between a rotor and a stator as shown in Fig. 1.

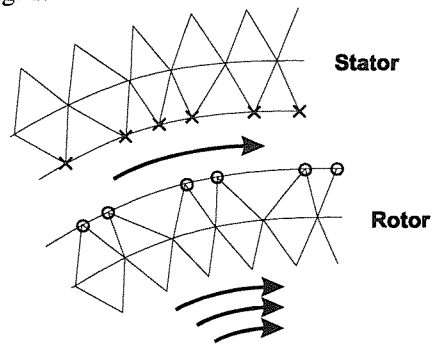

Fig.1. The detail of the mesh: The region between the Rotor and the Stator is meshed using overlapping shape functions.

The main features of the formulation may be summarised as follows :

- There is no re-meshing of the problem in a time -stepping procedure.
- There is a constant number of nodes in the finite-element mesh.
- The nodes on the stator and rotor are placed in an ordered list according to their angle around the rotation axis.
- An integration sector is defined by two adjacent nodes in the ordered list
- There is one integration sector per node
- The integration of the overlapping shape functions is carried out for all the sectors
- Full details of the shape function expressions are given in [1]

B. Details of the integration sectors

The mesh in the slip region is formed from a variable number of quadrilateral elements whose matrix contributions are recalculated at each time step.

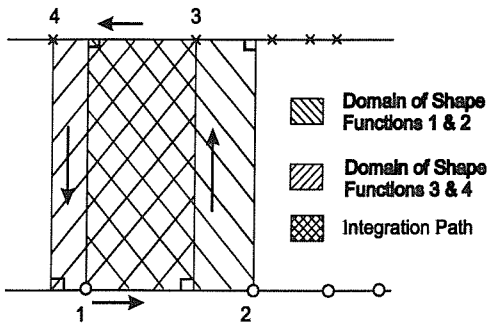

Fig. 2. The special quadrilateral elements using overlapping shape functions.

Figure 2 shows a typical integration sector in the slip region between the rotor and the stator. The integration of this sector follows the path: node 1, projection of node 3 on the rotor, node 3, projection of node 1 on the stator and back to node 1.

Consider the first side in the integration path of Fig. 2, (from node 1 to the projection of node 3). It can be clearly seen that only part of the domain of the shape function from node 1 contributes to the integration path.

Special cases which arise when, for example, the position of node 1 is coincident with the projection of 4, or the projection of node 3 and 4 lie between node 1 and 2 are all catered for by one general algorithm.

III. Torque Calculation by MSM

There are several methods of determining the forces on magnetic materials, including body forces method, virtual work principle and Mawell's stress method (MSM). We have chosen to use the MSM with the finite element overlapping shape functions in the slip region due to the simplicity and reliability of this method and because the position of the integration surface may be easily selected to be in the middle of the overlapping elements giving very accurate results [3].

In the MSM the torque is calculated on the basis of the magnetic field distribution on the closed surface in the air gap around the rotor

$$T = \oint_S \frac{1}{\mu_0}(\mathbf{r}\times\mathbf{B})(\mathbf{B}.\mathbf{n}) - \frac{1}{2\mu_0}\mathbf{B}^2(\mathbf{r}\times\mathbf{n})\, d\mathbf{S} \qquad (7)$$

To compute the integral, we have tried two different approaches. The numerical calculation can be performed in Cartesian coordinates or in polar coordinates. In a Cartesian coordinates system implementation, nearly degenerate overlapping elements are a source of errors. Such problems may be completely avoided by using a polar coordinates system. In other words, in polar coordinates, an algorithm allows to consider coincident points without extra assumptions about the calculation of the torque.

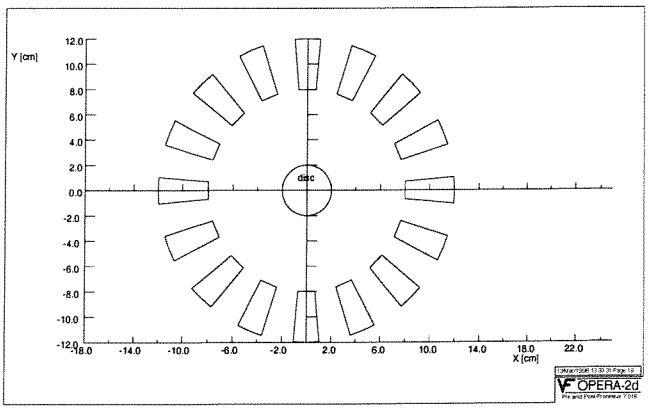

Fig. 3. Permanent magnet disc in the centre of the picture in a sinusoidal rotating field created by 16 coils with a 1Hz frequency

A detailed investigation of the torque calculation was performed for a permanent magnet disc moving at a constant

acceleration in a sinusoidal rotating field created by 16 coils with a frequency of 1 Hz. (Fig. 3).

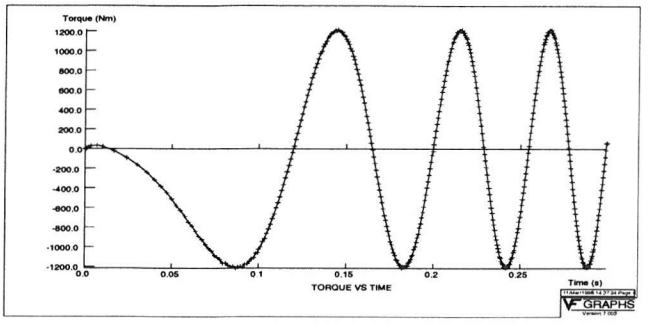

Fig. 4. Torque vs time calculated in cartesian coordinates for a rotor moving with a constant acceleration in a sinusoidal rotating field. with a frequency of 1Hz.

IV. Numerical Approach to the Mechanical Equation

First, the second order ordinary differential equation (6) has been transformed to a first order differential system (8)

$$\begin{cases} \dfrac{d\theta}{dt} = \omega \\ \dfrac{d\omega}{dt} = \dfrac{T}{\xi} \end{cases} \tag{8}$$

The first order ordinary differential system (8) can be solved by using many different numerical schemes. Three schemes are particularly popular: Euler schemes, explicit or implicit, midpoint scheme and Runge-Kutta schemes, explicit or implicit. We avoided implicit schemes, as the first order ordinary differential system (8) is nonlinear and time dependant. Implicit schemes would give a set of nonlinear equations that would need to be solved iteratively at each time step. In order to avoid such complications we have initially used an explicit Runge-Kutta scheme of order 4

To solve the system (8) we need to calculate an extrapolation of the torque by using a cubic Lagrange polynomial approximation obtained from previous calculated values of the torque.

Another future improvement is to consider the following set of mechanical equations in order to simulate the physical system more realistically.

$$\begin{cases} \dfrac{d\theta}{dt} = \omega \\ \dfrac{d\omega}{dt} = \dfrac{1}{\xi}\left[T - T_c - B\omega\right] \end{cases} \tag{9}$$

where T is the torque calculated with Maxwell Stress Tensor, T_c the load torque which may be a function of speed, ξ the inertia, ω the angular speed, θ the angular rotor displacement and B the viscous damping factor.

V. Numerical Examples

Two validations have been performed. Firstly, the overlapping shape functions were tested with a constant velocity. Secondly, the mechanical equations were tested using a simple case.

A. Validation of the overlapping shape functions

The method was validated in [3] for a constant velocity by comparing eddy currents in a rotating disc calculated by overlapping shape functions and by a coordinate transformation velocity solver (Fig. 5). The velocity solver produces a steady state solution, whereas the new solution shows all the transient effects. Thus the range of applications is not limited (as it would be in the velocity solver) by the fact that the cross section of the moving media must be invariant normal to the direction of the motion. To illustrate this advantage, a generator coupled to motion with a complex geometry was simulated and is shown in Fig. 6.

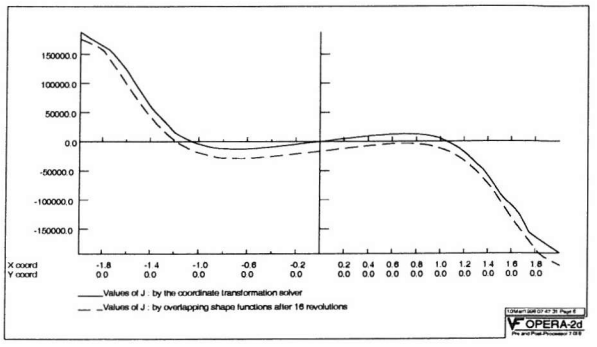

Fig. 5. Eddy currents in a rotating disc calculated by overlapping shape functions (dashed) and by a coordinate transformation solver (solid)

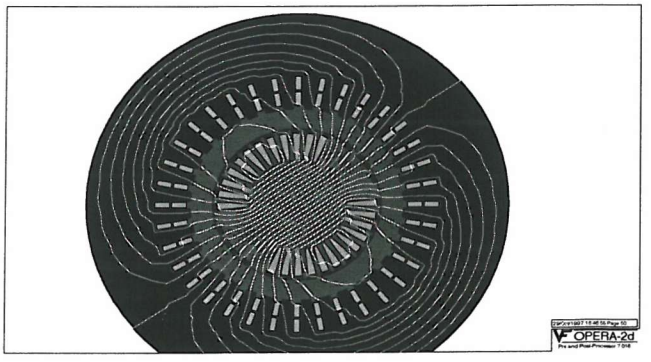

Fig. 6. The field in a generator example, after a rotation of 483 degrees

B. Validation of the mechanical equation

The algorithms were applied and tested for a permanent magnet disc surrounded by 16 coils creating a rotating field with a 1Hz frequency as described in Fig. 3. The torque over the time and the difference between the angles of the permanent magnet disc and the rotating field over time are shown in Fig. 7 and Fig. 8 respectively.

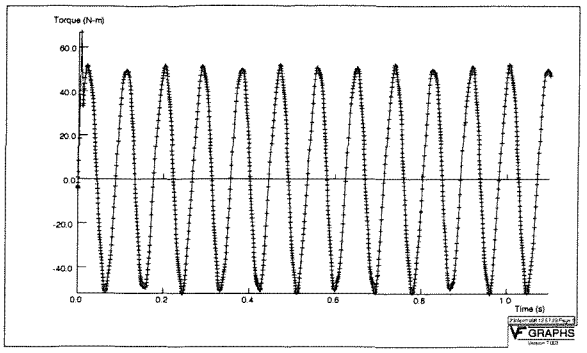

Fig. 7. The torque of the permanent magnet disc after one revolution for the electromechanical system described in Fig. 3.

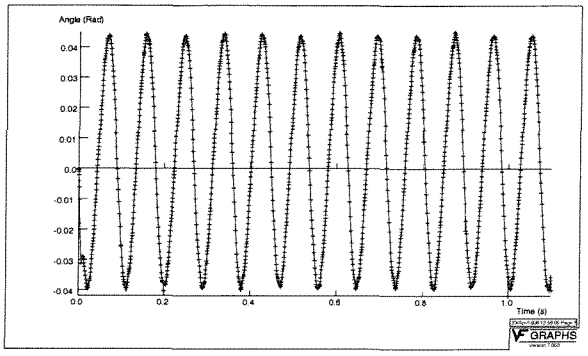

Fig. 8. The difference between the angles of the permanent magnet disc and the rotating field created by the 16 coils of Fig. 3 as a function of time.

This dynamic system is a good test to compare the accuracy of the different numerical schemes. The solution in the phase space (difference between the angles of the permanent magnet disc and the rotating field vs velocity) should be a closed loop. This is equivalent to the well-known mechanical pendulum oscillating with a small angle. To achieve this a scheme with a good accuracy is required.

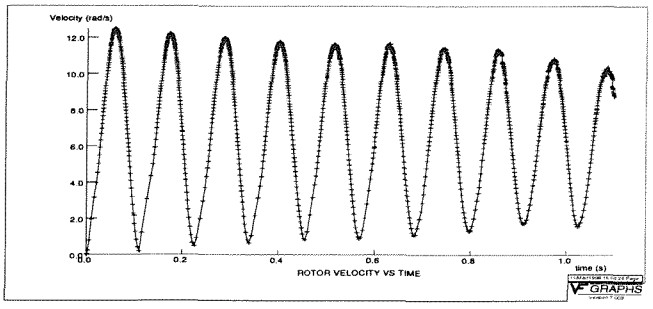

Fig. 9. The velocity of the permanent magnet disc after one revolution for the electromechanical system described in Fig. 3 using Euler's scheme.

It is well known that Euler's scheme is stable and consistent only for very small and constant time steps. In our analysis, however, we do not use a constant time step. The velocity amplitudes become therefore smaller and smaller as the time marches forward. If we reduce the tolerance, this phenomenon does not occur until after few cycles, as demonstrated in Fig. 9. To avoid this numerical difficulty, we propose a use of a Runge-Kutta scheme (Fig. 10.). At the moment, the torque is evaluated from the electomagnetic equations and used as a source term in the mechanical equation (8).Therefore, the coupling between the mechanical equations and the electromagnetic equations is a weak coupling [5]. A further improvement will be to use a predictor-corrector to evaluate the angle of the moving part in order to couple strongly the mechanical equations and the transient electromagnetic equations.

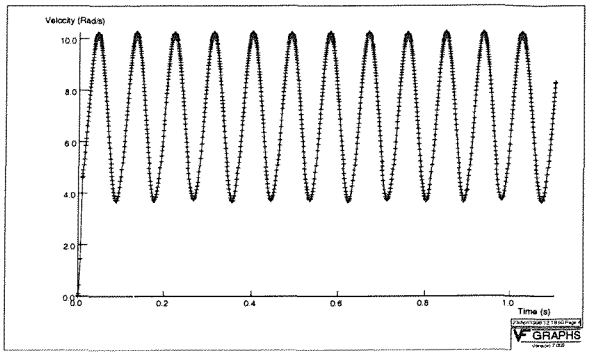

Fig. 10. The velocity of the permanent magnet disc after one revolution for the electromechanical system described in Fig. 3 using Runge-Kutta method.

VI. Conclusions

We have demonstrated a particular way in which rotational motion and arbitrary external circuits could be coupled to two dimensional finite element analysis. The solution time is minimized by using overlapping shape functions which allow for motion without reconstructing the finite element matrices, and by employing adaptive time stepping which only uses short time steps when the solution is changing rapidly. The Euler scheme is numerically is very simple to implement but haas to be used with caution. For instance, for stiff problem, which are not well conditioned, Euler schemes will generally fail. Therefore, to provide a robust analysis of many types of problems, more sophisticated methods, such as Runge-Kutta schemes are needed. Moreover, it might be beneficial to couple the mechanical equations and the transient magnetic equations more strongly by the use of a predictor-corrector to evaluate the angle of the moving part. Finally, the extension of the use of overlapping shape functions to 3D systems [6] will be needed to provide a complete solution of the electrical motor problem.

References

[1] I. A. Tsukerman "Overlapping finite elements for problems with movement," *IEEE Trans. Magn.*, Vol. 28, No.5 pp. 2247-2249, 1992

[2] M. Trlep, A. Hamler, B. Hribernik, "Various Approaches to Torque Calculations by FEM and BEM", in Proceedings of 7th International IGTE Symposium, 1996, pp. 416-419.

[3] C. S. Biddlecombe, J. Simkin, A. P. Jay, J. K. Sykulski, S. Lepaul, "Transient Electromagnetic Analysis Coupled to Electric Circuits and Motion," *IEEE Trans. Magn*, Vol 35, No.5 pp. 3182-3185. 1998.

[4] M. C. Costa et al "Simulation of Induction Machine by 2D Finite Element Method coupled with Electric Circuits using the Modified Nodal Analysis", presented at IEEE CEFC 1998.

[5] S. Lepaul, C. S. Biddlecombe, J. Simkin, A. P. Jay, J. K. Sykulski, "Transient Electromagnetic Analysis Coupled to Electric Circuits and Mechanical Systems," in Proceedings of the 4th International Workshop on Electric and Magnetic Fields, Marseille, May 1998, pp. 237-242.

[6] C. R. I. Emson et al "Modelling Eddy Currents in Rotating Systems", *IEEE Trans. Magn*, Vol 35, No.5 pp 2593-2596, 1998.